THE EFFECT OF FATTY ACID COMPOSITION ON THE COMBUSTION CHARACTERISTICS OF BIODIESEL

March 2008

Thet Myo

THE EFFECT OF FATTY ACID COMPOSITION ON THE COMBUSTION CHARACTERISTICS OF BIODIESEL

A Dissertation
Submitted to the Graduate School of Science and Engineering
In Partial Fulfillment of the Requirements
for the Degree of

Doctor of Philosophy in Engineering

at the
Kagoshima University

by
Thet Myo
Division of System Control Engineering,
Department of System Information Engineering,
Graduate School of Science and Engineering,
Kagoshima University
1-21-40, Korimoto, Kagoshima 890-0065, JAPAN

March 2008

TABLE OF CONTENTS

LIST OF FIGURES

LIST OF TABLES

LIST OF SYMBOLS AND ABBREVIATIONS

Hl : Low calorific value (MJ/kg)

L : Braking power (kW)

M : Electric dynamometer braking load (kg)

N : Engine speed (rpm)

BMEP, P_{me}: Brake mean effective pressure (MPa)

V : Stroke volume (cm^3)

B : Fuel consumption per hour (g/h)

NT : Fuel consumption per minute (g/min)

BSFC, b_e: Brake specific fuel consumption (g/MW.s)

η_v : Volumetric efficiency (%)

Q_{th} : Theoretical air charge (ℓ/min)

Q_a: Actual air charge (ℓ/min)

ΔP: Different pressure of laminar flow meter (mmHg)

C : Volume compensation coefficient

t_1 : Atmospheric temperature(˚C)

η_c : Charging efficiency (%)

ρ_a : Air density in suction surge tank (kg/m^3)

ρ_{20} : Air density at 760mmHg (kg/m^3)

H_{20} : Atmospheric pressure at 20˚C (mmHg)

H : Atmospheric pressure (mmHg)

t_2 : Temperature in surge tank (˚C)

G_a : Suction air quantity (g/s)

η_e : Brake thermal efficiency (%)

c_v : Specific heat at constant volume (kJ/kg.K)

Q : Calorific value (MJ/kg)

R : Gas constant (J/kg.K)

T : Absolute temperature of gas (K)

κ : Specific heat ratio

V : Stroke volume (m^3)

P : Cylinder pressure (Pa)

θ : Crank angle (deg.)

m : Mass of gas (kg)

U : Internal energy of gas (J)

l : Length of connecting rod (m)

r : Crank radius (m)

V_c : Clearance volume (m^3)

A : Cross sectional area of piston (m^2)

ABSTRACT

Biodiesel is an alternative fuel for diesel engines that can be manufactured from vegetable oils, animal fats and used cooking oils. It offers many advantages such as it is renewable, energy efficient, nontoxic, sulfur free and biodegradable, and also it usually takes cleaner combustion and reduces global warming gas emissions from the diesel engines. Specifically, the combustion of vegetable oil biodiesel does not add the net CO_2 to the atmosphere, because the next crop will reuse CO_2 to grow.

In this study, the objectives are to clarify the effect of fatty acid composition on the combustion characteristics of biodiesel and additionally to study the effect of fatty acid composition on the fuel properties and the exhaust emissions of biodiesels. Therefore, the experiments were conducted on five kinds of methyl ester type vegetable oils biodiesels, five kinds of common pure fatty acid methyl esters (FAMEs) and three kinds of unsaturated FAMEs with different degree of unsaturation, by using a single cylinder direct injection diesel engine. Furthermore, the fuel properties analysis, the exhaust gas emission measurements and development of a correlation program were carried out simultaneously.

In Chapter 1, the introduction of today world energy demand and supply concern, environmental concern and about the importance of renewable energy resources are expressed. A brief explanation about the concept of diesel engines and, fats and oils are also consisted in the introduction. In literatures reviews section, the transesterification process, the uses of vegetable oil and biodiesel in diesel engine, and biodiesel and fatty acid composition are given. At the end of the chapter, the objectives of this study are pointed out.

Chapter 2 introduces the experimental apparatus and procedures of the engine test experiments. The specifications of test engine, equipments and measurement devices are shown in this chapter. Also the detailed explanation of experimental procedure and, calculation and data analysis methods are mentioned.

In Chapter 3, the diesel combustion characteristics of various vegetable oil methyl esters were reported. The experiments were carried out on a single cylinder direct injection diesel engine by fuelling five kinds of FAME type

biodiesels and JIS No.2 diesel fuel. The FAME type biodiesels are coconut oil methyl ester (CME), palm oil methyl ester (PME), palm kernel oil methyl ester (PKME), rapeseed oil methyl ester (RME) and soybean oil methyl ester (SME). Also the fuel properties and the exhaust emission from these test fuels were measured. From the experimental results, saturated FAME type biodiesel, CME, PME and PKME have shown better combustion characteristics and lower emissions compared to unsaturated FAME type biodiesels like RME and SME.

Chapter 4 reports the diesel combustion characteristics of single composition of fatty acid methyl esters. The experiments were carried out on a single cylinder direct injection diesel engine by fuelling five kinds of pure FAMEs, three kinds of unsaturated FAME with different degree of unsaturation and JIS No.2 diesel fuel. Five kinds of pure FAMEs are methyl laurate, methyl myristate, methyl palmitate, methyl stearate and methyl oleate, and three kinds of unsaturated fatty acid methyl ester are high oleate safflower oil methyl ester ($SFME_{HO}$), high linoleate safflower oil methyl ester ($SFME_{HL}$) and linseed oil methyl ester (LME). From the experimental results, better combustion characteristics and lower emissions were found in saturated FAMEs and poor combustion characteristics and higher emission can be seen in most unsaturated FAMEs.

Chapter 5 expresses the effect of fatty acid composition on the combustion characteristics of biodiesel. Detailed discussions on the experimental results of chapter 3 and 4 based on the experimental results concerning the fuel properties, the combustion characteristics and the exhaust emissions of five kinds of FAME type biodiesels, five kinds of pure FAMEs and three kinds of unsaturated FAME type biodiesels with different degree of unsaturation are included. Furthermore, from these experimental results, the assumptions were made for the emissions (HC, CO, NOx, smoke) of seven kinds of single composition of FAME (methyl laurate, methyl myristate, methyl palmitate, methyl stearate, methyl oleate, methyl linoleate, methyl linolenate). By fairly adjusting to coincide the assumption data of these single type FAMEs emissions and the experimental emission data (CME, PME, RME, SME, $SFME_{HO}$, $SFME_{HL}$ and LME), a correlation program was developed for estimation of exhaust emissions from biodiesels.

Finally, the conclusions of this study based on the implementation of objectives are expressed in Chapter 6.

1. INTRODUCTION

1.1 Introduction

The demand for energy around the world is continuously increasing, specifically in the demand for petroleum-based energy. Petroleum is the largest single source of energy which has been consuming by the world's population, exceeding the other energy resources such as natural gas, coal, nuclear and renewable. According to International Energy Outlook 2007 published by the Energy Information Administration, the world consumption for petroleum and other liquid fuel will grow from 83 million barrels/day in 2004 to 97 million barrels/day in 2015 and just over 118 million barrels/day in 2025. Under these growth assumptions, approximately half of the world's total resources would be exhausted by 2025. Also, many studies estimating that the world oil production would peak sometime between 2007 and 2025 (01). Therefore the future energy availability is a serious problem for us.

Another major global concern is environmental concern or climate change such as global warming. Global warming is related with the greenhouse gases which are mostly emitted from the combustion of petroleum fuels. In order to control the emissions of greenhouse gases, Kyoto Protocol negotiated in Kyoto City, Japan in 1997 and came to effect since February, 2005. Now, Kyoto Protocol covers more than 160 countries globally and targeting to reduce the greenhouse gas emission by a collective average of 5% below 1990 level of respective countries. The Intergovernmental Panel on Climate Change (IPCC) concludes in the Climate Change 2007 that, because of global warming effect the global surface temperatures are likely to increase 1.1°C to 6.4°C between 1990 and 2100 (02).

To solve both the energy concern and environmental concern, the renewable energies with lower environmental pollution impact should be necessary. Nowadays several new and renewable energies have been emphasized and biomass energy is one of the renewable energies among them. Biomass energy includes liquid biofuels derived from biomass and which are promising as alternative fuels with low environmental pollution impact, to replace petroleum

based fuels. Some of the well known liquid biofuels are ethanol for gasoline engines and biodiesel for compression ignition engines or diesel engines.

Biodiesel is a renewable and environmental friendly alternative diesel fuel for diesel engine. It can be produced from food grade vegetable oils or edible oils, nonfood grade vegetable oils or inedible oil, animal fats and waste or used vegetable oils, by the transesterification process. Transesterification is a chemical reaction in which vegetable oils and animal fats are reacted with alcohol in the presence of a catalyst. The products of reaction are fatty acid alkyl ester and glycerin, and where the fatty acid alkyl ester is known as biodiesel.

Biodiesel is an oxygenated fuel and which containing 10% to 15% oxygen by weight. Also it can be said a sulfur-free fuel. These facts lead biodiesel to more complete combustion and less most of the exhaust emissions from diesel engine. But, comparing the fuel properties of biodiesel and diesel fuel, it has higher viscosity, density, pour point, flash point and cetane number than diesel fuel. Also the energy content or net calorific value of biodiesel is about 12% less than that of diesel fuel on a mass basis.

Using biodiesel can help to reduce the world's dependence on fossil fuels and which also has significant environmental benefits. The reasons for these environmental benefits are: using biodiesel instead of the conventional diesel fuel reduces exhaust emissions such as the overall life circle of carbon dioxide (CO_2), particulate matter (PM), carbon monoxide (CO), sulfur oxides (SOx), volatile organic compounds (VOCs), and unburned hydrocarbons (HC) significantly. On the other hand, most of the researchers have reported that 100% biodiesel emits lower tail pipe exhaust emissions compared to the diesel fuel; nearly 50% less in PM emission, nearly 50% less in CO emission and about 68% less in HC emission. Furthermore, since biodiesel can be said a sulfur-free fuel, it has 99% less SOx emission than the diesel fuel. However, most of the biodiesels produce 10% to 15% higher oxides of nitrogen (NOx) when fueling with 100% biodiesel (03).

Depending on the abundantly availability of feedstock in local region, the different feedstocks are focused for the biodiesel production. In the United States, the primary sources for biodiesel production is soy bean oil, while EU nations prefer to utilize rapeseed oil, and in South East Asia regions, palm oil, coconut oil

and jatropha oil are expected mainly for biodiesel productions. Growing the production of biodiesel in many countries around the world has been accompanied by the development of standards to ensure high fuel quality. Some biodiesel standards are ASTM D6751 in the United States and EN 14214 in EU nations. Also in Japan, there is a standard for biodiesel has been developing and will prescribe in near future. The properties of biodiesel are mainly determined by the structure of fatty acids alkyl esters in it. Particularly, the combustion characteristics such as ignition quality, and the fuel properties such as density, viscosity, pour point and oxidation stability of biodiesel are mostly affected by the structure of fatty acids alkyl esters (04).

1.1.1 Diesel Engines

It should be necessary to understand the basis concept of compression ignition engine or diesel engine before discussing about the combustion characteristics of biodiesel. Compression ignition engine was invented by Rudolf Diesel in1891, which is commonly known as diesel engine today. The engine cycle of the diesel engine is diesel cycle which is a modified Otto cycle and known as constant pressure cycle. Diesel engines are commonly four-stroke cycle engines. With the four-stroke cycle, air is drawn into the cylinder during the first stroke (intake stroke) followed by high compression during the second (compression stroke). Then the fuel is injected and burnt during the third stroke (power stroke) and the products of combustion are exhausted during the fourth (exhaust stroke). The diesel engine relies on a high compression ratio, typically greater than 14:1 to occur combustion. This higher compression ratio is in order to bring the air temperature to a level where auto ignition is promoted when the fuel is injected to the cylinder at the end of the compression stroke. A principal requirement of a fuel for diesel engine is, that must be auto ignited easily (05).

Diesel engines are usually classified into two categories; these are direct and indirect injection engines. Direct injection means the fuel is directly injected into the combustion chamber. The fuel is injected under high pressure through a nozzle with single or multiple tiny orifices. This results in a fuel spray with very fine droplets thus making it easier for the fuel to evaporate and burn. But in the

indirect injection engines, the fuel is injected into an auxiliary chamber that is adjacent and connected to the main combustion chamber. Most combustion start sooner in this chamber and burning gases exit the chamber with high velocities giving a greater ability for mixing of fuel and air. These types of engines are not very sensitive on the ignition ability of the fuels.

Generally, the combustion process in diesel engines can be divided into four steps (06):

(1) Ignition delay: it is a period between the start of injection and the start of combustion.

(2) Ignition: it is taken place after ignition delay period.

(3) Initial combustion or premixed combustion phase: which occurs after ignition and it consumes about 5% to 10% of injected fuel.

(4) Diffusion controlled or mixing controlled phase of combustion: it occurs after premixed combustion and produce high temperature and pressure in the combustion chamber. It consumes all of the remaining fuel.

During the ignition delay period many processes occur within the cylinder. Fuel has to be broken down into droplets, heated, vaporized, and mixed with air. Both physical and chemical delays are present and those two delays are not added since they are usually overlapping. Due to the high compression ratio the temperature and pressure of the air at the time of injection are normally well above those required to support chain-reaction in a uniform fuel-air mixture. Under these conditions, ignition of any element of the charge dose not require transfer of energy from another portion but will occur when the local temperature, pressure, and mixing of fuel and air make combustion possible (07). In general, the combustion of the fuel in the compression-ignition engine depend on the local condition in each part of the charge and does not depend on the spread of the flame through the charge like spark ignition engines. However, the local flame may assist the ignition of adjacent sections if the local conditions (e.g., fuel-air ratio) support combustion. Local flames may also reduce the reaction time of adjacent sections by raising their temperature and pressure. The combustion rate or heat release rate is thus a function of the state and distribution of the fuel as

well as the pressure and temperature in the combustion chamber, where the latter is initially dictated by the compression ratio (08). Other factors that influence the combustion process are injection timing, turbulence in the combustion chamber, engine revolution along with several other fuel properties such as cetane number, kinematic viscosity, density and distillation temperature.

The advantages of diesel engines are it has greater efficiency, durability and good fuel economy compared to gasoline engines. Therefore, the application range of diesel engines is very wide. Most of the applications of diesel engines are in major transportation sector such as bus, truck, train and ship, and heavy machinery like construction equipments.

1.1.2 Fats and Oils

In order to explain about biodiesel, it is also necessary to know about fats and oils or the origin of biodiesel. The different between a fat and oil is their physical state. The term fat usually defines the solid state, and oil in the liquid state. These terms are reversible depending on the temperature to which the compound is exposed. When the state is unimportant, the term fat is usually used. Vegetable oils and animal fats consist mainly of triglyceride. Its chemical structure consists of three fatty acids connected to the glycerol through ester linkages (09). This arrangement is shown in Figure 1.1. The type of triglyceride and its complexity is determined by: the number, kind and mode of arrangement of the individual fatty acids attached to the glycerol skeleton to form the specific glyceride; and the number and relative proportion of these glycerides that from the specific fat or oil. The fatty acids part of the triglyceride account for 90 to 94% of

$$\begin{array}{lcl} CH_2-OH & & CH_2-OOCR_1 \\ CH-OH & + R_2COOH \longrightarrow & CH-OOCR_2 \\ CH_2-OH & & CH_2-OOCR_3 \end{array} + 3H_2O$$

Glycerol + 3 fatty acids ⟶ Triglyceride + Water

R1, R2 and R3 are long hydrocarbon chains

Figure 1.1 Arrangement of three fatty acids

Table 1.1 Fatty acid compositions of some fats and oils (10)

Fatty acid	C:N	Fats and oils (wt%)								
		Lard	Tallow	Coconut	Palm	Palm Kernel	Rapeseed	Peanut	Soybean	Sunflower
Caproic	6:0	-	-	0.4	-	-	-	-	-	-
Caprylic	8:0	-	-	0.7	-	2.3	-	-	-	-
Capric	10:0	0.1	-	0.6	-	2.7	-	-	-	-
Lauric	12:0	-	-	47.5	0.3	44.1	-	-	-	-
Myristic	14:0	1.6	2.7	19.1	1.1	17.1	-	-	-	-
Palmitic	16:0	24.2	23.4	9.8	44.1	9.1	4.3	9.7	10.5	6.6
Palmitoleic	16:1	3.6	5.6	-	0.2	-	0.1	-	-	-
Stearic	18:0	14.1	16.5	3.8	4.5	2.6	1.9	3.3	3.8	5.5
Oleic	18:1	43.8	45.1	5.9	40.1	18.2	59.7	50.6	25	18.3
Linoleic	18:2	9.4	3.3	0.4	9.1	2.6	21.7	30.2	52.2	67.8
Linolenic	18:3	1.6	1.0	0.1	0.6	0.1	9.4	1.3	7.6	0.8
Gadoleic	20:1	-	-	-	-	-	1.5	0.9	0.3	0.1
Behenic	22:0	-	-	-	-	-	0.4	2.6	0.4	0.8
Erucic	22:1	0.3	-	-	-	-	0.6	-	-	-

C: no. of carbon, N: no. of carbon-carbon double bond

the compound's total molecular weight. Most of the fatty acids from vegetable oils and animal fats are usually with the carbon numbers ranging from C6 to C18. Table 1.1 shows the fatty acid composition of some commonly available fat and oils. The vegetable oil itself consists of several triglycerides in which the three fatty acids may vary.

Naturally occurring fatty acids are classified into two categories based on the presence or absence of multiple bonds in their hydrocarbon chain. These two categories of fatty acids are termed "saturated and unsaturated." Saturated fatty acids are those with no multiple bonds and unsaturated fatty acids are those with multiple bond. The degree of unsaturation of unsaturated fatty acids is determined by the number of double or triple bonds present in the structure, with a higher number of multiple bonds representing a higher degree of unsaturation. The detail explanation and the structure construction of saturated fatty acid and unsaturated fatty acid will be given in chapter 4.

1.2 Literature Review

1.2.1 Transesterification Process

The transesterification is a chemical reaction widely used in the production of biodiesel. In this reaction fatty acid in vegetable oil is reacted with an alcohol in a presence of a catalyst to form fatty acid alkyl ester. The most common type of alcohol used in biodiesel production is methanol. It is because of methanol takes high yield reaction quite easy and also the price of methanol is cheaper than the other alcohols. Indeed, the transesterification can take place with or without presences of a catalyst. Either an acid or alkali catalyst can be used in the transesterification to produce methyl, ethyl or butyl esters of fatty acids. In reaction, the stoichiometric ratio of alcohol to vegetable oil is 3:1 and the products are 3 mol of fatty acid alkyl ester and 1 mol of glycerol. The chemical equation of transesterification reaction is shown in Figure 1.2.

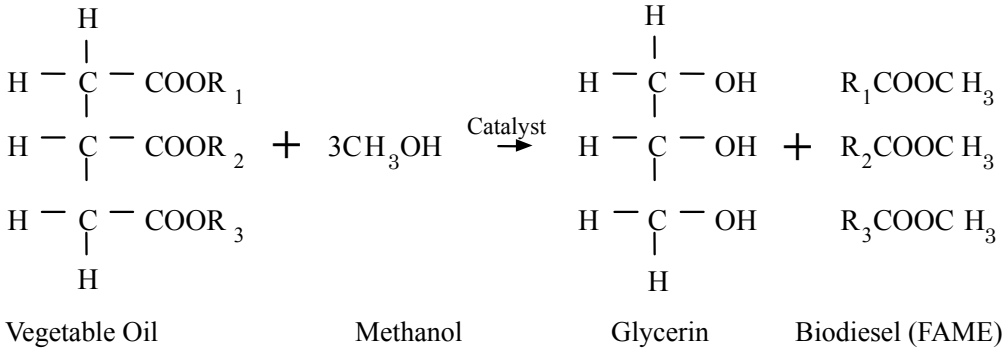

(R_1, R_2, R_3 represents the hydrocarbon chain of fatty acid)

Figure 1.2 Chemical equation of transesterification reaction

Mostly, the molar ratio of alcohol to vegetable oil is determining the ester conversion rates. It has been reported by several technical papers, a molar ratio of 6:1 of alcohol to vegetable oil that means two time of stoichiometry, gives the ester conversion rate over 90%. One of the factor influences on ester conversion rate is the fatty acid composition of vegetable oils. Higher saturated fatty acid compositions in vegetable oils like coconut oil and palm kernel make difficult for transesterification reaction and lower ester conversion rate.

Freedman et al (11) reported on the variables that affect the yield and purity of esters produced by way of the transesterification process. Sixty grams of edible-grade vegetable oil was mixes with 16.572 ml of methanol and sodium methoxide (0.5% by weight of oil) was used as the catalyst. It was expressed that 98% of the reaction was completed in approximately one hour. Several factors were found to significantly affect the yield and quality of the ester. The water content of all materials, including the catalyst and triglyceride, and the acid value of the triglyceride were required to be very low. An acid value of less than one (i.e., free fatty acid content of less than 0.5%) and water content of less than 0.3% (i.e., substantially anhydrous material) were recommended. Acid and water contents above those values were reported to cause a significant decrease in the ester yield.

Other important factors for transesterification are reaction time and temperature. The time required for the reaction to be completed was estimated to be 1 hr by Freedman et al. (11). The reaction temperature depended on the type of alcohol being used and was recommended to be a few degrees below the boiling point of the alcohols used (examples of reaction temperatures are: methanol 60 ^{o}C, ethanol 75 ^{o}C and butanol 114 $^{\circ}$C).

Noureddini and Zhu (12) found that increasing the reaction temperature for methyl esters from 30 to 70 $^{\circ}$C led to significant increases in the reaction rate with temperature up to 50 $^{\circ}$C, but little increase in reaction rate over 50 $^{\circ}$C. Work done by Allen and Watts (13) showed that reaction times in the range 15-30 minutes were adequate for greater than 98% conversion when canola oil was transesterified with methanol at 60 $^{\circ}$C.

By reviewing transesterification of vegetable oils, in order to clear the biodiesel standard such as ASTM or EU, more than 95% of ester conversion is necessary. Also it may be needed to investigate the method for higher ester conversion rate of saturated vegetable oils like as coconut oil and palm kernel oil.

1.2.2 The Uses of Vegetable Oil and Biodiesel in Diesel Engine

Vegetable oils were used as fuel for diesel engines to some extent since the invention of the compression ignition engine by Rudolf Diesel in the late 1800`s.

During the early stages of the diesel engine, strong interest was shown in the use of vegetable oils as fuel but this interest declined in the late 1950`s after the supply of petroleum products become abundant (14). During the early 1970`s, oil shock however caused a renewed interest in vegetable oil fuels. This interest evolved after it became apparent that the world's petroleum reserves were dwindling. At present, in order to replace a part of petroleum based diesel usage, the use of vegetable oil product biodiesel has been starting in some countries.

Vegetable oils are renewable energy source and significant environmental benefit can be derived from the combustion of vegetable oil based biodiesel rather than petroleum based diesel fuels. The CO_2 produced from combustion of biodiesels balances to CO_2 used by the plants from which they originate, therefore the net gain of CO_2 in the atmosphere is neutral unlike that which occurs with the combustion of petroleum based diesel. Vegetable oils also contain only trace quantities of sulfur, therefore the combustion of biodiesel emits 99% less SOx emission.

Generally, there are three forms to use vegetable oils as fuel in diesel engines. These are neat or pure vegetable oils, blends of vegetable oils and diesel fuel, and transesterified vegetable oils. The first and second forms have problems associated with the long term performance of diesel engines because of higher fuel viscosity. But the esters of vegetable oils have significantly lower viscosities than the neat or blended vegetable oil fuels thus the viscosity related problems are greatly reduced. The most promising applications of vegetable oils as diesel fuels are of course the ester of vegetable oils. Methyl, ethyl and butyl esters produced by means of the transesterification of vegetable oils are usually known. But the most common type of biodiesel is methyl esters as explained in the previous section. Presently, the well known method of biodiesel usage is blending with conventional diesel fuel. The common ratio is 80% conventional diesel fuel to 20% biodiesel, which is also known as "B20".

The application of ester of vegetable oils as diesel engine fuels was studied by several researchers [Peterson et al. (15), Schumacher et al., (16), Zubik et.al. (17), Ali et al. (18), Wagner et,al. (19), Van Gerpen (20), Mittelbach and Trillhart (21), A. Shaheed et.al. (22), K. Hamasaki et.al. (23), Eiji Kinoshita et.al(24)].

Most of their findings were similar and typical ones are given below.

Peterson et al. (15) found that the engine performance of a diesel engine fueled with methyl and ethyl esters of rapeseed oil was comparable to standard diesel No. 2 fuel with the ester showing slightly lower power output and associated higher brake specific fuel consumption. The methyl ester was reported to produce slightly more power than the ethyl ester. Schumacher et al., (16) found that 100% soydiesel (methyl ester of soybean oil) produced slightly more power on average than low sulfur diesel fuel.

Results of tests done by Zubik et al. (17) showed that the methyl esters of sunflower oil produced higher maximum cylinder pressure and rate of pressure rise than diesel No.2 fuel. The combustion process was also analyzed to be the same as diesel fuel, with a delay period followed by rapid combustion and then a slower diffusion controlled phase. Ali et al. (18) investigated in cylinder characteristics of methyl ester of beef tallow and blends with diesel fuel and ethanol. They found that the peak pressures of 100% esters and some of blends were 5-9% lower than that of diesel No.2 fuel. The rate of pressure rise was found the same.

Wagner et al. (19) reported that the cetane number of esters of soybean oil was higher than that of diesel No.2 fuel and thus a shorter delay period was assumed to be present although no cylinder pressure monitoring was done. Also they expressed that the cetane number was positively proportional to the molecular weight of the alcohol used in the transesterification process. Van Gerpen (20) found that the longer fatty acid carbon chains and saturated fatty acid molecules resulted in higher cetane values.

Mittelbach and Trillhart (21) investigated the used of transesterified used-frying-oil in diesel engines. They tested these methyl esters on a 1.6 litre Volkswagen car and reportedly found no significant difference in the performance of the engine when compared with diesel fuel. A. Shaheed at el. (22) investigated the performance and exhaust emission evaluation of a small diesel engine fueled with coconut oil methyl esters. They showed coconut oil methyl ester had comparative engine performance to diesel fuel and emission characteristics were equally as good as or better than diesel fuel for most of the exhaust constituents.

K. Hamasaki et al. (23) developed the way to utilize the waste vegetable oil as a diesel fuel by investigating the combustion characteristics of waste vegetable oil methyl ester. They pointed out that the exhaust gas emissions from the waste vegetable oil methyl ester were acceptable and smoke emission was lower than that of the JIS No. 2 diesel fuel. Eiji Kinoshita et al. (24) determined the usefulness of palm oil biodiesel as alternative diesel fuel. They showed that the ignition ability of palm oil methyl ester was better than that of JIS No.2 diesel fuel. And also they found the NOx and smoke emissions from palm oil methyl ester were lower than those of JIS No.2 diesel fuel.

The above mentioned references expressed the advantages of biodiesel usages. However, there are some problems related with the biodiesel usages. Most of the research reports expressed that biodiesels produce 10% to 15% higher oxides of nitrogen (NOx) compare to diesel fuel when fueling with 100% biodiesel. Some of reports on the defects of biodiesel are given below.

Mittelbach and Trillhart (21) in their tests with methyl esters of frying oil found that the level of NOx was high due to the high combustion temperature. This high temperature was attributed to the high oxygen content of the ester fuel. However, all other emissions, including polycyclic aromatic hydrocarbons (PAH), were low. Also Eiji Kinoshita et al. (24) reported that the lower air-fuel ratio of rapeseed oil methyl ester compared to diesel fuel caused less air amount for combustion and resulting higher combustion temperature and higher NOx emission.

Clark et al (25) found that the viscosity of the lubricating oil decreased continuously with engine operation during the 200 hour durability test suggesting that the esters caused some amount of dilution. The same problem was also observed by Wagner et al. (19).

Peterson et al. (15) found that the ethyl ester of rapeseed oil produced the same amount of injector coking as diesel fuel while methyl esters of the oil produced slightly higher amounts. The viscosities of these two ester types (methyl and ethyl) were approximately twice that of the diesel No.2 fuel. Goodrum et al. (26) also investigated fuel injector tip deposits with tricaprylin (C:8), tributryin (C4:0) and peanut oil. The coking indices, derived from pixel counts of a photo

image were 0.77, 0.56 and 1.26 respectively compared to diesel No.2 fuel which was given an index of 1.00. Therefore, one could deduce that the shorter chained fatty acids have a lesser tendency to coke than longer chain fatty acids.

Schumacher et al. (16) found that the use of methyl soyate caused rapid deterioration of components of the fuel system made of rubber. This may be of concern when biodiesel fuels are used in current vehicles and power systems.

Apart from some minor technical problem, biodiesel is offering potentially viable alternative fuel for petroleum based diesel fuels.

1.2.3 Biodiesel and Fatty Acid Composition

Since biodiesel is produced from vegetable oils and animal fats, the properties of finished biodiesel depend mainly on the feedstock. On the other hand, the main components of vegetable oils and animal fats are fatty acids and therefore fatty acid compositions influence the properties of biodiesel. These properties are both physical and chemical properties, including the fuel properties (cetene number, viscosity, density, bulk modulus and pour point), combustion characteristics (fuel injection timing, ignition delay and ignition timing) and exhaust emissions (HC, CO, NOx and smoke). The effects of fatty acid composition on biodiesels were studied by researchers [Gerhard Knothe et al., (27), Gerhard Knothe and Kevin R Steidley (28), M. S. Graboski and R. L. McCormick (29), Koji Yamane et al., (30)].

Gerhard Knothe et al. (27) pointed out that biodiesel from vegetable oils with high amounts of saturated fatty acids (low iodine numbers) will have a higher cetane number while the low-temperature properties are poor. But biodiesel from vegetable oils with high amounts of unsaturated fatty acids (high iodine numbers) will have low cetane number while the low-temperature properties are better. Gerhard Knothe and Kevin R Steidley (28) investigated the kinematic viscosity of numerous fatty acid compounds which mainly contain in biodiesel. They found that the kinematic viscosity of fatty compounds is significantly influenced by compound structure and influencing factors are chain length, position, number and nature of double bonds, as well as nature of oxygenated moieties.

M. S. Graboski and R. L. McCormick (29) expressed in their paper that the chemical composition of fat and oil esters is dependent upon the length and degree of unsaturation of the fatty alkyl chains. Also they stated that the cetane number of fatty acid increases with the chain length, decrease with number of double bound and carbonyl groups move toward the center of the chain. Koji Yamane et al. (30) carried out a study in order to investigate the effect of fatty acid methyl ester content on the peroxide value and acid value of biodiesel. Base on their investigation they reported that polyunsaturated fatty acid methyl ester, such as linolenic acid methyl (C18:3) can be oxidized easier than linoleic acid methyl (C18:2) and oleic acid methyl (18:1).

By reviewing these literatures on fatty acid composition on biodiesel, most of the researches were emphasis on the fuel properties of biodiesel such as viscosity, pour point, cetane number and oxidation stability. However, the researches related to the effect of fatty acid composition on the combustion characteristics of biodiesel are rare. Therefore more researches are required to understand the effect of fatty acid composition on the combustion characteristics of biodiesel.

1.3 Objectives

To clearly understand the effect of fatty acid composition on the combustion characteristics of biodiesel, it is required to know the diesel combustion characteristics of different fatty acids type biodiesels (saturated and unsaturated types) and also the combustion characteristics of single composition fatty acids which mainly contain in biodiesels.

Thus the specific objectives are decided based on these requirements and the objectives of this study are to:

(1) Determine the diesel combustion characteristics of saturated and unsaturated type vegetable oil methyl esters

(2) Determine the combustion characteristics of single composition of fatty acid methyl esters (FAMEs) and the effect of degree of unsaturation of FAMEs on combustion

(3) Determine the effect of fatty acid composition on the combustion characteristics of biodiesel

Additionally, to study the effect of FAME composition on fuel properties and exhaust emissions of biodiesel related with combustion characteristics is an objective. And also the development of the correlation between single composition of fatty acid and exhaust emissions of biodiesel are intended to investigate in this study.

1.4 Thesis Outline

In order to accomplish the objectives of this study, experiments were carried out on five kinds of vegetable oil methyl esters, five kinds of pure fatty acid methyl esters and three kind of unsaturated fatty acid methyl esters. Based on the volume of the experiments, the thesis is divided into six chapters. The outlines of each chapter are given as follows.

Chapter 1 expresses the introduction of today world energy demand and supply concern, environmental concern and about the importance of renewable energy resources. A brief explanation about diesel engines and fats and oils are consisted in the introduction. In literatures reviews section, the transesterification process, the uses of vegetable oil and biodiesel in diesel engine, and biodiesel and fatty acid composition are included. The objectives of this study are also expressed in this chapter.

Chapter 2 describes the experimental apparatus and procedures of the engine test experiments. The specifications of test engine, equipment and measurement devices are shown in this chapter. Also the detailed explanation of experimental procedure and, calculation and data analysis methods are expressed.

Chapter 3 examines the diesel combustion characteristics of various vegetable oil methyl esters. The annual production of vegetable oils, the explanation on the experimental used five kinds of vegetable oils, test fuel making processes and fuel properties comparison are given in this chapter. The experiments were carried out on a single cylinder direct injection diesel engine by fuelling five kinds of FAME type biodiesels and JIS No.2 diesel fuel. The FAME type biodiesels are coconut oil methyl ester (CME), palm oil methyl ester (PME), palm kernel oil methyl ester (PKME), rapeseed oil methyl ester (RME) and soybean oil methyl ester (SME). The discussions on engine experimental results based on the fatty acid composition of biodiesel, combustion characteristics and exhaust emissions are also expressed.

Chapter 4 reports the diesel combustion characteristics of single composition of fatty acid methyl esters. In this chapter, the introduction to influence of fatty acids on biodiesel and the types of fatty acids is included and the two experimental results on pure fatty acid methyl esters and unsaturated fatty

acid methyl ester are explained. The experiments were carried out on a single cylinder direct injection diesel engine by fuelling five kinds of pure FAMEs, three kinds of unsaturated FAME with different degree of unsaturation and JIS No.2 diesel fuel. Five kinds of pure FAMEs are methyl laurate, methyl myristate, methyl palmitate, methyl stearate and methyl oleate, and three kinds of unsaturated fatty acid methyl ester are high oleate safflower oil methyl ester ($SFME_{HO}$), high linoleate safflower oil methyl ester ($SFME_{HL}$) and linseed oil methyl ester (LME). Comparison of the experimental results and the effect of fatty acid composition on the fuel properties, combustion characteristics and exhaust emissions are discussed in detail.

Chapter 5 expresses the effect of fatty acid composition on the combustion characteristics of biodiesel. Detailed discussions on the experimental results of chapter 3 and 4 based on the experimental results concerning fuel properties, combustion characteristics and exhaust emissions of five kinds of FAME type biodiesels, five kinds of pure fatty acid methyl esters and three kinds of unsaturated FAME with different degree of unsaturation are included. Furthermore, from these experimental results, the assumptions were made for the emissions (HC, CO, NOx, smoke) of seven kinds of single composition of FAME (methyl laurate, methyl myristate, methyl palmitate, methyl stearate, methyl oleate, methyl linoleate, methyl linolenate). By fairly adjusting to coincide the assumption data of these single type FAMEs emissions and the experimental emission data (CME, PME, RME, SME, $SFME_{HO}$, $SFME_{HL}$ and LME), a correlation program was developed for estimation of exhaust emissions from biodiesels.

Chapter 6 describes the general conclusions of this study based on the implementation of the objectives.

2. EXPERIMENTAL APPARATUS AND PROCEDURES

In this chapter, the apparatus those were used in the experiments and the procedures followed in this study are described. The chapter is divided into four sections. These are experiment apparatus, procedures, calculations and analysis, and expressed in each section respectively.

2.1 Experimental Apparatus

2.1.1 Test Engine and Measurement Devices Set-up

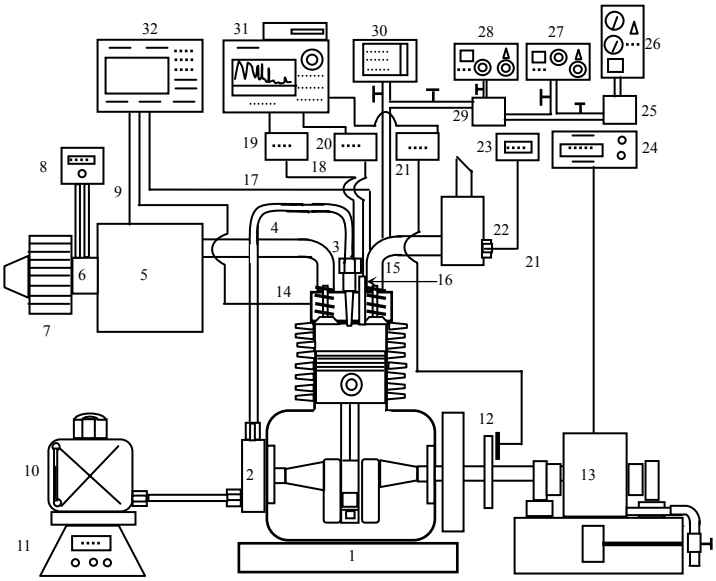

1. Engine
2. Fuel injection pump
3. Fuel injection nozzle
4. Intake manifold
5. Intake air surge tank
6. Air flow meter
7. Air cleaner
8. Digital manometer
9. Intake air temp sensor
10. Fuel tank
11. Digital weighting scale
12. Crank angle detector
13. Electric dynamometer
14. Coolant temp sensor
15. Exhaust manifold
16. Compression pressure transducer
17. Exhaust gas temp sensor
18. Injector needle lift sensor
19. Needle lift amplifier
20. Signal amplifier
21. Pulse amplifier
22. Air-fuel ratio sensor
23. A/F meter
24. Dynamometer control panel
25. Dehumidifier
26. HC meter
27. NOx meter
28. CO meter
29. Heater
30. Smoke meter
31. Digital scope recorder
32. Data recorder

Figure 2.1 Schematic diagram of experimental set-up

Figure 2.1 shows test engine and measurement devices set-up.

2.1.2 Test Engine

Test engine used in the experiments is a single cylinder direct injection diesel engine. It is a naturally aspirated water-cooled four stroke diesel engine.

Table 2.1 Test engine specifications

Type	Yanmar NF-19
Number of cylinders	1
Combustion chamber	Direct injection
Valve arrangement	OHV
No. of stroke per cycle	4
Cooling system	Water-cooled
Compression ratio	16.3
Bore×stroke	110mm×106mm
Stroke volume	1007cc
Max. power (at 2400rpm)	19ps (14kW)
Injection pump	Bosch type
Injection nozzle	4-Hole nozzle
Nozzle hole diameter	0.33mm
Injection timing	19 BTDC
Nozzle opening pressure	19.6 MPa

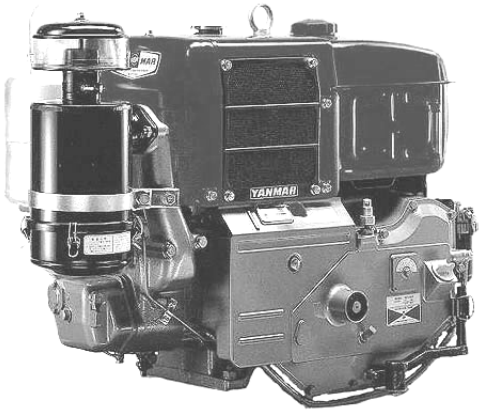

Figure 2.2 Test engine

The test engine's specifications are shown in Table 2.1 and the photograph is shown in Figure 2.2. The diagram of valve timing of test engine is shown in Figure 2.3. Also the injection nozzle of the test engine is shown in Figure 2.4.

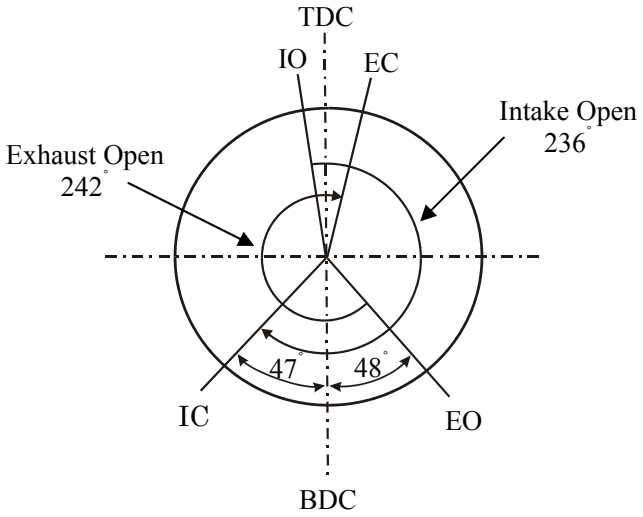

TDC: Top dead center, BDC: Bottom dead center

I: Intake, E: Exhaust, O: Open, C: Close

Figure 2.3 Valve timing of test engine

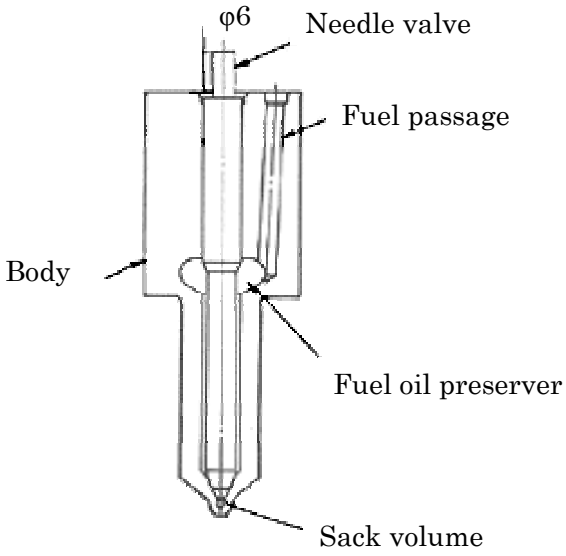

Figure 2.4 Injection nozzle of test engine

2.1.3 Electric Dynamometer

An electric dynamometer used in this study was a high speed type Eddy-current electro brake dynamometer. The specifications of dynamometer and expansion type controller unit are shown in Table 2.2 and Table 2.3.

Table 2.2 Electric dynamometer specifications

Type	EWS-100-L (Tokyo Meter Co., Ltd.)
Maximum absorbing power	100ps (73.5 kW)
Maximum revolution	13000 rpm
Maximum absorbing torque	235 Nm
Inertia of moment	0.034 J
Cooling water quantity	42 l/min
Supply water pressure	60 kPa
Automatic control	Constant rpm with boost control
Dynamo graph	Digital counter and load cell device
Speed sensor type	Electromagnetic

Table 2.3 Electric dynamometer expansion type controller specifications

Type	EDC-240-EB (Tokyo Meter Co., Ltd.)
Input signal	Speed signal 60P/R, load cell signal 2mv/v
Output signal	Speed (0~10V) F.S, Torque (0~10V) F.S
Control method	PID control method
Control mode	Constant speed control(ASR), constant speed control(ATR) Proportional control(APR), constant current control(ACR)
Input interlock	Cooling water(Pressure low and temp rise)
Output interlock	At abnormal C contact 1 point
Excite current	10A
Power source	AC100V or 200V

2.1.4 Inlet Air Measurement Devices

To determine the amount of inlet air that flowed into the engine, a laminar flow (LFE 50B) type air flow meter was used. The air flow meter was fitted between air cleaner and intake air surge tank. The specifications of air flow meter are given in Table 2.4.

In order to record the pressure differences between the two parts of air flow meter, a digital manometer was coupled with air flow meter in this study. The specifications of digital manometer are as shown in Table 2.5.

Table 2.4 Air flow meter specifications

Model	LFE 50B (Tsukasa soken Co., Ltd.)
Rated flow rate	0~50 l/s
Maximum flow rate	75 l/s
Rated pressure	0~60 mm Aq
Inner diameter	128 mm
Outer diameter	142 mm
Length	100 mm
Flange outer diameter	166 mm
Pipe connection size	φ51

Table 2.5 Digital manometer specifications

Model	DM 3300(Cosmo Instrument Co., Ltd.)
Allowance pressure	Up to 500 kPa
Accuracy	±0.15 % of F.S. ±1 digit
Rated pressure	0~50 mm Aq
Display digits	4 digits (0000 to± 9999)
Sampling time	250 ms
Power sources	100 VAC ±10 V 50/60 Hz 0.5 A

2.1.5 Fuel Consumption Measurement Devices

To calculate the break specific fuel consumption and fuel consumption gram per minute, a digital weighing scale and a stopwatch were used in this study. The specifications of digital weighing scale are shown in Table 2.6.

Table 2.6 Digital weighing scale specifications

Type	EB-6200 S (Shimadzu Co., Ltd.)
Capacity	0.1~6200 g
Standard deviation	0.1 g
Temperature drift	±5ppm/˚C
Indication renewal period	5 or 10 times per second
Power sources	100 VAC ±10 V 50/60 Hz 0.5 A

2.1.6 Temperature Measurements Devices

The temperatures of intake air, exhaust gas and engine coolant were measured in this study. The electronic siginal that from thermocouples fitted in intake air surge tank, exhaust manifold and radiator of the engine were connected to a portable hybrid recorder, and the temperatures of those points were recorded periodically. The portable hybrid recorder specifications are shown in Table 2.7.

Table 2.7 Portable hybrid recorder specifications

Type	YEW-3087(Yokokawa electric corporation)
Input signal	Thermocouple
Available channel	12 Nos.
Measurement ranges	Type K:-200~400˚C(range code 16)
	Type T: -200~400˚C(range code 16)
Voltage ranges	10,20,50,100,200,500mV, 1,2,5,10,20,50V
Input resistance	1MΩ constant on all voltage ranges
Power source	100 VAC

A T type thermocouple (Cu 55 %+Ni 45 %) was installed inside the intake air surge tank in order to measure intake air temperature. To measure the exhaust gas temperature, a K type chromel-alumel thermocouple (Ni 89%, Cr 10%, Al 1% and Ni 94%, Mn 2.5%, Al 2%, Si 1%) was fitted at the center of exhaust pipe and which was 50 mm apart from flange surface. Also a thermocouple (Cu 55 %+Ni 45 %) was set inside the radiator to measure the engine coolant temperature. The wires from thermocouples were connected with hybrid recorder and the electromotive forces from thermocouples were transformed to the temperature, ˚C. The temperatures of intake air system, exhaust system and radiator of the engine were recorded periodically. The position of thermocouple placed in exhaust pipe is shown in Figure 2.5 and dimensions are shown in Table 2.8.

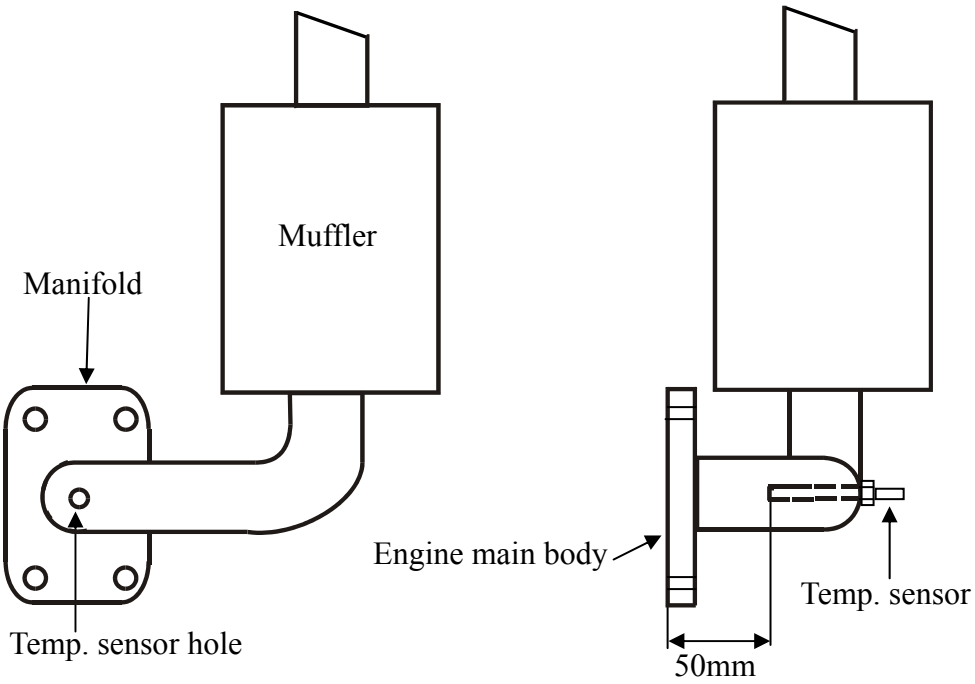

Figure 2.5 Thermocouple position in exhaust manifold

Table 2.8 K type thermocouple dimensions

Type	K type chromel-alumel thermocouple
Diameter	0.4 mm
Length	800 mm

2.1.7 Air Fuel Ratio Measurement Devices

In order to measure the air fuel ratio, an air fuel or oxygen sensor was installed at the center of exhaust muffler of the test engine. The output signal from air fuel sensor was sent to the air fuel ratio analyzer. Air fuel ratio, O_2 content and λ (excess air ratio) were measured in this study. The air fuel ratio analyzer specifications are shown in Table 2.9 and the place of air fuel ratio sensor in exhaust muffler is shown in Figure 2.6.

Table 2.9 Air fuel ratio analyzer specifications

Type	MEXA-110λ (Horiba Co., Ltd)
Measurement ranges	A/F 0.00~99.99(H/C=1.85, O/C=0.00)
	λ0.00-9.999(H/C=1.85, O/C=0.00)
	O_2: 0~25 vol%
Accuracy	±0.3 A/F when 9.5 A/F
	±0.1 A/F when 14.7 A/F
	±0.3 A/F when 20 A/F
Power source	AC100V 50/60Hz

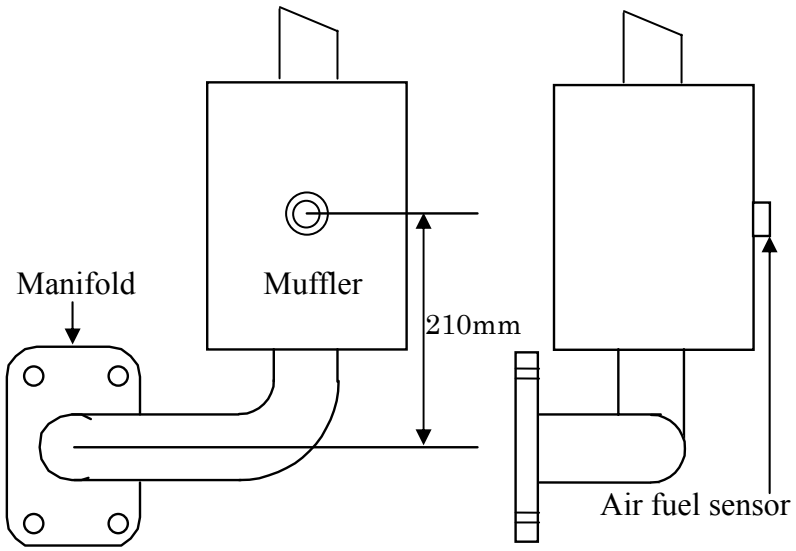

Figure 2.6 Position of air fuel ratio sensor in exhaust muffler

2.1.8 Combustion Characteristics Measurement Devices

In order to investigate the combustion characteristics, the fuel injection timing measurement, the combustion pressure measurement and the crank angle detection were carried out. Fuel injection timings were detected by lift amount of a needle valve of the fuel injection nozzle. To detect the lift amount of needle valve, a needle lift sensor was installed in the fuel injector nozzle. The needle lift sensor detects the lift amount of needle valve of the fuel injector nozzle and produces signal representing the lift amount. The output signal of the needle lift sensor was converted to rectangular wave form by mean of an amplifier to achieve the determined threshold level. Then the output amplified signal or rectangular wave from the amplifier was recorded by the digital scope recorder. The calculation of timing for fuel ignition was made by the basis of the rectangular wave in accordance with the crank angle or driving condition of the engine. The data conversion program was used for fuel injection timings related to the crank angles. A Zexel made needle lift sensor was used in this study and the position of sensor in the jet nozzle of the fuel injector is shown in Figure 2.7.

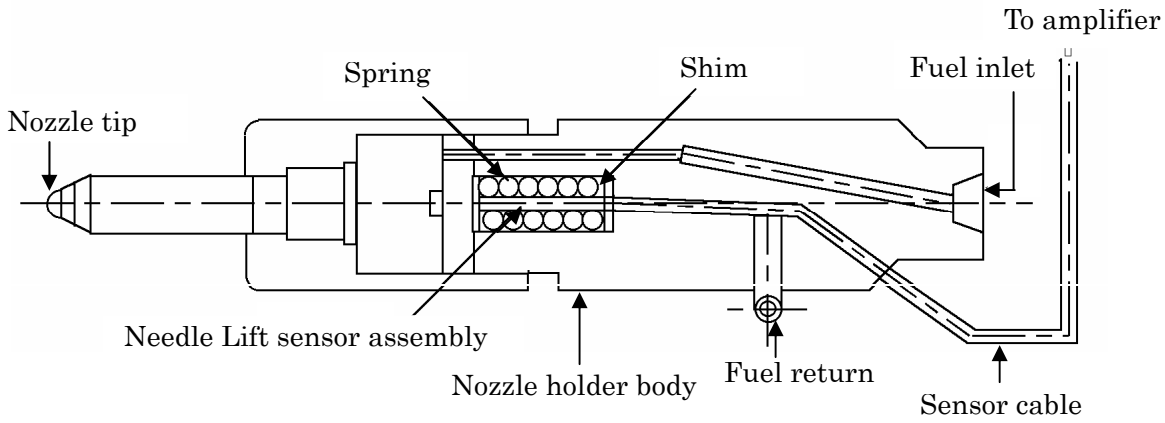

Figure 2.7 Needle lifter sensor installation position

Pressure measurement for ascertaining the combustion chamber pressure is necessary, in order to obtain in each instance imformation regarding prevailing in the combustion chamber of the engine. Information regarding the pressure prevailing in the combustion chamber in each instance is important for

monotoring the combustion. By mean of this information, it can trace combustion characteristics such as combustion start timing, ignition timing and combustion end timing from pressure history of the combustion chamber. Therefore, to measure the combustion chamber pressure of the test engine, a strain gage pressure tranducer was installed in the upper side of combustion chamber or engine head assembly. Strain gauge, which surve as the pressure detection element, fetures self-temperature- compasating gage developed by superior micro technology give minimal fluctuations in sensitivity minimal caused by temperature changes and zero-point fluctuations, enabling usage over a broad temperature range. To achieve the actual combustion pressure, the strain or minute mechanical changes occurred response to combustion pressure was traced and, signals detected by the pressure tranducer were sent to digital scope recorder through an amplifier. Photo and out line drawing of engine pressure tranducer are shown in Figure 2.8 and specifications are shown in Table 2.10. The position of pressure transducer unit in the engine head assembly is shown in Figure 2.9.

As expressed in the above paragraph, to investigate the combustion characteristics of the engine, the crank angle detection is one of the important works. On the other hand, to correctly determine the fuel injection timing and ignition timing, the accuracy of the rotational direction of crankshaft or crank angle is important. To detect the crank angle of the test engine, crank angle detector assembly (a slit disc and optical detector) was used in this study. Crank angle detector assembly was fitted on the crank shaft of the test engine. The out-

Table 2.10 Pressure sensor specifications

Type	PE-200KWS (Kyowa Electronic Instrument Co., Ltd)
Rated capacity	20 MPa
Non linearity	±1% RO
Hysteretic	±1% RO
Rated output	0.5 mV/V (1000×10^{-6} strain) or higher

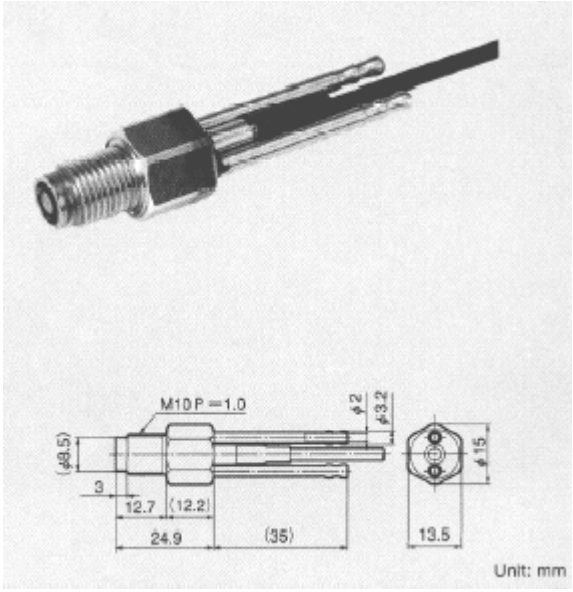

Figure 2.8 Photo and out line drawing of engine pressure tranducer

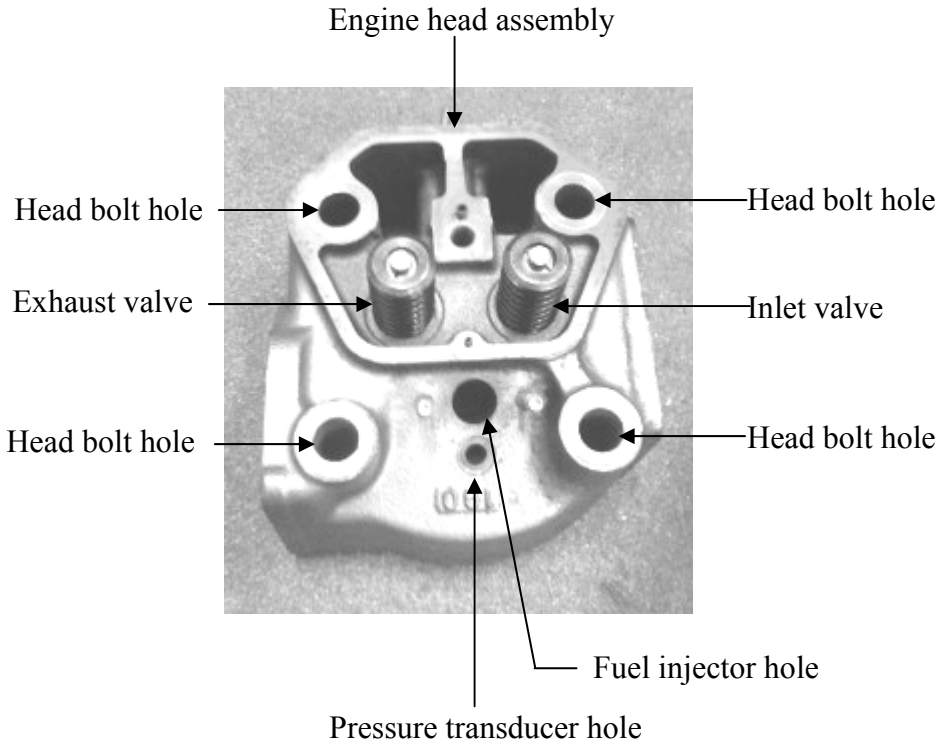

Figure 2.9 Position of pressure transducer in engine head assembly

Table 2.11 Crank angle detector assembly (Slit disc) specifications

Type	PP-010A (Ono Sokki Co., Ltd.)
Diameter	200 mm
Material	Acrylic
Speed range	0~6000 rpm
Slit disc thickness	0.5 mm

Table 2.12 Crank angle detector assembly (Optical detector) specifications

Type	PP 932 (Ono Sokki Co., Ltd.)
DC resistance	600~700Ω
Material	SUS 410
Weight	100 gm
Heat proof type	150˚C max

Table 2.13 Crank angle amplifier specifications

Type	PA-500 (Ono Sokki Co., Ltd.)
Output power supply	DC 65 ±5V, 1A
Input power supply	DC 12V, 0.1A
Load	10 kΩ
Input and output signal difference	< 2μs

put signal from crank angle detector assembly was sent to crank angle detector amplifier and then sent to digital scope recorder. The specifications crank angle detector assembly and amplifier are shown in Table 2.11, 2.12 and 2.13 respectively.

To record and save the data, a digital scope recorder was used in this study. The data of injector needle lift, compression pressure and crank angle were sampled at every crank angles and average on 50 cycles were recorded. There are two types of files recorded in the hard disk of the digital scope recorder, they are HDR and WVF. The specification of digital scope recorder is shown in Table 2.14.

Table 2.14 Digital scope recorder specifications

Type	DL 750 (Yokogawa Electric Corporation)
Channel available	64 CH
Input impedance	1 MΩ±1.0%
Logic input	16 bit (8 bit×2)
Max. sampling rate	10MS/s
Max. record length	50MW
Bandwidth	3MW
Internal HDD	40 GB (optional)
Power source	AC100V 50/60Hz

2.1.9 Exhaust Gas Emissions Measurements Devices

In this study, hydrocarbon (HC), carbon monoxide (CO), nitrogen oxides (NOx) and smoke emissions from the exhaust gas of the test engine were measured. Exhaust gas was sampled from exhaust pipe of the test engine. The position of exhaust gas sampling pipe is shown in Figure 2.10.

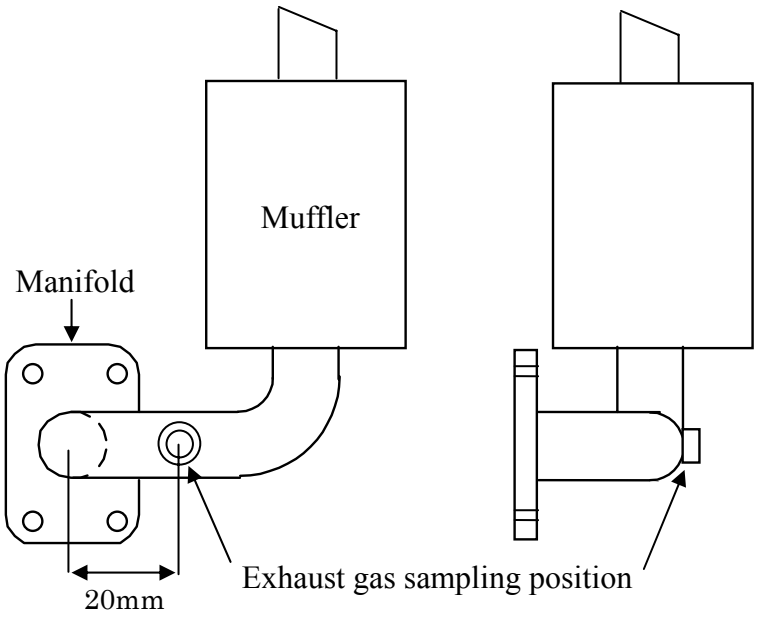

Figure 2.10 Exhaust gas sample position

The HC emission from the test engine was measured by a flame ionization detector type HC analyzer. The exhaust gas from the test engine was piped to the filter, dehumidifier and the dehumidified exhaust gas was sent to the HC analyzer. The HC analyzer specifications are shown in Table 2.15.

The CO emission of the test engine was measured by a non-dispersive infrared detector type CO analyzer. Before entering the CO analyzer, the exhaust gas from test engine was heated by a heater and pass through a filter. The CO analyzer specifications are shown in Table 2.16.

Table 2.15 HC analyzer specifications

Model	HCM-1B (Shimadzu Corporation)
Measuring component	Total hydro carbon
Measurement method	Flame ionization detection method
Measurement ranges	1,5,10,50,100,500,1000,5000,10000 ppm C
Accuracy	±1.0%
Response speed	Less than 2 Sec.
Required gas	Hydrogen and standard gas(for span setting)
Hydrogen consumption rate	About 50 ml/min
Power source	AC100 V 50/60 Hz

Table 2.16 CO analyzer specifications

Model	BCO-511 (Best Instrument Co., Ltd.)
Measuring component	Carbon monoxide (CO)
Measuring principle	Non-dispersive infrared detection method
Measurement ranges	1~2000, 5000 ppm
Calibrating period	Within 4 Hours
Required gas	standard gas(for span setting)
Noise	Less than ± 1.0 %FS
Power source	AC100 V 50/60 Hz

The NOx emission from the test engine was measured by chemical luminescent detector type NOx analyzer. Sample exhaust gases taken from exhaust pipe of the test engine were passed through a filter and then entered to the NOx analyzer. The NOx analyzer specifications are shown in Table 2.17.

Also the smoke emission from the test engine was measured in this study. In order to measure smoke emission, an opacity type smoke meter was used. The exhaust gas from the test engine was connected to the smoke meter and recorded the smoke emission. The smoke meter specification is shown in Table 2.18.

Table 2.17 NOx analyzer specifications

Model	BCL-611(Best Instrument Co., Ltd.)
Measuring component	Nitrogen oxides (NOx)
Measuring principle	Chemical luminescent detection method
Measurement ranges	0~50,100,250,500,1000, 2000 ppm
Calibrating period	Within 4 Hours
Reproducibility	Less than ± 1.0 %FS
Required gas	standard gas(for span setting)
Noise	Less than ± 1.0 %FS
Power source	AC100 V 50/60 Hz

Table 2.18 Smoke meter specifications

Model	MEXA-130S(Horiba Co., Ltd)
Measuring component	Smoke from diesel engine
Measuring principle	Opacity method
Measurement ranges	Opacity 0-100%
	K value 0-10.00 1/m
Sampling method	Partial flow
Input/output	Digital
Power source	AC100 V 50/60 Hz

2.2 Experimental Procedures

Before starting the engine experiments, the fuel tank, engine oil level, coolant and other proper conditions of the test engine were checked. And the test engine was started by lower engine speed (1000 rpm) until achieving the stable idling condition. Then the engine speed was increased gradually up to 2000 rpm. At the same time, the dynamometer, all analyzers and meters for measurements were switched on and the proper preparations and settings for measurements were carried out as the recommended methods by the makers' instruction manuals. When the test engine got stable condition and preparations and settings for the measurements were finished the experiments were started. The type of experiment is a study state engine test. The applications of loads were five levels and they were 0%, 25%, 50%, 75% and 100% loads respectively. The engine speeds at all load levels were adjusted for constant engine speed and fixed at 2000 rpm. In each load levels, the measurements of intake air, fuel consumption, intake air temperature, exhaust gas temperature, engine coolant temperature, air fuel ratio, fuel injection timing, combustion pressure, crank angle, hydrocarbon (HC) emission, carbon monoxide (CO) emission, nitrogen oxides (NOx) emission and smoke emission were carried out and recorded the data. The same conditions, methods and procedures were used for both the experiments of biodiesel and diesel fuels. After the engine experiments for all kinds of fuels were finished, the experimental data calculation and the analysis were done. The calculation and analysis methods are expressed detail in next sections.

2.3 Calculation Procedures

2.3.1 Brake Power Calculation

The brake power of the test engine was calculated for every load levels. The equation for brake power calculation is as follow:

$$L = \frac{M \times n}{33330} \qquad \text{(kW)}$$

where:

L= brake power (kW)

M = electric dynamometer braking load (N)

n = engine speed (rpm)

2.3.2 Brake Mean Effective Pressure Calculation

The brake mean effective pressure of the test engine was calculated for every load levels. The equation of brake mean effective pressure is as follow:

$$P_{me} = \frac{2 \times L \times 60 \times 1000}{n \times V} \qquad \text{(MPa)}$$

where:

P_{me}= brake mean effective pressure

L = brake power (kW)

n = engine speed (rpm)

V= stroke volume (cm^3)

2.3.3 Fuel Consumption Calculation

The fuel consumption of the test engine was calculated for each load levels.

The equation of fuel consumption rate is as follow:

$$B = NT \times 60 \qquad \text{(g/h)}$$

where:

B=fuel consumption rate (g/h)

NT = Fuel consumption per minute (g/min)

The fuel consumption rate of the test engine was calculated in every load levels. The equation of fuel consumption rate is as follow:

$$b_e = \frac{B}{3.6 \times L} \qquad \text{(g/MW.s)}$$

where:

b_e=fuel consumption rate (g/MW.s)

B= fuel consumption (g/h)

L= brake power (kW)

2.3.4 Volumetric Efficiency Calculation

The volumetric efficiency of the test engine was calculated at all load levels. The equation of volumetric efficiency is as follow:

$$\eta_v = \frac{Qi}{Q_{th}} \times 100 \quad (\%)$$

$$Q_{th} = \frac{V \times n}{2 \times 1000} \quad (\lambda/\text{min})$$

Qi = 0.700 x 60 x ΔP x C (λ/min)

$$C = \frac{380 + t_1}{400} \times \left(\frac{293}{273 + t_1} \right)^{3/2}$$

where:

η_v = volumetric efficiency (%)

Q_{th} =theoretical air charge (*l*/min)

Qi =air charge (*l*/min)

ΔP =differential pressure of laminar flow meter (mmHg)

C =volume compensation coefficient depended on the temperature

t_1 =atmospheric temperature (^{O}C)

V= stroke volume (cm^3)

n = engine speed (rpm)

2.3.5 Charging Efficiency Calculation

The charging efficiency of the test engine was calculated for each load levels. The equation for charging efficiency is as follow:

$$\eta_c = \eta_v \times \frac{\rho_a}{\rho_{20}} \quad (\%)$$

$$\rho_a = \rho_{20} \times \frac{293}{273 + t_2} \times \frac{H_{20}}{760}$$

$$H_{20} = \frac{H}{1 + 0.0001627(t_2 - 20)}$$

where:

η_c = charging efficiency (%)

η_v = volumetric efficiency (%)

ρ_a =: air density in a suction surge tank (kg/m^3)

ρ_{20} = air density in 760mmHg 20 ^{0}C (kg/m^3)

H_{20} = atmospheric pressure in 760 mmHg at 20 ^{0}C (mmHg)

H = atmospheric pressure (mmHg)

t_2 = aspiration temperature (temperature in a surge tank) (^{0}C)

2.3.6 Suction Air Quantity Calculation

The suction air quantity of the test engine was calculated for all load levels. The equation of suction air quantity is as follow:

$$G_a = \frac{Q \times \rho_a}{60} \qquad (g/s)$$

where:

G_a=suction air quantity (g/s)

Q= air charge (l/min)

ρ_a =air density in a suction surge tank (kg/m^3)

2.3.7 Brake Thermal Efficiency Calculation

The brake thermal efficiency of the test engine was calculated at every load levels. The equation of brake thermal efficiency is as follow:

$$\eta_e = \frac{1000}{Hl \times b_e} \times 100 \qquad (\%)$$

where

η_e =brake thermal efficiency

Hl=low calorific value of fuel

b_e=fuel consumption rate

2.4 Analysis

2.4.1 Combustion Chamber Pressure Analytical Method

Motoring of the test engine was taken in order to derive a pressure curve related to combustion chamber pressure of the test engine and the output data of the digital scope recorder. A pressure transducer was installed in one side of the compression pressure tester. The compression pressure tester was fitted in the injector hole of the test engine and the combustion chamber pressure was adjusted from 1.078MPa to 8.918Mpa by increasing 0.98MPa in each step. The data from pressure transducer was recorded in the digital scope recorder. The recorded data were copied to the computer and plotted combustion chamber pressure vs. data point graph. Base on this graph, an equation or function was derived to satisfy the relation between the combustion chamber pressure and the data point. But the data point can vary within the motoring and actual experiment because of the combustion temperature difference. Therefore, when carried out motoring of the test engine, select 10 points between the crank angles from -60˚ to -51˚ after top death center for standardization of compression pressure. The equation or function of standard pressure and. data is expressed as follow and the graph is shown in Figure 2.11.

$$P = 2.0 \times 10^{-4} \cdot Y - 0.879 \times 10^{-1}$$

where:

P : compression pressure (MPa)

Y : Data Point (the data of Y axis reading in digital scope recorder)

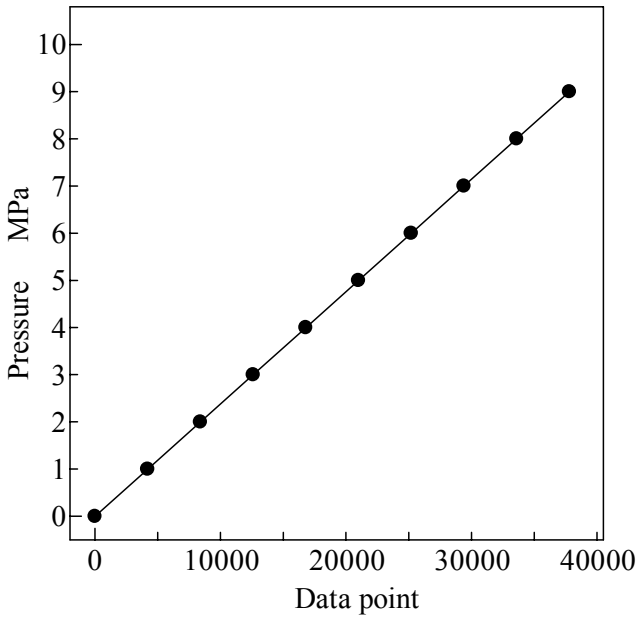

Figure 2.11 Pressure indicator of combustion chamber

From this relation the combustion chamber pressure analysis of the test engine were carried out. Figure 2.12 shows combustion chamber pressure related to the crank angle.

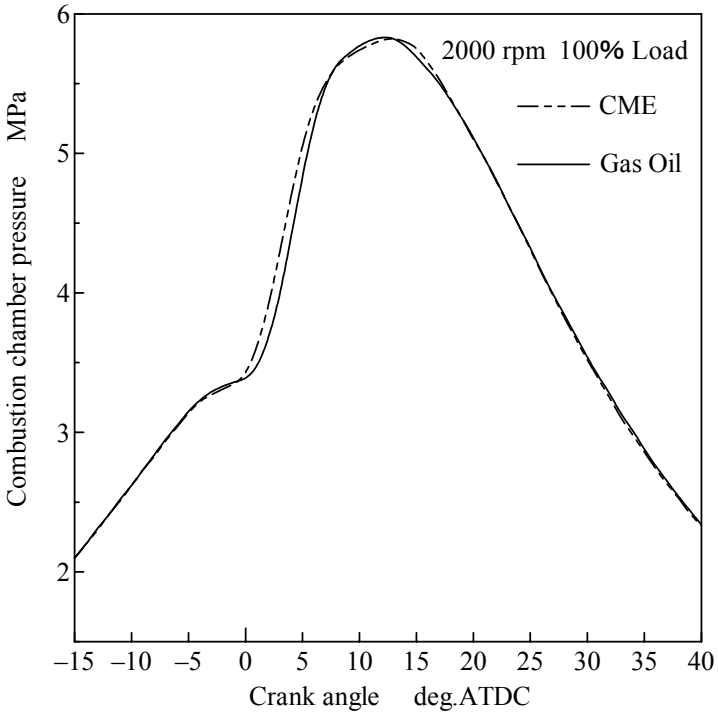

Figure 2.12 Combustion chamber pressure related to crank angle

2.4.2 Heat Release Rate Analytical Method

To understand the combustion and to make comparisons between diesel fuel and biodiesel, heat release rate analysis was conducted. The basic heat release rate calculation used in this study included three assumptions. The first is that the charge air-fuel mixture inside the combustion chamber behaves as an ideal gas. The second is that the charge in the cylinder is a uniform single zone of constant composition from the intake valve closing to the exhaust valve opening. And the last one is that the energy released due to fuel consumption is due to fuel combustion can be considered as a heat addition to the combustion chamber. When the first law of thermodynamics was applied to this system, Equation 2.1 and 2.2 can be written as follow:

$$dQ = dU + PdV \tag{2.1}$$

Alternatively, the heat capacity per crank angle is given by

$$\frac{dQ}{d\theta} = \frac{dU}{d\theta} + P\frac{dV}{d\theta} \tag{2.2}$$

If the gas in a cylinder is considered to be ideal gas, the internal energy is

$$dU = mC_v dT$$
$$C_v = \frac{R}{\kappa - 1} \tag{2.3}$$

then, substitute in equation 2,

$$\frac{dQ}{d\theta} = \frac{mR}{\kappa - 1}\frac{dT}{d\theta} + P\frac{dV}{d\theta} \tag{2.4}$$

substituting the ideal gas equation (PV = mRT),

$$V \cdot dP + P \cdot dV = m \cdot R \cdot dT \tag{2.5}$$

therefore,

$$\frac{dQ}{d\theta} = \frac{1}{\kappa - 1}\left(V \cdot \frac{dP}{d\theta} + \kappa P\frac{dV}{d\theta}\right) \tag{2.6}$$

where:

C_v : Specific heat at constant volume

Q : Heat

R : Gas constant number

T : Absolute temperature

κ : Specific heat ratio of gas

V : Cylinder volume

P : Cylinder pressure

θ : Crank angle

m : Mass of gas

U : Internal energy

While, cylinder volume per crank angle dV/d θ can be derived from the following equation.

$$V = V_c + A \cdot r\left[1 - cos\left(\frac{\pi\theta}{180}\right) + \frac{1}{\lambda}\left\{1 - \sqrt{1 - \lambda^2\, sin^2\left(\frac{\pi\theta}{180}\right)}\right\}\right]$$

$$\frac{dV}{d\theta} = \left(\frac{\pi A}{180}\right) \times r\left\{sin\left(\frac{\pi\theta}{180}\right) + \frac{\lambda\, sin^2\left(\frac{\pi\theta}{180}\right)}{2\sqrt{1 - \lambda^2\, sin^2\left(\frac{\pi\theta}{180}\right)}}\right\} \qquad (2.7)$$

$$\lambda = \frac{l}{r}$$

where

l : Connecting rod length

r : Crank radius

V_c : Clearance volume

A : Cross-section area of a piston

The example of heat release rate related to the crank angle is shown in Figure 2.13. From this figure, the combustion start timing, the trend of heat release rate and the combustion end timing against the crank angle can be seen.

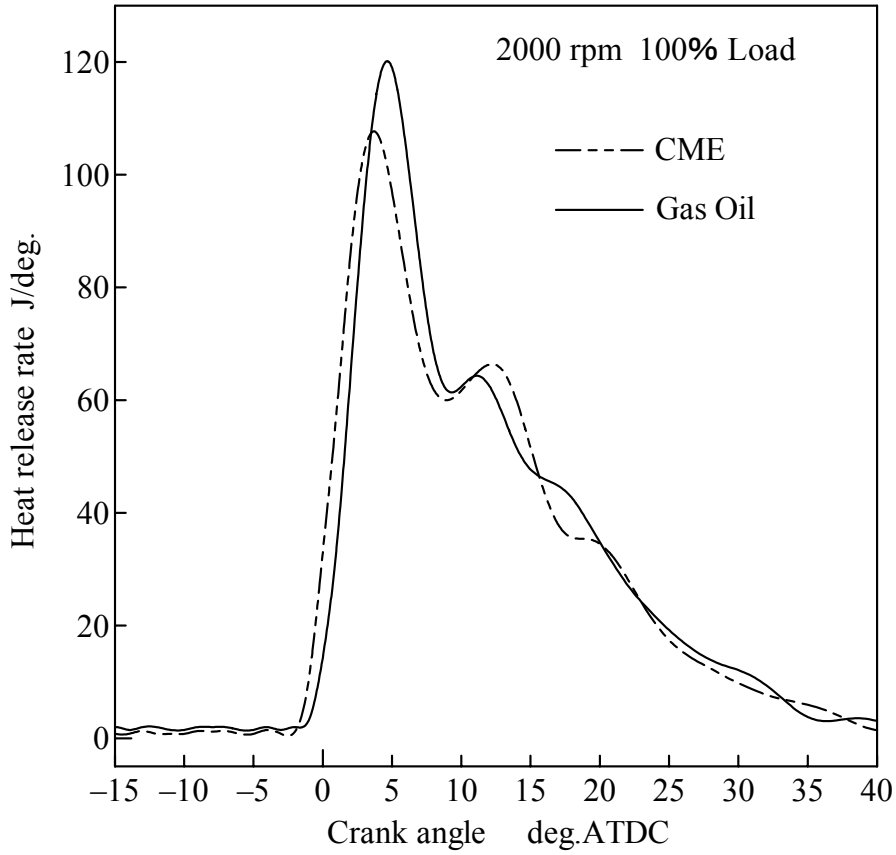

Figure 2.13 Heat release rate related to crank angle

2.4.3 Needle Lift Analytical Method

To determine the injection timing such as start and end of fuel injection of the injector of the test engine and to compare between diesel fuel and biodiesel, needle lift analysis was conducted. The start and end of fuel injection were analyzed from the lift of the needle. The needle lift data gives the real needle opening, so it is reliable and accurate. Example of needle lift is given in Figure 2.14. In Figure 2.14 needle lift data are presented in volts per crank angle degree for coconut oil biodiesel (CME) and JIS No.2 diesel fuel. Since these data are

used only for determination of the start and end of the fuel injection, and the actual needle movement corresponding to a certain voltage or signal level is not needed.

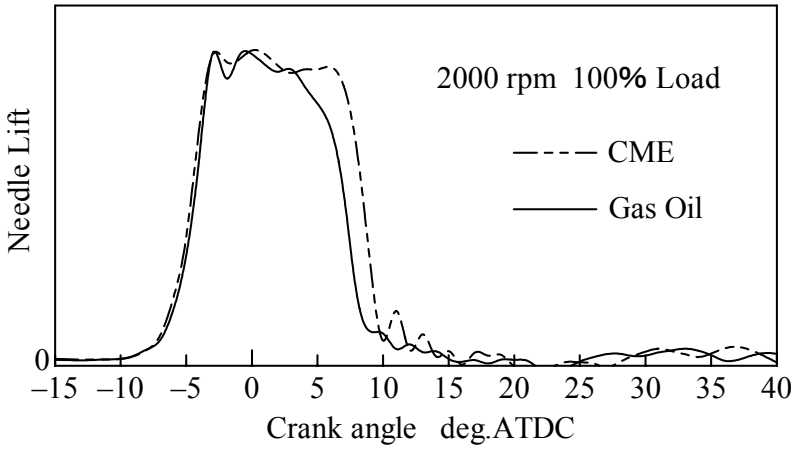

Figure 2.14 Needle lift vs. crank angle

2.4.4 Analytical Program

The fuel injection timing, the combustion chamber pressure and the crank angle of the test engine were analyzed by a program. The program used for analysis was a data conversion program. The signal from needle lift sensor, pressure transducer and crank angle detector were recorded as binary data by the digital scope recorder. They were HRD and WVF type files and then converted to text data. From these data the injection timing, the pressure of combustion chamber and rate of heat release of the test engine in every crank angles were calculated. However, the data often contains high amplitude oscillations or noises. These oscillations make significant impact on analysis and even small oscillations in the data lead to significant errors in analysis. Therefore, in order to reduce the errors in analysis, the data smoothing was done by using low pass digital filter. Figure 2.15 and 2.16 show the combustion pressure (100% load level) of JIS No. 2 diesel fuel before and after passing the low pass digital filter. The flow diagram of the data conversion program is shown in Figure 2.17.

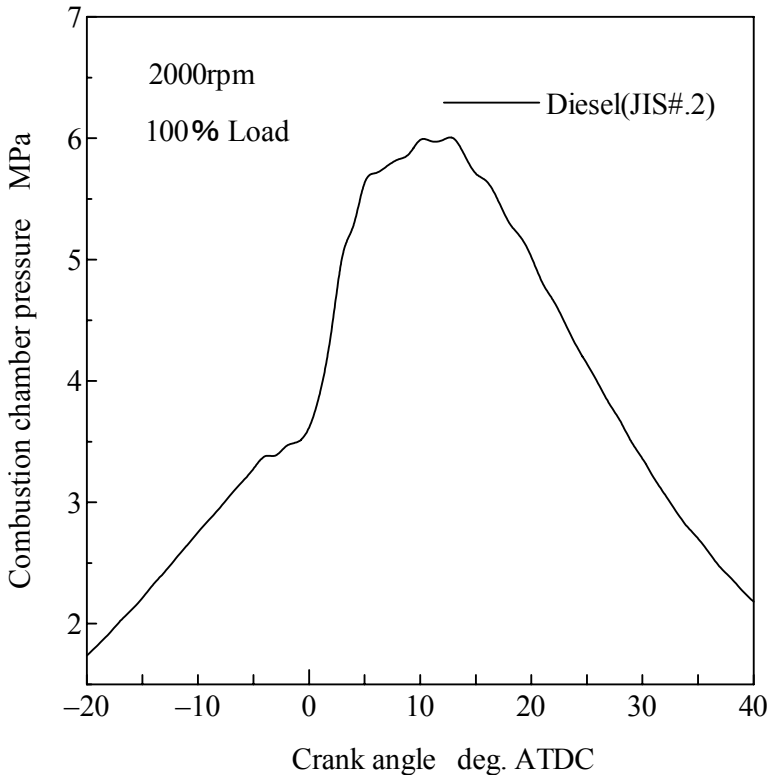

Figure 2.15 Combustion chamber pressure before low pass digital filter

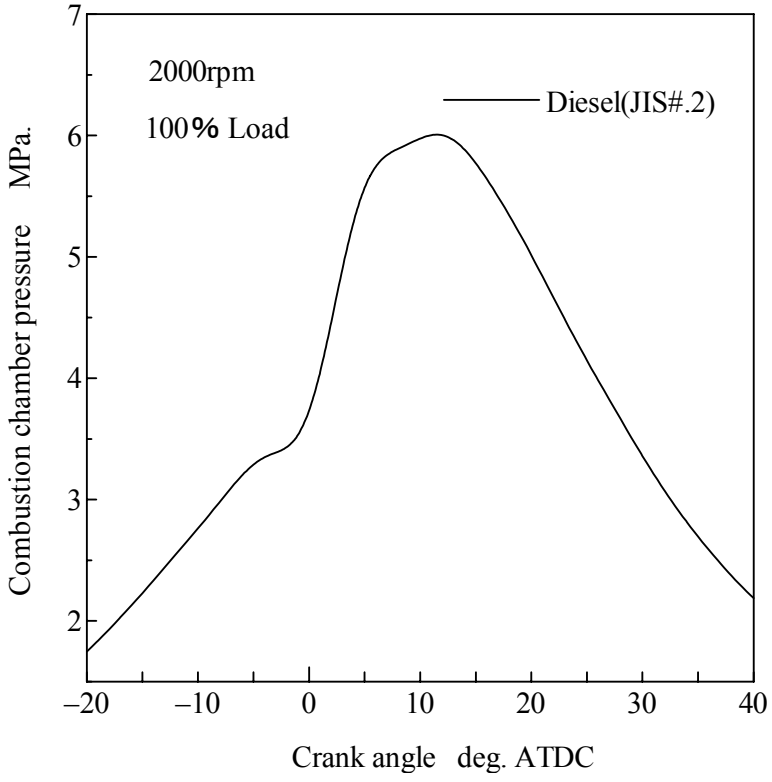

Figure 2.16 Combustion chamber pressure after low pass digital filter

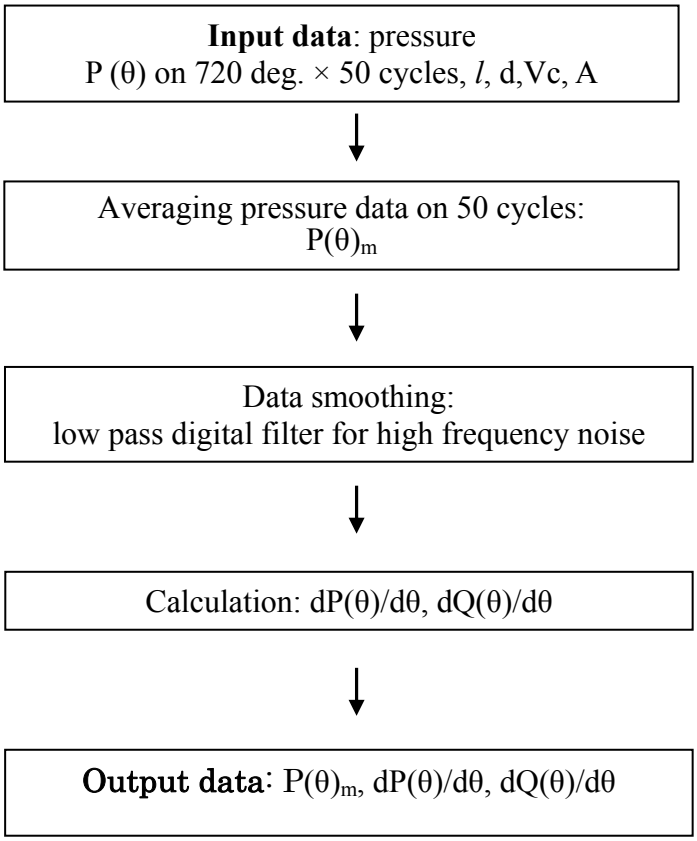

where

l : Stroke length

d: piston diameter

V_c : Clearance volume

A : Cross-section area of a piston

Figure 2.17 Flow diagram of the data conversion program

3. DIESEL COMBUSTION CHARACTERISTICS OF VEGETABLE OIL METHYL ESTERS

3.1 Introduction

Biodiesel can be derived from food grade vegetable oils or edible oils, nonfood grade vegetable oils or inedible oil, animal fats and waste or used vegetable oils. The most common types of biodiesel fuels are methyl, ethyl and butyl esters produced by means of the transesterification of vegetable oils. Therefore, the most promising applications way of vegetable oils as biodiesel fuels, can be termed as the ester of vegetable oils. Depending on the abundantly availability of feedstock in local region, the different feedstocks have been focused for biodiesel production. Consequently, in the United States, the primary sources for biodiesel production is soy bean oil while EU nations prefer to utilize rapeseed oil and in South East Asia regions, palm oil and coconut oil are promising for biodiesel productions. Global annual productions of major vegetable oils (31) are as shown in table 3.1.

Generally, most of vegetable oils contain fatty acids usually with the carbon numbers ranging from C6 to C18. Some of these fatty acids are saturated, while the others are unsaturated. It is expected that, the fatty acid composition and differing levels of saturation of the origins or vegetable oils may affect on the fuel properties and combustion characteristics of biodiesels.

Table 3.1 Global productions of major vegetable oils (31)

Year	2003/04	2004/05	2005/06
Soy bean oil	30859	32857	34822
Palm oil	29877	33328	35260
Rapeseed oil	14381	15734	17665
Sunflower oil	9602	9399	10540
Palm kernel oil	3472	3941	4112
Coconut oil	3135	3162	3283

(unit: 1000Mt.ton)

3.2 Vegetable Oils

Brief explanations on the fatty acid composition, productivity and annual production of vegetable oils used in this study are as follows.

3.2.1 Coconut oil

Coconut oil from coconut palm (*Cocus nucifera*) contains larger amount of saturated fatty acids with small carbon numbers such as lauric acid and myristic acid. Over 90% of its fatty acids composition is saturated fatty acids. The fatty acid composition of coconut oil is shown in Table 3.2. The productivity of coconut oil is 2260 kg oil/ha and it is the second most productivity among the vegetables oils. Annual production of coconut oil exceeds 3 million tons (Table 3.1) and produces mainly from Indonesia and the Philippines. Coconut oil has been considered as one of the feedstock for biodiesel fuel production in South East Asia countries.

3.2.2 Palm oil

Palm oil is produced from fleshy endosperm of the oil palm (*Elaies guinensis*). Palm oil contains mainly palmitic acid and oleic acid. About 52% saturated fatty acids and 47% unsaturated fatty acids include in palm oil. The fatty acid composition of palm oil is shown in Table 3.2. Annual production of palm oil is about 35 million tons in 2005/06 and which is the highest production compared to the others vegetable oils (Table 3.1). Also the productivity of palm oil is over 4000 kg oil/ha and it is the highest productivity among the vegetable oils. Oil palm grows in the tropical region of Asia, Africa and America and predominantly in Malaysia and Indonesia. Therefore, palm oil with highest production and productivity is a promising feedstock for biodiesel production especially in South East Asia regions.

3.2.3 Palm kernel oil

Palm kernel oil is produced from kernel of the oil palm. Annual production of palm kernel oil is about 4 million tons and increasing with the rising of palm oil production (Table 3.1). Although palm oil and palm kernel oil seemed similar, the

fatty acid compositions between them are so different. But the fatty acid composition of palm kernel oil is quite similar to that of coconut oil. Palm kernel oil contains larger amount of saturated fatty acids with small carbon numbers such as lauric acid and myristic acid. Over 80% of its fatty acids composition is saturated fatty acids. The fatty acid composition of palm kernel oil is shown in Table 3.2. By considering the annual production and fatty acid composition of palm kernel oil, it may also be a favorable feedstock for biodiesel production like coconut oil.

3.2.4 Rapeseed oil

Rapeseed oil is produced from rapeseed (Brassica napus or B. campestris). Rapeseed oil contains mainly unsaturated fatty acid such as oleic acid and linoleic acid. The fatty acid composition of rapeseed oil is expressed in Table 3.2. Over 90% of its fatty acid composition is unsaturated fatty acids. The production of rapeseed oil was about 17 million tons in 2005/6 (Table 3.1). It is grown mainly in Europe, China, India, Canada (where the canola varieties were developed) and Japan. Annual production of rapeseed oil is after soybean oil and palm oil, and the third largest production among the global annual vegetable oils. Rapeseed oil has been widely used for biodiesel fuel production in EU countries.

3.2.5 Soybean oil

Soybean oil is produced from soybean (*Glycine soja*). Soybean oil contains mainly unsaturated fatty acid such as linoleic acid and oleic acid. The fatty acid composition of soybean oil is expressed in Table 3.2. About 85% of its fatty acid composition is unsaturated fatty acids. The annual production of soybean oil is about 35 million tons in 2005/06 (Table 3.1). The production of soybean oil is second largest in vegetable oils. Soybean oil has been produced primarily in the United States, Brazil, Argentina and China. Because of high production, soybean oil is one of the promising candidates for biodiesel production. Today biodiesel produced from soybean oil is commercially available in some states in the United States.

Table 3.2 Fatty acid composition of vegetable oils (10)

Fatty acid	C:N	Vegetable oil, wt%				
		Coconut	Palm	Palm Kernel	Rapeseed	Soybean
Caproic	6:0	0.4	-	-	-	-
Caprylic	8:0	0.7	-	2.3	-	-
Capric	10:0	0.6	-	2.7	-	-
Lauric	12:0	47.5	0.3	44.1	-	-
Myristic	14:0	19.1	1.1	17.1	-	-
Palmitic	16:0	9.8	44.1	9.1	4.3	10.5
Palmitoleic	16:1	-	0.2	-	0.1	-
Stearic	18:0	3.8	4.5	2.6	1.9	3.8
Oleic	18:1	5.9	40.1	18.2	59.7	25
Linoleic	18:2	0.4	9.1	2.6	21.7	52.2
Linolenic	18:3	0.1	0.6	0.1	9.4	7.6
Gadoleic	20:1	-	-	-	1.5	0.3
Behenic	22:0	-	-	-	0.4	0.4
Erucic	22:1	-	-	-	0.6	-

3.3 Test fuels

In this study in order to investigate the combustion characteristics of saturated fatty acids type and unsaturated fatty acids type biodiesels, five kinds of vegetable oils were selected based on the saturated and unsaturated fatty acid compositions. These are coconut, palm and palm kernel oils which mostly contained saturated fatty acids and soybean oil and rapeseed oil which mostly contain unsaturated fatty acids. From these vegetable oils, the fatty acid methyl ester (FAME) type biodiesels such as coconut oil methyl ester (CME), palm oil methyl ester (PME), palm kernel oil methyl ester (PKME), soy bean oil methyl ester (SME) and rapeseed oil methyl ester (RME) were processed and used as test fuels for the engine experiments.

3.3.1 Coconut Oil Methyl Ester

Coconut oil was selected for this study and transesterified to coconut oil methyl ester (CME). CME was used as one of the test fuels in the engine experiments. In order to do transesterification reaction, the saponification value of coconut oil was carried out by titration. The saponification value of coconut oil was 252 mg/g. In transesterification reaction, the molar ratio of methanol to coconut oil was 6:1 and 1% mass of KOH to coconut oil was used. The reactions were taken for two hours at reaction temperature 60˚C. After the end of the reaction, the mixtures were kept at the ambient temperature 20- 25˚C for eight hours and then the settled glycerin layer was drained off. At last the residual methanol in methyl ester mixtures was evaporated. Then the finished product is coconut oil biodiesel or CME. The ester conversion rate of CME was over 95%. From fatty acid composition, CME can be said a saturated fatty acid type biodiesel. The FAME composition of CME measured by gas chromatograph and the properties of CME are expressed in table 3.3 and 3.4.

From the fuel properties of CME; the viscosity of was measured according to JIS K 2283 by using Redwood viscosity meter and Engler viscosity meter. The density was measured according to JIS K 2249 by using a hydrometer. The pour point was measured according to JIS K 2269 by using a rapid pour point tester. The carbon, hydrogen, oxygen contents were calculated from FAME composition

Table 3.3 FAME composition of CME

Fatty acid	C:N	Content (%)
Caprylic	8:0	6.0
Capric	10:0	4.9
Lauric	12:0	52.4
Myristic	14:0	16.9
Palmitic	16:0	8.6
Stearic	18:0	2.3
Oleic	18:1	6.5
Linoleic	18:2	1.4
Linolenic	18:3	0.3
Others	-	1.0

Table 3.4 Properties of CME

Properties		CME
Cetane number		57
Net calorific value	(MJ/kg)	35.22
Density@288K	(kg/m^3)	874
Kinematic viscosity@313K	(mm^2/sec)	2.7
Pour point	(˚C)	-5.0
C	(% mass)	73.2
H	(% mass)	12.3
O	(% mass)	14.5
Sulphur	(mass ppm)	2
Water	(% mass)	0.04
Potassium	(mg/kg)	<5.0
Methanol	(% mass)	<0.013
Monoglyceride	(% mass)	0.03
Diglyceride	(% mass)	0.15
Triglyceride	(% mass)	0.02
50% Distillation temperature	(˚C)	275
Stoichiometric air-fuel ratio		11.99

The monoglyceride, diglyceride, triglyceride and methanol contents in CME were analyzed by gas chromatography. The 50% distillation temperature was measured according to JIS K 2254. The net calorific value of CME was calculated by the carbon, hydrogen and oxygen contents and the calculation is as follow.

The equation of high calorific value is

$$Hh = 33900C + 142000\left(H - \frac{O}{8}\right)$$

From high calorific value, we can write low calorific value equation as

$$Hl = Hh - 2443 \times 9H$$

where: C=wt% of carbon content
H=wt% of hydrogen content
O=wt% of oxygen content

3.3.2 Palm Oil Methyl Ester

Transesterified palm oil, which is palm oil methyl ester (PME), was used as a test fuel in this study. The saponification value of palm oil was 199 mg/g and measured by titration method. From this value the amount of catalyst for transesterification reaction was calculated. In transesterification reaction, the molar ratio of methanol to palm oil was 6:1 and 1% mass of KOH to palm oil was used. The reactions were taken for two hours at reaction temperature 60˚C. After the end of the reaction, the mixtures were kept at the ambient temperature 20-25˚C for eight hours and then the settled glycerin layer was drained off. At last the residual methanol in methyl ester mixtures was evaporated. Then the finished product is palm oil biodiesel or PME. The ester conversion rate of PME was over 95%. The FAME composition measured by gas chromatograph and the properties of PME are expressed in table 3.5 and 3.6. The cetane number of PME is from reference 32. The carbon, hydrogen and oxygen contents were measured by analysis. The net calorific value of PME was measured according to JIS K 2279. The rest fuel properties of PME were measured the same method as those of CME.

Table 3.5 FAME composition of PME

FAME	C:N	Content (%)
Caprylic	8:0	-
Capric	10:0	-
Lauric	12:0	0.3
Myristic	14:0	1.1
Palmitic	16:0	48.8
Stearic	18:0	1.7
Oleic	18:1	38.4
Linoleic	18:2	9.1
Linolenic	18:3	0.5
Others	-	0.1

Table 3.6 Properties of PME

Properties		PME
Cetane number		64.5*
Net calorific value	(MJ/kg)	36.85
Density@288K	(kg/m^3)	879
Kinematic viscosity@313K	(mm^2/sec)	4.5
Pour point	(˚C)	12.5
C	(% mass)	75.6
H	(% mass)	12.9
O	(% mass)	11.5
Sulphur	(mass ppm)	2
Water	(% mass)	0.04
Potassium	(mg/kg)	<5.0
Methanol	(% mass)	<0.001
Monoglyceride	(% mass)	0.073
Diglyceride	(% mass)	0.178
Triglyceride	(% mass)	0.007
50% Distillation temperature	(˚C)	329
Stoichiometric air-fuel ratio		12.6

* from reference no.32

3.3.3 Palm Kernel Oil Methyl Ester

Palm kernel oil was used to process palm kernel oil methyl ester (PKME) in this study. PKME was prepared by transesterification reaction. In order to take transesterification reaction, the saponification value of palm kernel oil was carryout by titration. The saponification value of palm kernel oil was 243 mg/g. In transesterification reaction, the molar ratio of methanol to palm kernel oil was 6:1 and 1% mass of KOH to palm kernel oil was used. The reactions were taken for two hours at reaction temperature 60˚C. After the end of the reaction, the mixtures were kept at the ambient temperature 20- 25˚C for eight hours and then the settled glycerin layer was drained off. At last the residual methanol in methyl ester mixtures was evaporated. Then the finished product is palm kernel oil biodiesel or PKME. The ester conversion rate of PKME was over 95%. The FAME composition and properties of PKME are expressed in table 3.7 and 3.8. From FAME composition of PKME, it can be said that PKME is a saturated fatty acid type biodiesel. The cetane number of PKME was calculated from the composition of fatty acids and cetane number of fatty acids. The rest fuel properties of PKME were measured the same methods, analysis and calculation used those of CME.

Table 3.7 FAME composition of PKME

FAME	C:N	Content (%)
Caprylic	8:0	3.3
Capric	10:0	3.0
Lauric	12:0	50.8
Myristic	14:0	15.0
Palmitic	16:0	8.0
Stearic	18:0	2.1
Oleic	18:1	15.1
Linoleic	18:2	2.4
Linolenic	18:3	0.1
Others	-	0.2

Table 3.8 Properties of PKME

Properties		PKME
Cetane number		58
Net calorific value	(MJ/kg)	35.61
Density@288K	(kg/m^3)	877
Kinematic viscosity@313K	(mm^2/sec)	2.9
Pour point	(˚C)	-5.0
C	(% mass)	73.9
H	(% mass)	12.3
O	(% mass)	13.8
Sulphur	(mass ppm)	-
Water	(% mass)	0.03
Potassium	(mg/kg)	<5.0
Methanol	(% mass)	<0.001
Monoglyceride	(% mass)	0.39
Diglyceride	(% mass)	0.31
Triglyceride	(% mass)	0.04
50% Distillation temperature	(˚C)	273
Stoichiometric air-fuel ratio		12.1

3.3.4 Rapeseed Oil Methyl Ester

Rapeseed oil was used for rapeseed oil methyl ester (RME) processing in this study. RME was prepared by transesterification reaction. In order to take transesterification reaction, the saponification value of rapeseed oil was carryout by titration. The saponification value of rapeseed oil was 198 mg/g. In trans-esterification reaction, the molar ratio of methanol to rapeseed oil was 6:1 and 1% mass of KOH to rapeseed oil was used. The reactions were taken for two hours at reaction temperature 60˚C. After the end of the reaction, the mixtures were kept at the ambient temperature 20- 25˚C for eight hours and then the settled glycerin layer was drained off. Finally, the residual methanol in methyl ester mixtures was evaporated. Then the finished product is rapeseed oil biodiesel or RME. The ester

Table 3.9 FAME composition of RME

Fatty acid	C:N	Content (%)
Caprylic	8:0	-
Capric	10:0	-
Lauric	12:0	-
Myristic	14:0	-
Palmitic	16:0	4.5
Stearic	18:0	-
Oleic	18:1	63.8
Linoleic	18:2	19.8
Linolenic	18:3	10.4
Others	-	1.5

Table 3.10 Properties of RME

Properties		RME
Cetane number		54
Net calorific value	(MJ/kg)	36.55
Density@288K	(kg/m^3)	886
Kinematic viscosity@313K	(mm^2/sec)	4.5
Pour point	(^0C)	-7.5
C	(% mass)	77.6
H	(% mass)	11.9
O	(% mass)	10.5
Sulphur	(mass ppm)	6
Water	(% mass)	0.03
Potassium	(mg/kg)	<5.0
Methanol	(% mass)	<0.001
Monoglyceride	(% mass)	0.07
Diglyceride	(% mass)	0.17
Triglyceride	(% mass)	0.01
50% Distillation temperature	(^0C)	340
Stoichiometric air-fuel ratio		12.53

conversion rate of RME was over 95%. The FAME composition and properties of RME are expressed in table 3.9 and 3.10. From FAME composition of RME, it can be said that, RME is an unsaturated fatty acid type biodiesel. The cetane number of RME was measured by CFR engine. The carbon, hydrogen and oxygen contents were measured by analysis. The net calorific value of RME was measured according to JIS K 2279. The rest fuel properties of RME were measured the same methods, analysis and calculation used as those of CME.

3.3.5 Soybean Oil Methyl Ester

In this study, soybean oil was transesterified to make soybean oil methyl (SME). The saponification value of soybean oil is 191 mg/g and which was analyzed by titration. In transesterification reaction, the molar ratio of methanol to soybean oil was 6:1 and 1% mass of KOH to soy bean oil was used. The reaction was taken for two hours at reaction temperature 60˚C. After the end of the reaction, the mixture was kept at the ambient temperature 20- 25˚C for eight hours and then the settled glycerin layer was drained off. At last the residual methanol in methyl ester mixtures was evaporated. Then the finished product is soybean oil biodiesel

Table 3.11 FAME composition of SME

Fatty acid	C:N	Content (%)
Caprylic	8:0	-
Capric	10:0	-
Lauric	12:0	-
Myristic	14:0	0.4
Palmitic	16:0	10.6
Stearic	18:0	2.4
Oleic	18:1	23.5
Linoleic	18:2	51.2
Linolenic	18:3	8.5
Others	-	2.5

Table 3.12 Properties of SME

Properties		SME
Cetane number		-
Net calorific value	(MJ/kg)	38.22
Density@288K	(kg/m^3)	883
Kinematic viscosity@313K	(mm^2/sec)	6.63
Pour point	(^0C)	0
C	(% mass)	76.9
H	(% mass)	12.2
O	(% mass)	10.9
Sulphur	(mass ppm)	-
Water	(% mass)	0.03
Potassium	(mg/kg)	<5.0
Methanol	(% mass)	<0.001
Monoglyceride	(% mass)	0.083
Diglyceride	(% mass)	0.02
Triglyceride	(% mass)	0.018
50% Distillation temperature	(˚C)	329
Stoichiometric air-fuel ratio		12.47

or SME. The ester conversion rate of SME was over 95%. From FAME composition of soybean oil, SME can be said an unsaturated fatty acid type biodiesel. The FAME composition and properties of SME are expressed in table 3.11 and 3.12. The fuel properties of SME were measured the same methods, analysis and calculation used those of CME.

3.3.6 Diesel fuel

Diesel fuel (JIS No.2) was used as test fuel for comparison between biodiesel fuels and diesel fuel. The properties of diesel fuel are as shown in table 3.13.

Table 3.13 Properties of diesel fuel

Properties		Diesel
Cetane number		56
Net calorific value	(MJ/kg)	43.12
Density@288K	(kg/m^3)	832
Kinematic viscosity@313K	(mm^2/sec)	4.7
Pour point	(^0C)	-12.5
C	(% mass)	87.3
H	(% mass)	12.5
O	(% mass)	0
Sulphur	(mass ppm)	<50
Water	(% mass)	-
Potassium	(mg/kg)	-
50% Distillation temperature	(^0C)	278
Stoichiometric air-fuel ratio		14.2

3.4 Fuel Properties Comparison

The fuel properties of test fuels are expressed in Table 3.14. From Table 4.13 it can be said as follows. The cetane number of CME, PME and PKME are higher than the diesel fuel. But RME has lower cetane number. Generally, methyl ester fuels used in this study have suitable cetane numbers for diesel combustion process. The net calorific values of methyl ester fuels are about 15% lower than that of the diesel fuel. Comparing the net calorific values in methyl ester fuels, CME has lowest and SME has highest. From this fact, it can be said that the more oxygen content in methyl ester fuel makes the less net calorific value. Furthermore, less net calorific value make more fuel consumption for combustion. The densities of methyl ester fuels are higher than that of the diesel fuel. The density of CME is 874 kg/m^3 and it is lowest in the methyl ester fuels. The kinematics viscosities of methyl ester fuels are higher than that of the diesel fuel. The higher density and kinematics viscosity cause negative effects on the combustion process such as advance fuel injection timing and poor combustible mixture formation. But CME and PKME have lower kinematics viscosity compared to the other methyl ester fuels and their values are close to that of the diesel fuel. The pour points of all methyl ester fuels are higher than that of the diesel fuel. Among the methyl ester fuels, the pour point of RME is the lowest and PME is highest. One distinctive fuel property of methyl ester fuels is they contain oxygen more than 10%. The oxygen content of CME, PME, PKME, RME and SME are 14.5%, 11.5%, 13.8%, 10.5% and 10.8% respectively. Oxygen in fuel supports complete combustion process. The residual impurities of methyl ester fuels such as triglycerides, methanol and water in methyl ester fuels are very small and they are within the limits of ASTM and EU biodiesel standard. The 50% distillation temperatures of CME and PKME are lower than those of PME, RME and SME, and nearly the same as that of the diesel fuel. From the distillation temperatures of CME and PKME, it is expected that they have good volatility and fuel air mixture formation for combustion process, as diesel fuel. The stiochiometric air-fuel ratios of methyl ester fuels are lower than that of the diesel fuel. It means stiochiometric air amount in combustion of methyl ester fuel is less than that of the diesel fuel.

Table 3.14 Properties of test fuels

Properties		CME	PME	PKME	RME	SME	JIS#2
Cetane number		57	64.5[32]	58	54	-	56
Net calorific value	(MJ/kg)	35.22	36.85	35.61	36.55	38.22	43.12
Density@288K	(kg/m^3)	874	879	877	886	883	826
Kinematic viscosity@313K	(mm^2/sec)	2.7	4.5	2.9	4.5	4.1	2.5
Pour point	(^0C)	-5.0	12.5	-5.0	-7.5	0	-12.5
C	(% mass)	73.2	75.6	73.9	77.6	76.9	87.3
H	(% mass)	12.3	12.9	12.3	11.9	12.2	12.5
O	(% mass)	14.5	11.5	13.8	10.5	10.9	0
Sulphur	(mass ppm)	2	2	-	6	-	<50
Water	(% mass)	0.04	0.04	0.03	0.03	0.03	-
Potassium	(mg/kg)	< 5.0	<5.0	<5.0	<5.0	<5.0-	-
Methanol	(% mass)	<0.013	<0.001	<0.001	<0.001	-	-
Monoglyceride	(% mass)	0.03	0.073	0.39	0.07	0.083	-
Diglyceride	(% mass)	0.15	0.178	0.31	0.17	0.2	-
Triglyceride	(% mass)	0.02	0.007	0.04	0.01	0.018	-
50% Distillation temperature	(^0C)	275	329	273	340	329	278
Stoichiometric air-fuel ratio		11.99	12.6	12.1	12.58	12.47	14.2

3.5 Experimental Procedures

The experiments were started from engine warming up to achieve the stable condition. When test engine get stable condition, the application of loads and measurements were started. The engine speed was fixed at 2000 rpm and the loads were applied from 0% to 25, 50, 75,100% by using an electric dynamometer. At 100% load condition the brake mean effective pressure (*Pme*) of the test engine was 0.67 MPa. The exhaust gases, the CO emission was measured by a non-dispersive infrared detector (NDIR) type analyzer, the HC emission was measured by a flame ionization detector (FID) type analyzer, the NOx emission was measured by chemiluminescent detector (CLD) type analyzer and the smoke emission was measured by light transmitting type smoke meter (Opacimeter). The same conditions, methods and procedures were used for both biodiesel and diesel fuels. In order to get the same weather condition such as temperature and humidity, all experiments were carried out on sunny days. At least four set of engine experiments were done on each kind of the test fuel for data confidence.

3.6 Results and Discussion

3.6.1 Brake Thermal Efficiency and Brake Specific Fuel Consumption

Brake thermal efficiency is the ratio of brake power output to power input. Brake thermal efficiency of test fuels are shown in Figure 3.1. Brake thermal efficiencies rise from lower to higher load level. It is because of higher power output or work done at high load level makes higher brake thermal efficiency. Therefore at 0 load level, there is no work done and no brake thermal efficiency. From Figure 3.1 it can be seen that brake thermal efficiency of CME, PME, PKME, RME and SME are slightly higher than that of diesel fuel at all load levels. From this result, methyl ester fuels with more than 10% oxygen content may take better combustion and therefore they have better energy conversion rate compared to diesel fuel.

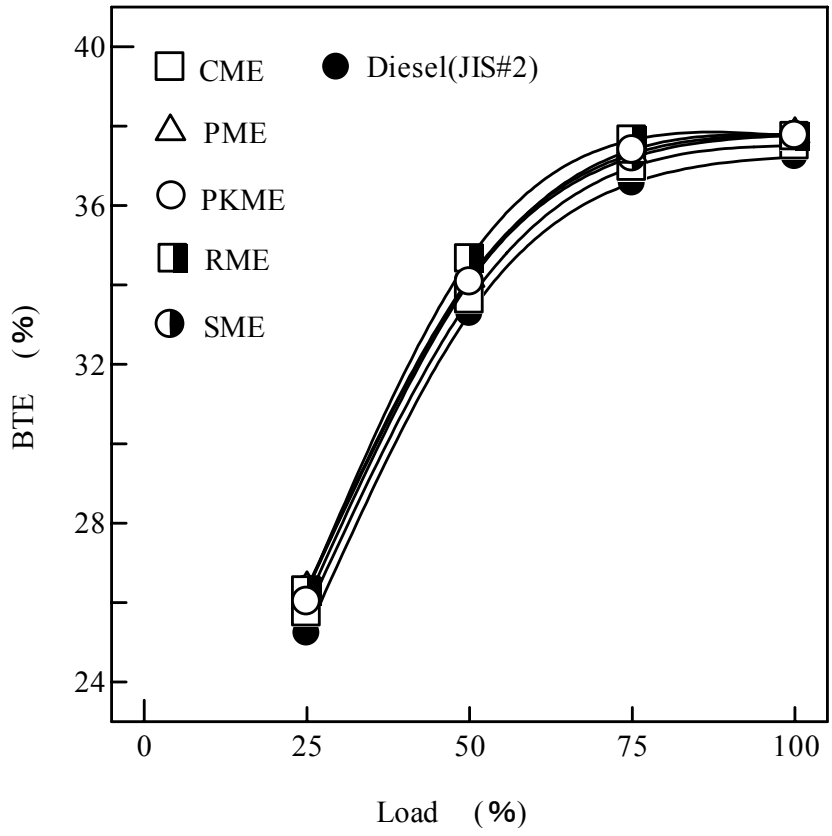

Figure 3.1 Brake thermal efficiency of the test fuels

Brake specific fuel consumption is the rate of fuel consumption divides by the rate of power production. Brake specific fuel consumption of test fuels are shown in Figure 3.2. Brake specific fuel consumptions descend from lower to higher load level. It is related with brake thermal efficiency. At higher load level the brake thermal efficiency is increased and brake specific fuel consumption decreased. From Figure 3.2 it can be seen that the brake specific fuel consumption of CME, PME, PKME, RME and SME are higher than that of the diesel fuel. In the combustion process, to occur the combustion process or to produce the same amount of heat, more amount of fuel is necessary for lower net calorific value fuel compared to the higher one. Therefore, the higher brake specific fuel consumption of methyl ester fuels are due to the lower net calorific value of these fuels. CME with the lowest net calorific value among the test fuels shows the highest brake specific fuel consumption.

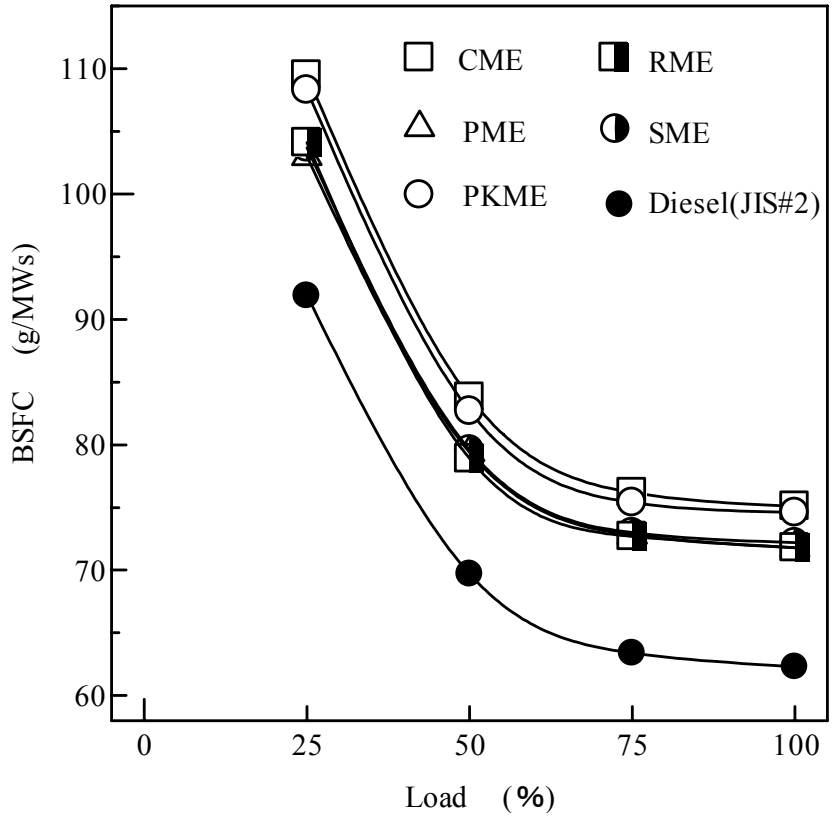

Figure 3.2 Brake specific fuel consumption of the test fuels

3.6.2 Combustion characteristics

Combustion in a diesel engine is physical and chemical processes. The combustion depends on many different parameters, such as injection fuel amount, ignition delay time and ignition timing. The proper combustion processes after fuel injection are atomization, vaporization, fuel air mixing, self ignition and finally combustion. Figure 3.3 shows injection timing, ignition delay and ignition timing of the test fuels. This figure was illustrated by the data from the needle lift of the fuel injector and heat release rate of the combustion chamber of the test engine. The injection start timing of PME, RME and SME are faster than that of diesel fuel. However CME and PKME have almost the same fuel injection start timing as that of the diesel fuel. The fuel injection timing is mainly influenced by the physical properties of the fuel, especially the bulk modulus, density and kinematics viscosity of the fuel. The higher bulk modulus, density and kinematics viscosity make faster injection timing. Therefore higher density and kinematics viscosity of PME, RME and SME show faster injection timings. The faster injection timing causes negative effect on the combustion process such as the faster combustion and incomplete combustion.

As it was expressed in reference (33), the buck modulus of saturated fatty acid methyl ester is lower than that of unsaturated fatty acid methyl ester. Considering fatty acid composition of biodiesels, biodiesels containing mostly unsaturated fatty acids have higher bulk modulus, density and kinematics viscosity compared to the diesel fuel. On the other hand, saturated fatty acids type biodiesels have closed bulk modulus, density and kinematics viscosity compared to the diesel fuel. Accordingly, saturated fatty acids type biodiesel CME and PKME have almost the same fuel injection timing as the diesel fuel.

The ignition delay is a symbol of ignition ability of a fuel. The shorter ignition delay means the better ignition ability. From the experimental results, the ignition delays of methyl ester fuels are shorter than that of the diesel fuel at every load levels. From this result, it can be said that the ignition abilities of methyl ester fuels are better than that of the diesel fuel. Comparing the ignition ability of methyl ester fuels, PME has the best ignition ability and the descending order is PKME, CME, RME and SME. This order is matching with the cetane number

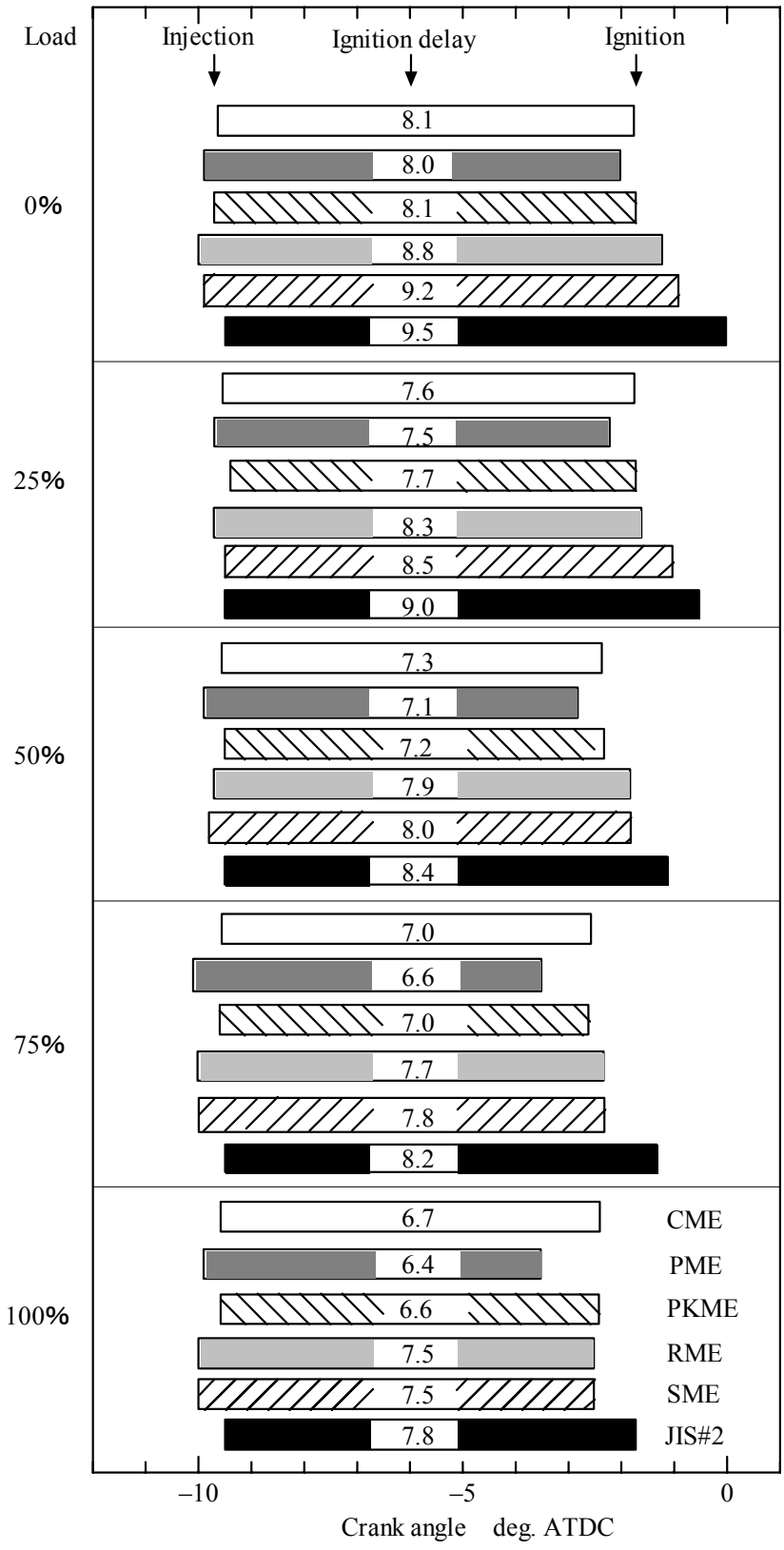

Figure 3.3 Injection, ignition delay and ignition

order of the methyl ester fuels as shown in Table 3.13. The same order of ignition delay times can be found at every load levels. The other factor influence on ignition ability of methyl ester fuels is the residual impurities in the fuels. These residual impurities such as monoglyceride, diglyceride, triglyceride, glycerine, methanol and water in methyl ester fuels may reduce the ignition ability. But methyl ester fuels used in this study contain only small amount of residual impurities, therefore, they showed good ignition ability as the cetane number.

The heat release rate depends on fuel injection amount, ignition delay and ignition timing. The heat release rate of combustion chamber and the needle lift of fuel injector of test engine at 100% load level are shown in Figure. 3.4. The needle lift interval of fuel injector shows the fuel injection time of the fuel injector. The longer needle lift interval means more fuel injection amount injected to the combustion chamber. From Figure 3.4 it can be seen clearly that, the needle lifts interval of methyl ester fuels are longer than that of the diesel fuel. It indicates more amount of methyl ester fuels are necessary compared to the diesel fuel. It is related with lower net calorific value of methyl ester fuels. To occur the combustion process, the necessary heat amount for combustion is the same, thus the fuel with lower net calorific is needed more fuel amount compared to higher one. Comparing the needle lift intervals of methyl ester fuels, the lowest net calorific value CME shows the longest interval. Also this result coincides with the specific fuel consumption of CME explained in above.

From the result of heat release rate, the peak heat release rate of CME, PME, PKME and RME are lower than that of the diesel fuel. However, the peak heat rate of SME can be said almost the same as that of the diesel fuel. The rapid heat release rate emitted just after ignition is due to the combustion of combustible fuel air mixture. The combustible fuel air mixture is formed in ignition delay time. Therefore it can be considered as that longer ignition delay makes greater amount of combustible fuel air mixture and it causes higher peak heat release rate at initial combustion stage. From Figure 3.3 and 3.4, the ignition delay time is directly proportional to the peak of the heat release rate. The combustion ending of all test fuels are almost the same.

By comparing the experimental results on injection timing, ignition delay and

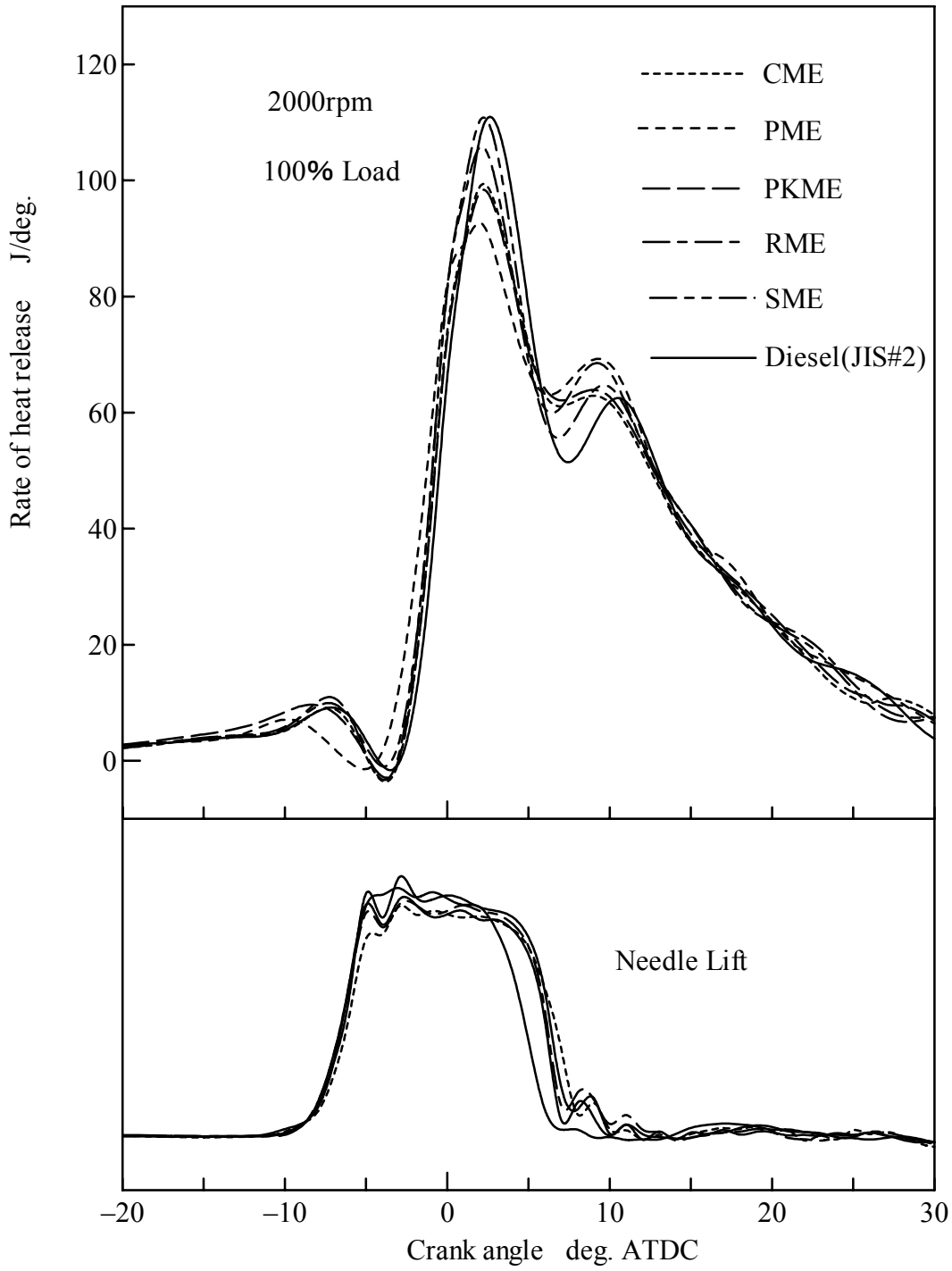

Figure 3.4 Heat release rates and needle lifts of the test fuels

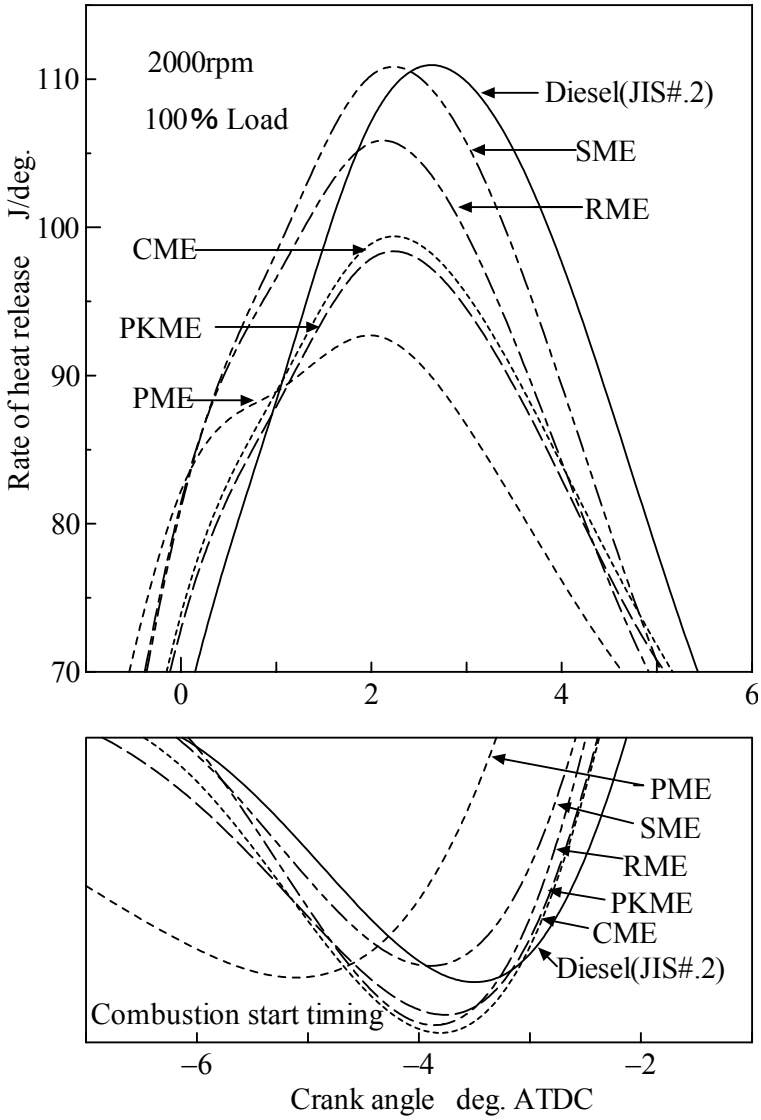

Figure 3.5 Heat release rates and needle lifts of the test fuels (enlarged)

ignition timing of methyl ester fuels the following can be said. CME and PKME with good fuel properties such as much oxygen content in fuel, suitable cetane number, lower density, lower viscosity and lower distillation temperature may have better combustion process. These fuel properties of CME and PKME may carry out proper fuel injection timing, atomization, vaporization, fuel air mixing and self ignition in the combustion process. Therefore CME and PKME take better combustion process than the other test fuels. Also it can be seemed from the exhaust emissions, because complete combustion reduces most of the exhaust emissions.

3.6.3 Exhaust Emission

The HC emissions of the test fuel are shown in Figure 3.6. The cause of HC emission is mostly depending on the combustion. Incomplete combustion produces more HC emission or unburned fuel emission (34). If a fuel-rich mixture does not has enough oxygen to react with all the carbon, result high level of HC emission. From the experimental results, the HC emissions from all methyl ester fuels are lower than that of the diesel fuel. The lower HC emission from methyl ester fuel is probably due to the oxygen in methyl ester fuel. The present of fuel oxygen allows the fuel to burn completely, so fewer unburned fuel emission result. Therefore, more oxygen in CME and PKME show more reductions in HC emission.

The CO emissions from test fuels are shown in Figure 3.7. The cause of CO emission is similar as HC emission. Generally, CO is generated when there is not enough oxygen to convert all carbon to CO_2, some fuel does not get burned and

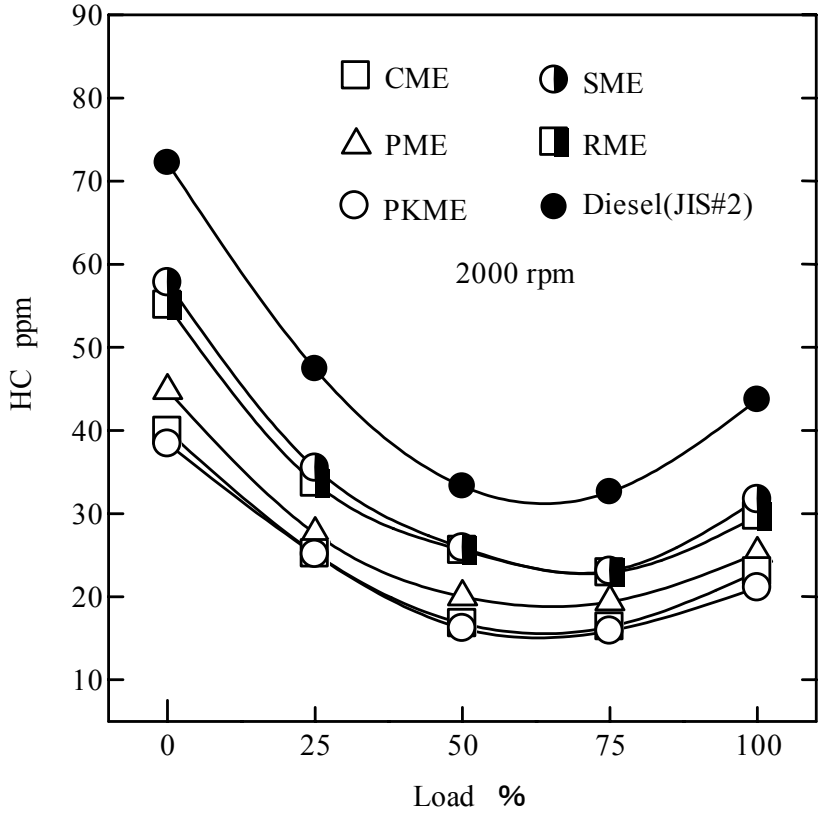

Figure 3.6 HC emission of the test fuels

some carbon ends up as CO (34). The other factors of CO emission are poor fuel air mixing, local fuel rich region and incomplete combustion will create some CO. From the experimental results, the CO emission from CME, PME and PKME are lower than that of the diesel fuel at all load levels. While RME and SME are higher CO emission compared to the diesel fuel. Also CO emission from methyl ester fuels may be influenced by the oxygen content in the fuel. Therefore, more oxygen in CME and PKME show more reductions in CO emission.

The NOx emissions from the test fuel are shown in Figure 3.8. The NOx formation in diesel engine combustion is complicated. But the NOx formation in combustion process is mainly controlled by the combustion temperature. On the other hand, the combustion temperature is depended on the injection timing of the fuel, ignition delay time and combustion pattern. In general, biodiesels with higher speed of sound and buck modulus cause the faster propagation of pressure

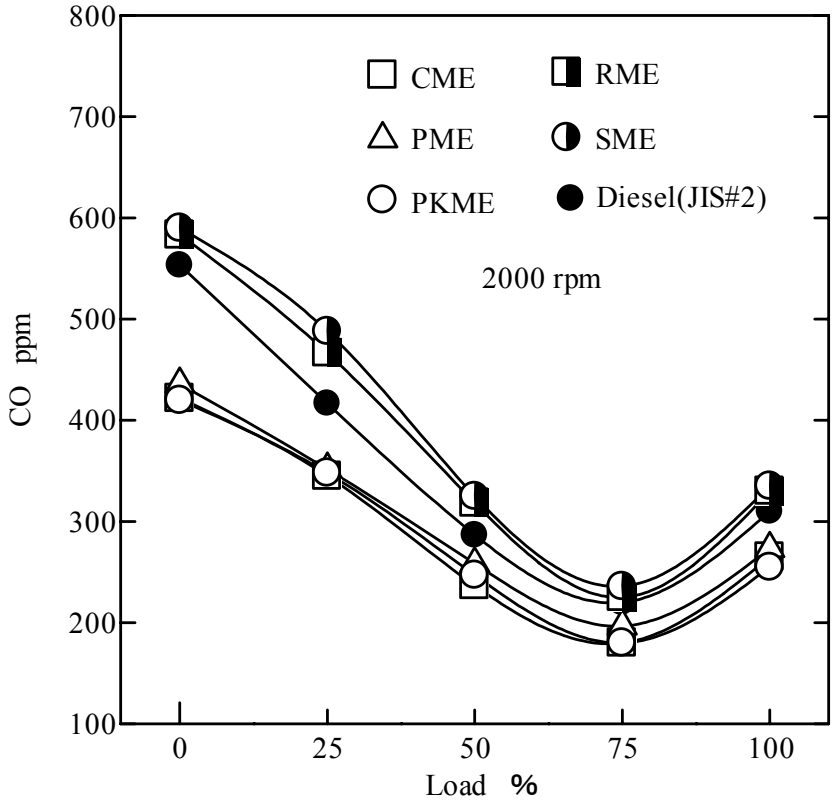

Figure 3.7 CO emission of the test fuels

waves and more rapid pressure rise, and which may shift the injection timing from optimum timing and driving to earlier combustion. The earlier combustion can result higher combustion temperature and higher NOx emission (35). From the experimental results, there are no differences in NOx emissions of methyl ester fuels and the diesel fuel at lower load level. But at 75- 100% load level, 5-10% reduction can be seen in CME and PKME, and about 10% increase occurred in RME and SME. The reduction of NOx emission from CME and PKME compared to that of RME and SME, are probably due to the lower combustion temperature related with the shorter ignition delay and lower heat release rate of CME and PKME. In case of PME, although PME has shorter ignition delay and lower heat release rate than those of CME and PKME, but the NOx emission from PME is slightly higher. It may be caused by faster injection

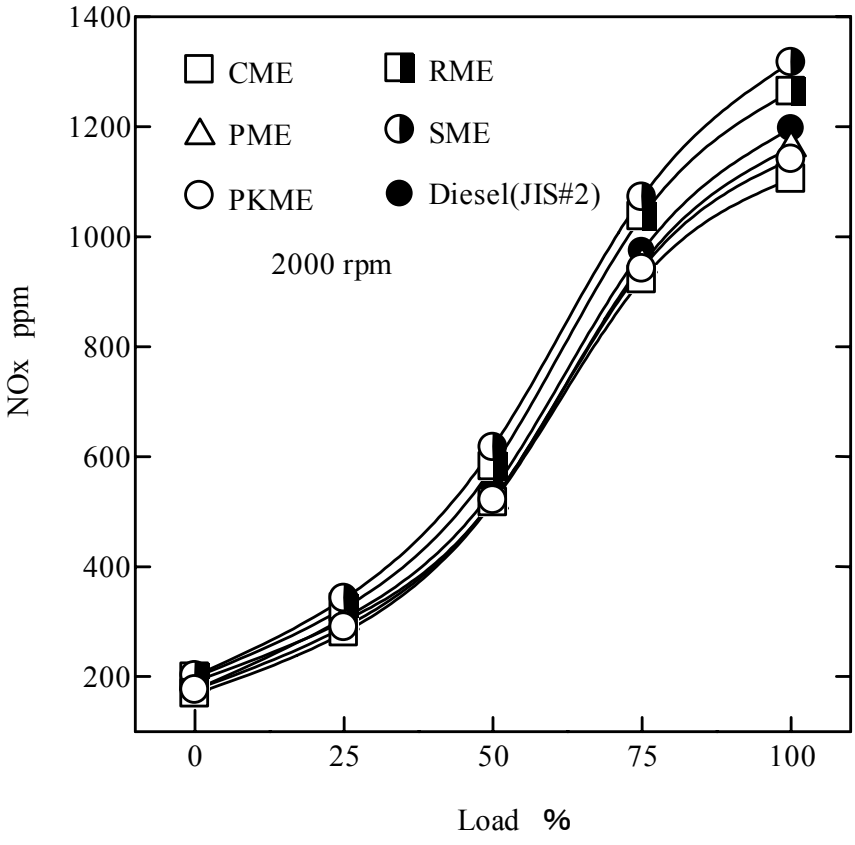

Figure 3.8 NOx emission of the test fuels

timing leading to earlier combustion and resulting higher combustion temperature and the NOx emission increase.

The smoke emissions from test fuels are shown in Figure.3.9. The smoke contains solid carbon soot particles that are generated when the fuel has no enough oxygen to react with all the carbon or in the fuel rich zone of combustion chamber during combustion process (34). From the experimental results, the smoke emission from methyl ester fuel and the diesel fuel are a few differences in 0% to 25% load level. But at 50% to 100% load level the smoke emission from all methyl ester fuels are lower than that of the diesel fuel. Comparing the smoke emissions in methyl ester fuels, CME and PKME emit lower smoke emission than the PME, RME and SME. The smoke emission in methyl ester fuels vary with the oxygen content of the fuel and the less smoke emission can be found in the fuel with the more oxygen content.

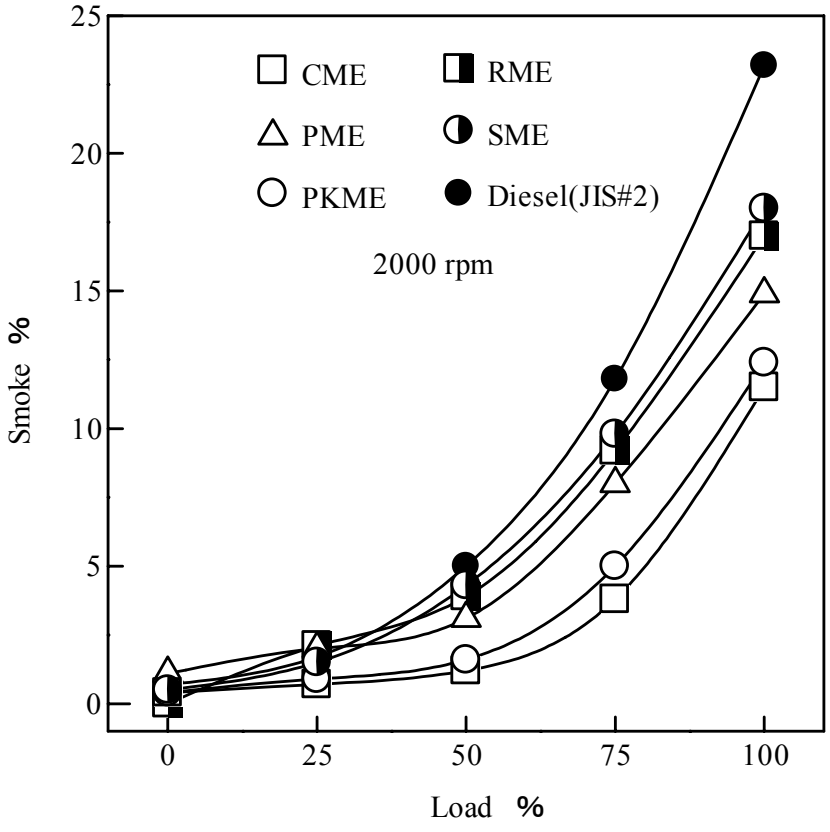

Figure 3.9 smoke emission of the test fuels

3.6.4 Exhaust Emissions Comparison

The comparisons of HC, CO, NOx and smoke emissions of methyl ester fuels to diesel fuel are shown in Figure 3.10, 3.11, 3.12 and 3.13 respectively. From these figures it can be seen that, at 100% load level the HC emissions from CME is about 48% lower, from PME is about 42% lower, from PKME is about 52% lower, from RME is about 32% lower and from SME is about 28% lower than that of the diesel fuel. The CO emission from CME is about 15% lower, from PME is about 12% lower, from PKME is about 18% lower, from RME is about 6% higher and from SME is about 8% higher than that of the diesel fuel. The NOx emissions from CME is about 8% lower, from PME is about 3% lower, from PKME is about 5% lower, from RME is about 5% higher and from SME is about 10% higher than that of the diesel fuel. The smoke emissions from CME is about 51% lower, from PME is about 36% lower, from PKME is about 47% lower, from RME is about 27% lower and from SME is about 23% lower than that of the diesel fuel. The reduction of all emissions can be seen in those of CME, PME and PKME.

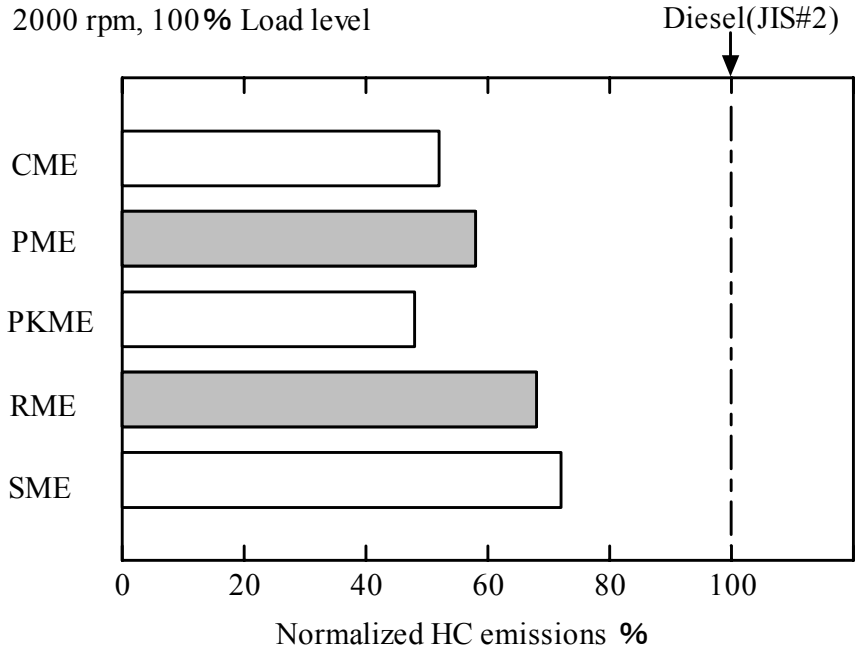

Figure 3.10 Comparison of HC emission

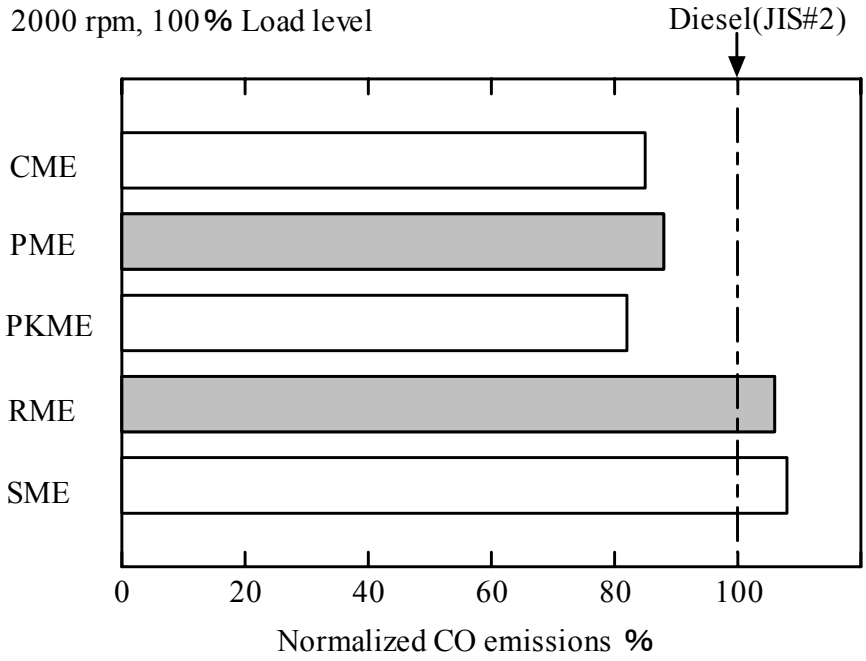

Figure 3.11 Comparison of CO emission

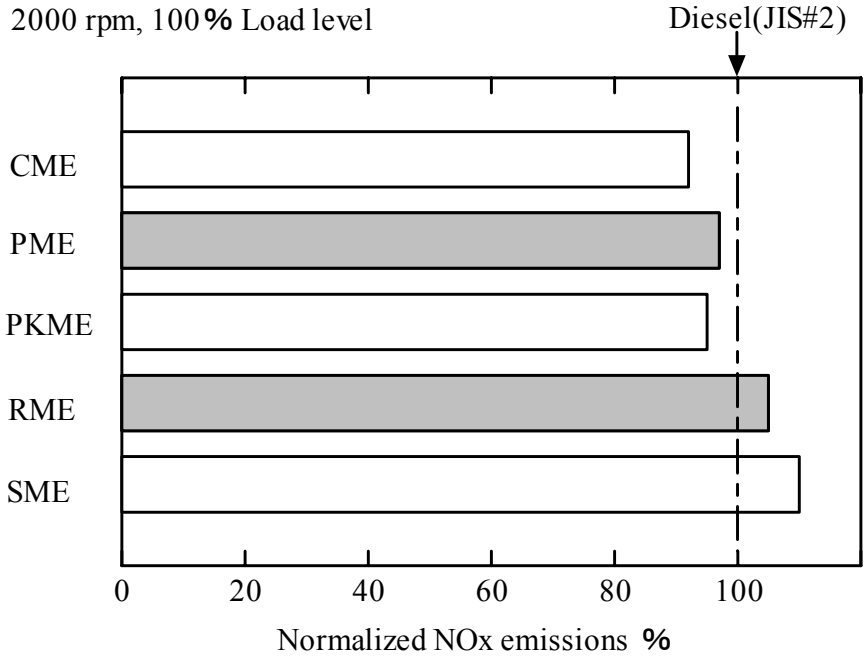

Figure 3.12 Comparison of NOx emission

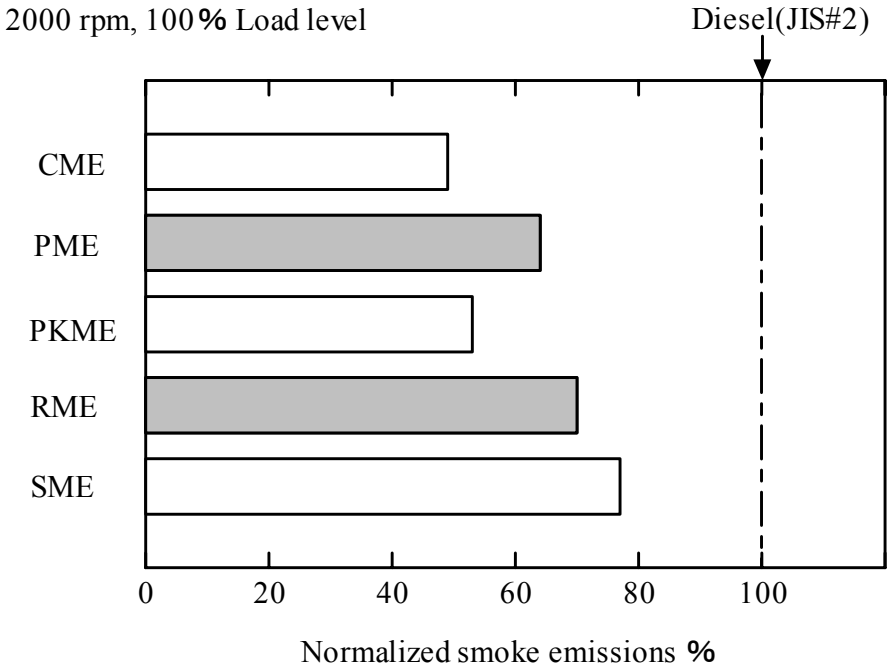

Figure 3.13 Comparison of smoke emission

3.7 Conclusions

The analysis and engine experiments were carried out to compare the fuel properties, the combustion characteristics and the exhaust emissions of CME, PME, PKME, RME and SME. From the analytical and experimental results the following conclusions can be drawn.

Fuel properties

(1) The density and kinematics viscosity of CME and PKME are lower than that of PME, RME and SME.

(2) The net calorific value of CME and PKME are lower than that of PME, RME and SME.

(3) The oxygen content of CME is 14.5%, PME is 11.5%, PKME is 13.8%, RME is 10.5% and SME is 10.9 % respectively.

(4) The distillation temperature of CME and PKME are lower than that of the PME, RME and SME.

Combustion characteristics and exhaust emissions

(1) The fuel injection timing of PME, RME and SME are faster than that of CME and PKME.

(2) The fuel injection time of CME and PKME are longer than that of PME, RME and SME.

(3) The ignition delay time of PME is shortest in the other methyl ester fuels and CME and PKME have shorter ignition delay time relative to RME and SME.

(4) The heat release rate of PME at 100% load level is lowest in the methyl ester fuels and CME and PKME have lower heat release rate compared to RME and SME.

(4) The thermal efficiency of the methyl ester fuels have only small differences between them.

(5) CME, PME and PKME have lower HC, CO, NOx and smoke emissions compared to those of RME and SME.

4. DIESEL COMBUSTION CHARACTERISTICS OF SINGLE COMPOSITION OF FATTY ACID METHYL ESTERS

4.1 Introduction

Since biodiesel is produced from vegetable oils and animal fats, the properties and characteristics of finished biodiesel depend mainly on its original feedstock. On the other hand, the main components of vegetable oils and animal fats are fatty acids and therefore fatty acid compositions influence the properties and the characteristics of biodiesel. These properties are both physical and chemical properties, including fuel properties such as cetene number, density, kinematic viscosity, bulk modulus and pour point, and characteristics such as combustion and exhaust emissions. Generally, most of vegetable oils contain fatty acids usually with the carbon numbers ranging from C6 to C18. Some of these fatty acids are saturated, while others are unsaturated. The saturated fatty acid does not contain carbon-carbon double bond and while unsaturated fatty acids have carbon-carbon double bond(s). The hydro carbon construction chains of saturated and unsaturated fatty acids are shown in Figure 4.1 and 4.2. Figure 4.1 shows lauric acid, it is a medium chain length saturated fatty acid and which does not contain carbon-carbon double bond. But in Figure 4.2, oleic acid contains one carbon-carbon double bond and the actual chain construction is not straight and bending because of double bond. The fatty acid composition and differing levels of saturation of the origins or vegetable oils may affect the combustion characteristics of biodiesels.

In the previous chapter, the experiments on the combustion characteristics and exhaust emissions of three kinds of saturated fatty acids type and two kind of unsaturated fatty acids type vegetable oil biodiesels were explained. Additionally in order to understand detail on the combustion characteristics of biodiesel, it is necessary to know the combustion characteristics of single composition of fatty acid methyl ester (FAME). Therefore, five kinds of single composition of FAMEs which mostly contain in methyl ester type biodiesel were selected for this study. These five kinds of FAMEs are methyl laurate, methyl myristate, methyl palmitate,

methyl stearate and methyl oleate. Additionally, in order to investigate the effect of unsaturation degree of FAMEs on the combustion characteristics of diesel engine, high oleate safflower oil, high linoleate safflower oil and linseed oil methyl esters were used for experiments. This chapter is divided into two sections. In the first section, the experiments of single composition of FAMEs are expressed and in the second section the experiments of unsaturated FAMEs with three different unsaturation degrees are expressed.

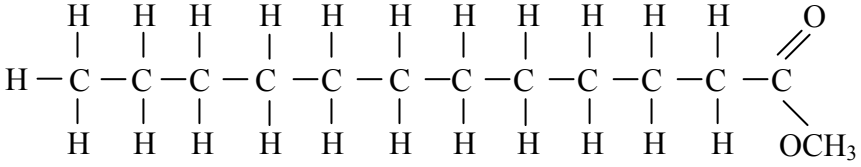

Figure 4.1 Example of saturated fatty acid (lauric acid)

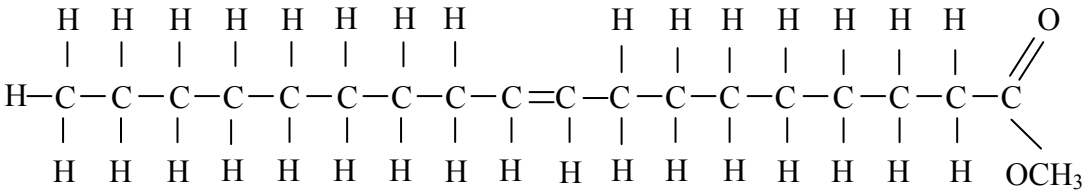

Figure 4.2 Example of unsaturated fatty acid (Oleic acid)

4.2 Combustion Characteristics of Single Composition of Five FAMEs

4.2.1 Test Fuels

In order to investigate the combustion characteristics of single composition of FAMEs, five kinds of pure FAMEs were chosen. Experimental used five FAMEs are methyl laurate (minimum 98% purity), methyl myristate (minimum 98% purity), methyl palmitate (minimum 98% purity), methyl stearate (minimum 80% purity) and methyl oleate (minimum 70% purity). These FAMEs were purchased from Wako Pure Chemical Industries LTD., Japan. From these five kinds of FAMEs, six kinds of pure and blended FAME fuels were prepared. Some FAMEs such as methyl palmitate and methyl stearate are high pour point FAMEs, which are in solid state at ambient temperature about 30˚C. Therefore, it is necessary to blend with the others lower pour point FAMEs to use as a fuel in diesel engine.

In the test fuel preparing process, lower pour point methyl oleate was used as a base for blending. The six kind of FAME fuels are expressed in table 4.2. The six FAME fuels are methyl laurate (ML100), methyl oleate (MO100), methyl laurate 50wt%+methyl oleate 50wt% blend (MOL50), methyl myristate 50wt%+methyl oleate 50wt% blend (MOM50), methyl palmitate 50wt%+methyl oleate 50wt% blend (MOP50) and methyl stearate 50wt%+methyl oleate 50wt% blend (MOL50). The JIS no. 2 diesel fuel was also used as a test fuel for comparison. The properties of test fuels are shown in table 4.1.

Table 4.1 Six kinds of FAME fuels

Name of fuel	Base fuel	Additive fuel
ML100	Methyl laurate 100wt%	
MO100	Methyl oleate 100wt%	
MOL50	Methyl oleate 50wt%	Methyl laurate 50wt%
MOM50	Methyl oleate 50wt%	Methyl myristate 50wt%
MOP50	Methyl oleate 50wt%	Methyl palmitate 50wt%
MOS50	Methyl oleate 50wt%	Methyl stearate 50wt%

Table 4.2 Properties of test fuels

Properties		ML100	MO100	MOL50	MOM50	MOP50	MOS50	Diesel*
Cetane number		-	-	-	-	-	-	56
Net calorific value	(MJ/kg)	36.64	38.8	37.72	38.27	38.7	39.07	43.12
Density@288K	(kg/m^3)	865	878	870	872	872	875	832
Kinematic Viscosity@293K	(mm^2/sec)	4.1	7.1	5	5.63	7.1	6.5	4.7
Pour point	(˚C)	2.5	-15	-12.5	2.5	10	25	-12.5
C	(% mass)	72.9	77.03	74.9	75.7	76.29	76.77	87.3
H	(% mass)	12.5	12.16	12.16	12.28	12.38	12.46	12.5
O	(% mass)	14.95	10.81	12.88	12.02	11.33	10.77	0
Sulphur	(wt%)	-	-	-	-	-		0.05

* JIS No. 2 diesel fuel

From Table 4.2, the net calorific values of FAME fuels were calculated from the Carbon, Hydrogen and Oxygen contents. Comparing the net calorific value of FAME fuels, ML100 is the lowest in the FAME fuels and MOS50 is the highest. But the net calorific value of all FAME fuels is about 10-15% lower than that of the diesel fuel. The densities of FAME fuels are between 865-878 kg/m^3 and those of ML100 and MO100 are the lowest and the highest respectively. The densities of all FAME fuel are higher than that of the diesel fuel. The kinematic viscosity of ML100 and MOL50 are lower than the other FAME fuels and their value is closer to that of the diesel fuel. The pour point of MOS50 is 25˚C and MO100 is -15˚C. MOL50 has the same pour point that of the diesel fuel and which is -12.5˚C. The oxygen content in FAME fuels vary between 10.77-14.95 wt%. ML100 contains 14.95wt% of oxygen and it is highest content in the FAME fuels. The more oxygen in fuel reduces the net calorific value of FAME fuels.

4.2.2 Experimental Procedures

The experimental procedures of this experiment are the same procedures as expressed in the Chapter 3.

4.2.3 Results and Discussion

Figure 4.3 shows the injection timing, the ignition delays, and the ignition timing of the test fuels. These values were derived from the needle lift of fuel injector and the heat release rate of the combustion chamber of the test engine. The fuel injection timing of MO100 and MOS50 are slightly faster than the other FAME fuels and ML100 is almost the same as that of the diesel fuel. Faster injection timings are probably due to the higher density and buck modulus of these fuels. The relation of pressure and buck modulus of some FAMEs are shown in Figure 4.4.

The ignition delay time of MOS50 is shorter than those of the other FAMEs fuels at all load levels and the ignition delay times increase as the following ascending order; MOS50<MOP50<MOM50<MO100<MOL50<ML100. The shorter ignition delay time mean the better ignition ability. There-fore it can be estimated that the ignition ability of single composition of FAMEs may also be in

the following ascending order; methyl laurate<methyl oleate<methyl myristate<methyl palmitate<methyl stearate. Generally, the saturated fatty acid with long chain and unbranched have higher cetane number and better ignition ability while unsaturated fatty acid with carbon-carbon double bonds have lower cetane number and poor ignition ability (36). From experimental results, the ignition delays of saturated FAMEs(methyl laurate, methyl myristate, methyl palmitate and methyl stearate) decrease with the longer straight chain of hydrocarbon molecules, and among FAMEs with the same carbon numbers (methyl oleate and methyl stearate), the ignition delays increase with increasing carbon-carbon double bond. Comparing the ignition delays between FAME fuels and diesel fuel, all FAME fuels have shorter ignition delay times. From this result, FAME fuels used in experiments may have larger cetane numbers and better ignition ability that of the diesel fuel. Table 4.3 shows the properties of some saturated FAMEs. The ignition ability order of saturated FAMEs in this experiment is matching with the cetane number order expressed in Table 4.3.

The heat release rate of combustion chamber and the needle lift of fuel injector of test engine at 100% load level are shown in Figure. 4.5 and 4.6. The fuel injection timing of the test fuels also explained in previous paragraph can be seen clearly in Figure 4.6. The fuel injection period of ML100 is longest in the FAME fuels because of lowest net calorific value. All FAME fuel have longer fuel injection period relative to the diesel fuel is also because of 10-15% lower in net calorific values. The combustion start timing of ML100 and MOL50 is later than the other FAME fuels and their timing is closer to that of the diesel fuel. Comparing the peak heat release rates of FAME fuels, ML100 is highest and MOS 50 is lowest. The descending order of peak heat release rate of FAME fuels is ML100>MOL50>MO100>MOM50>MOP50>MOS50. It can be seen from this order, the peak heat release rates of FAME fuels rising with the longer ignition delay times. In the longer ignition delay time, the time for formation of combustible mixture is more and more mixture is formed. So these cause higher peak heat release rate just after ignition as well as initial combustion stage. The combustion end timing of all FAME fuels and diesel fuel are almost the same.

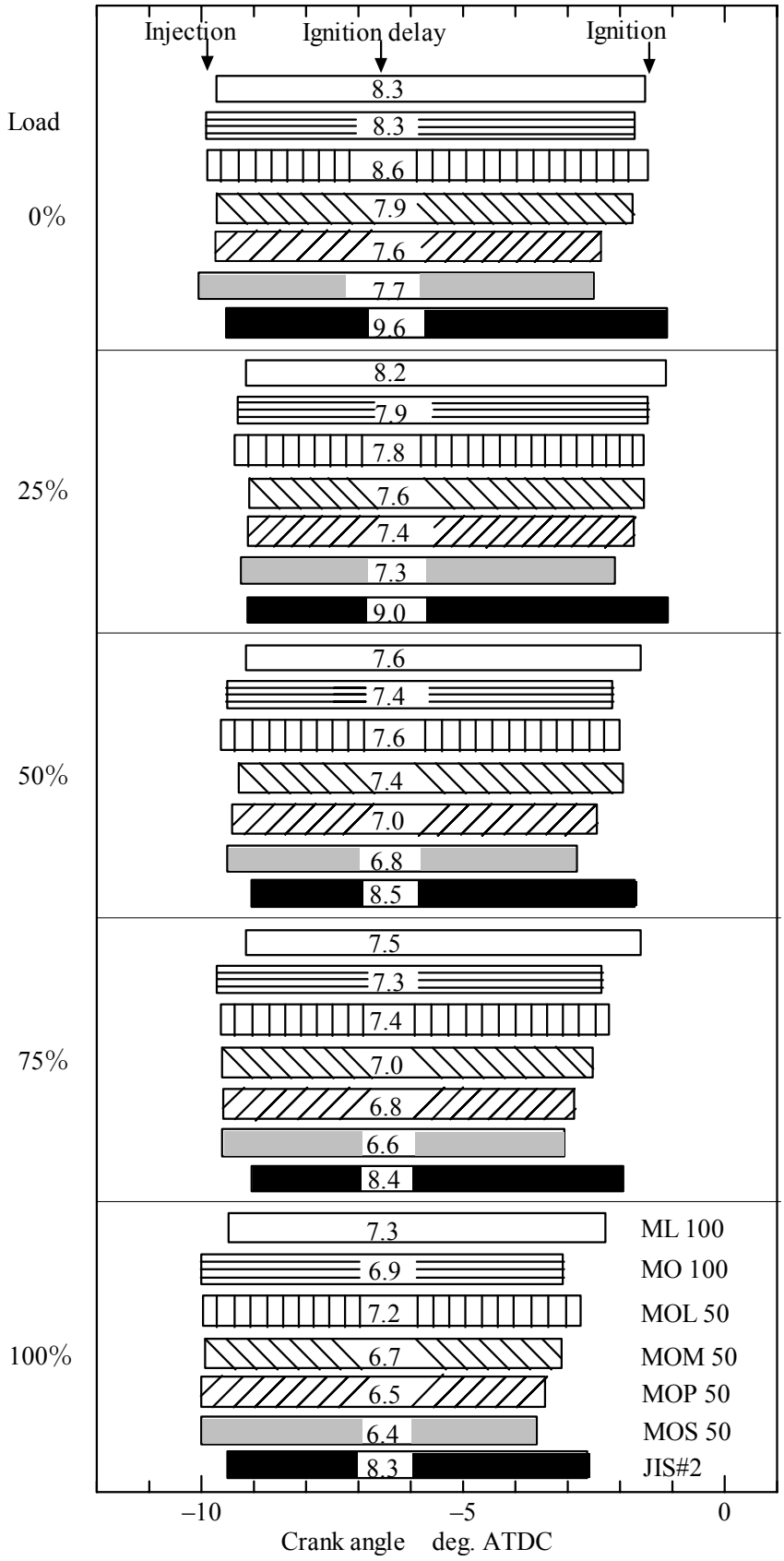

Figure 4.3 Injection, ignition delay and ignition

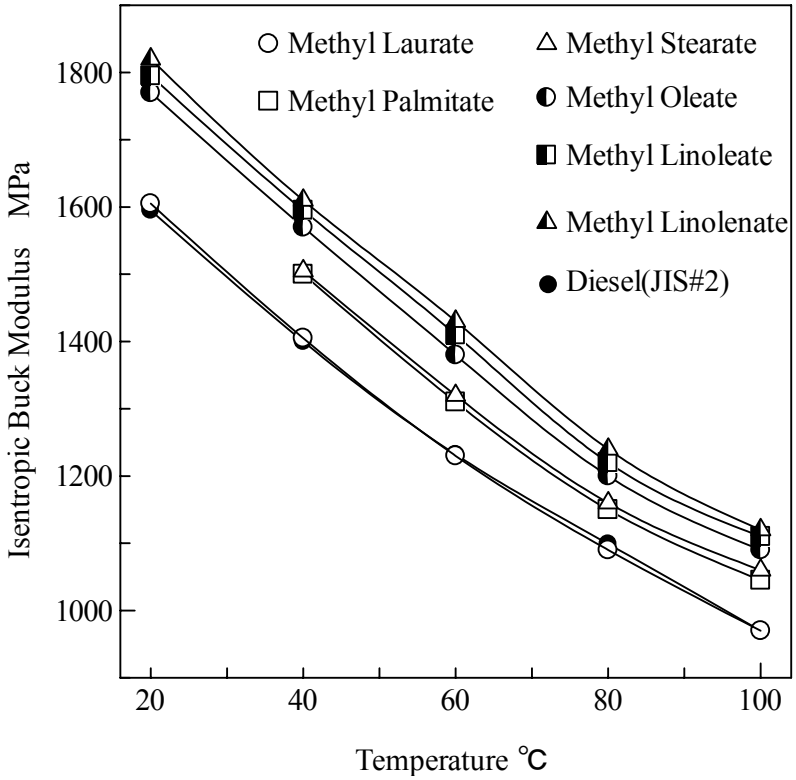

Figure 4.4 Buck modulus of some FAMEs (33)

Table 4.3 Properties of some FAMEs

Methyl	C:N	Boiling point(˚C) 760mm	Melting Point(˚C)	Measured cetane number	Viscosity (mm^2/s) @313K
Caproate	6:0	151 [a]	-71 [a]	18.0 [a]	0.785 [a]
Caprate	10:0	224 [a]	-18 [a]	47.9 [a]	1.69 [a]
Laurate	12:0	262 [a]	5 [a]	60.8 [a]	2.28 [a]
Myristate	14:0	323 [a]	18.4 [a]	73.5 [a]	3.23 [a]
Palmitate	16:0	330 [a]	28 [a]	74.3 [a]	4.32 [a]
Stearate	18:0	356 [a]	39 [a]	75.6 [a]	5.61 [a]
Oleate	18:1	-	-20 [c]	56 [b]	4.45 [b]
Linoleate	18:2	-	-35 [c]	45.9 [b]	4.43 [b]
Linolenate	18:3	-	-57 [c]	41.7 [b]	3.99 [b]

C: no. of carbon, N: no. of carbon-carbon double bond

a: from reference no. (37), b: from reference no. (38), c: from reference no. (39)

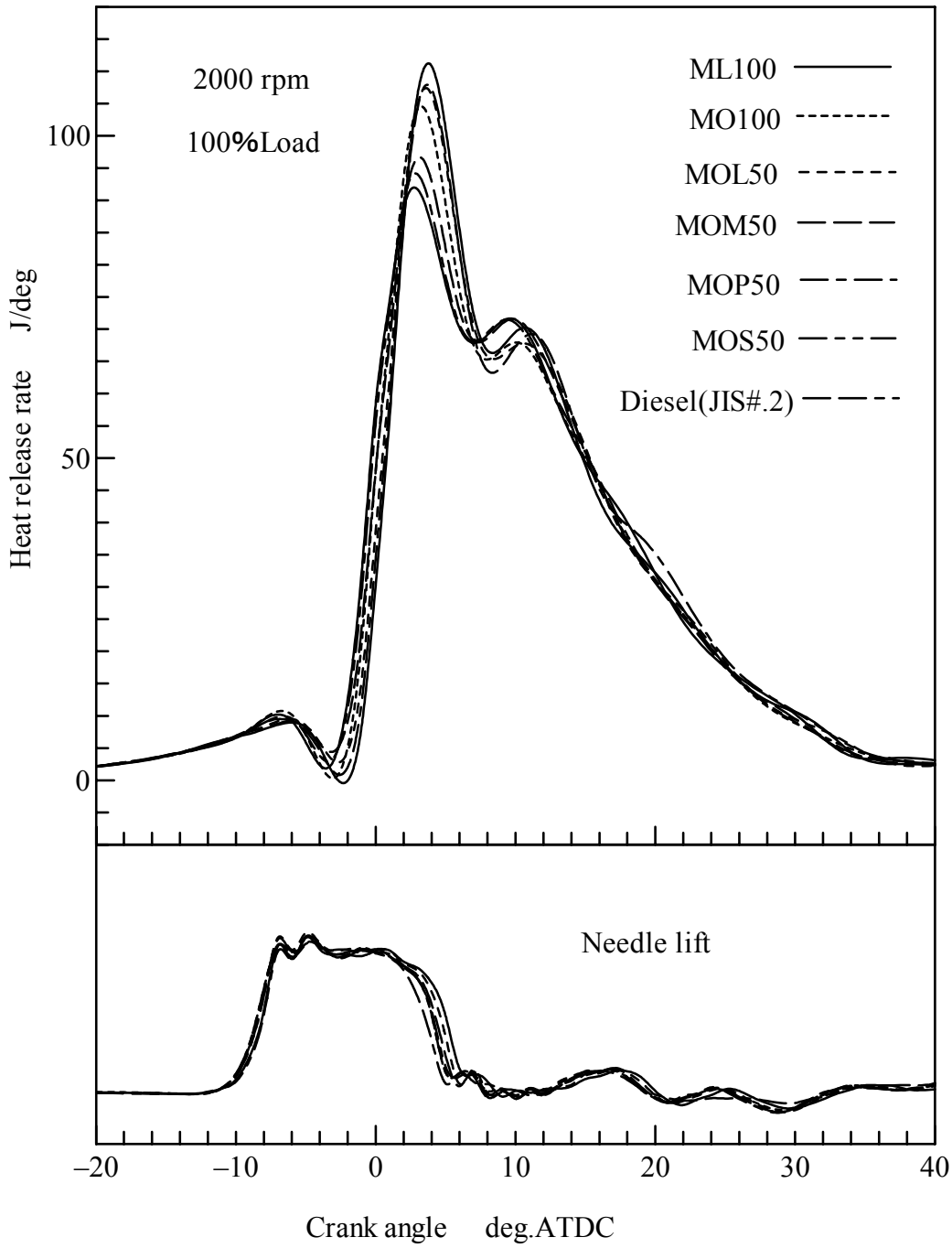

Figure 4.5 Heat release rate and needle lift

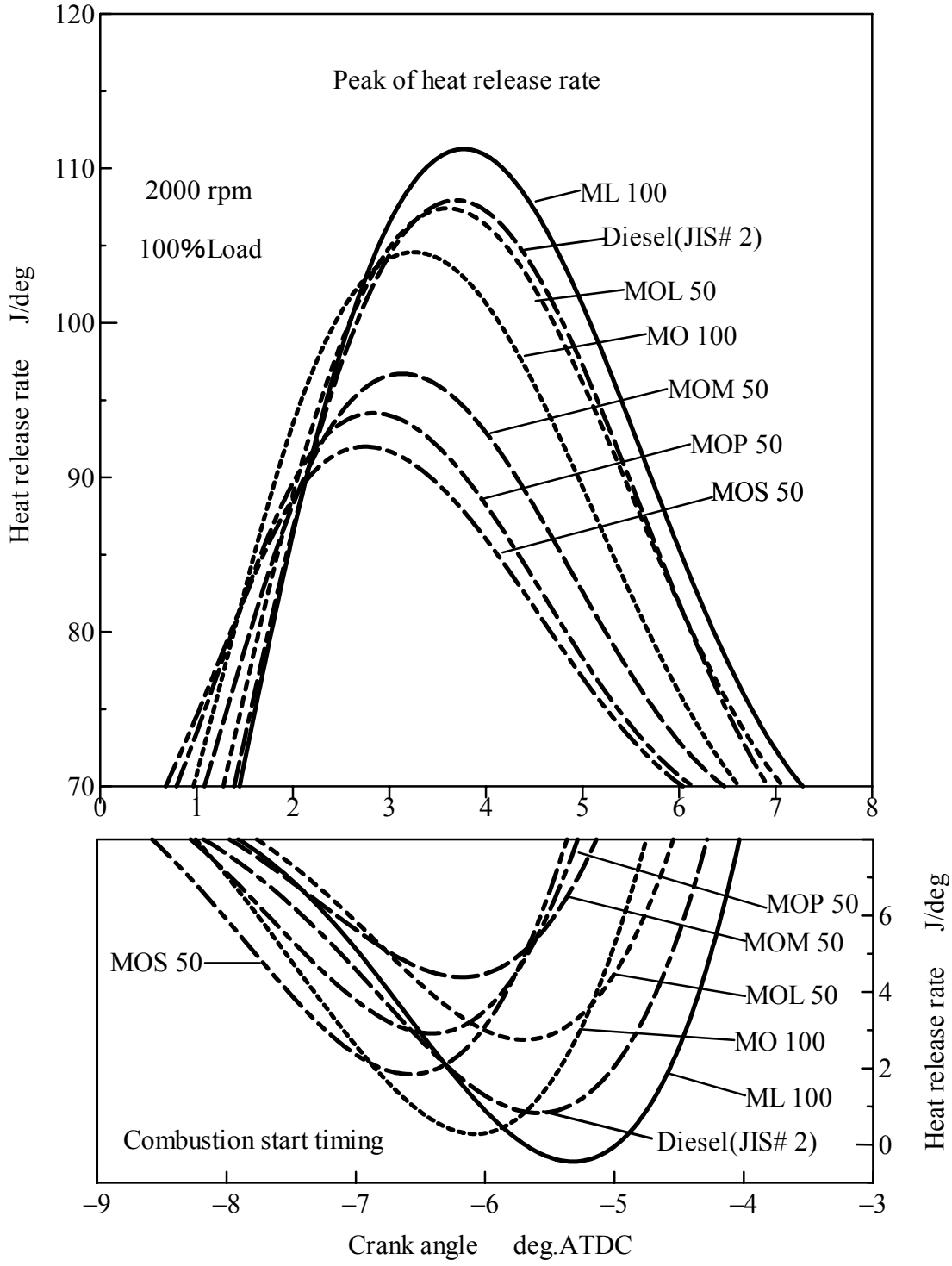

Figure 4.6 Heat release rate and needle lift (enlarged)

Brake thermal efficiencies of the test fuels are shown in Figure. 4.7. Brake thermal efficiencies of FAME fuels have only very small differences between each other. But all FAME fuels show slightly higher brake thermal efficiencies than that of the diesel fuel. From this result, FAME fuels with more than 10% oxygen content may take better combustion process and therefore they have better energy conversion rates compared to the diesel fuel. Brake specific fuel consumption of the test fuels are shown in Figure 4.8. In the FAME fuels, brake specific fuel consumption of ML100 is the highest because of its lowest net calorific value. The brake specific fuel consumption is changing with the net calorific value of the fuels and application of load levels. The higher brake specific fuel consumption of FAME fuels are due to the about 15% lower in net calorific value of these fuels compared to the gas oil.

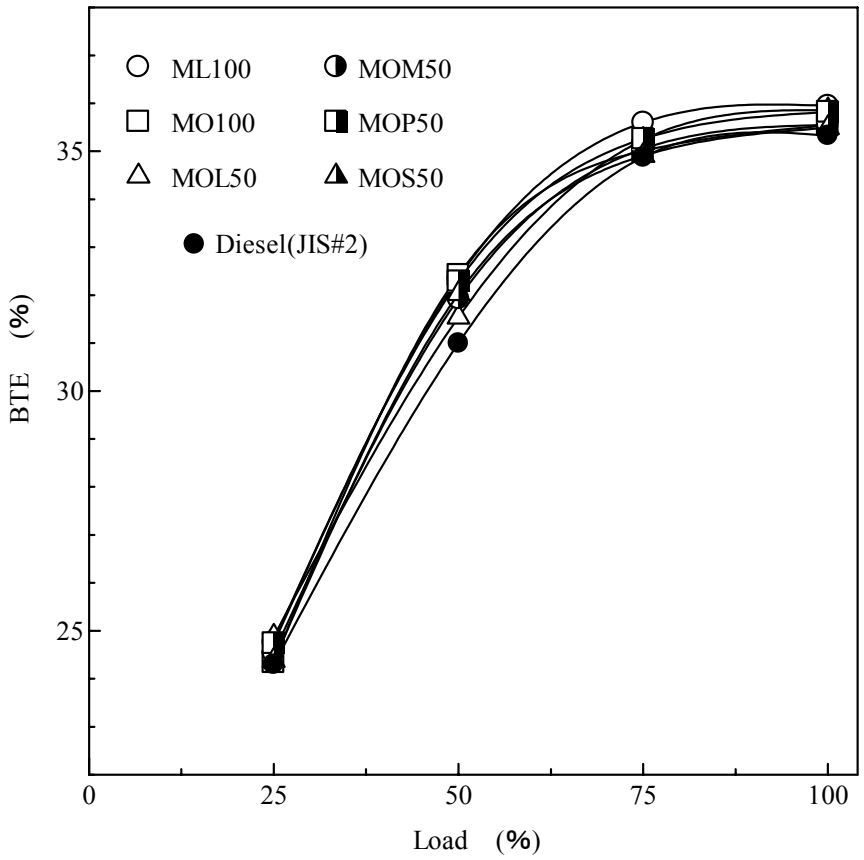

Figure 4.7 Brake thermal efficiencies of the test fuels

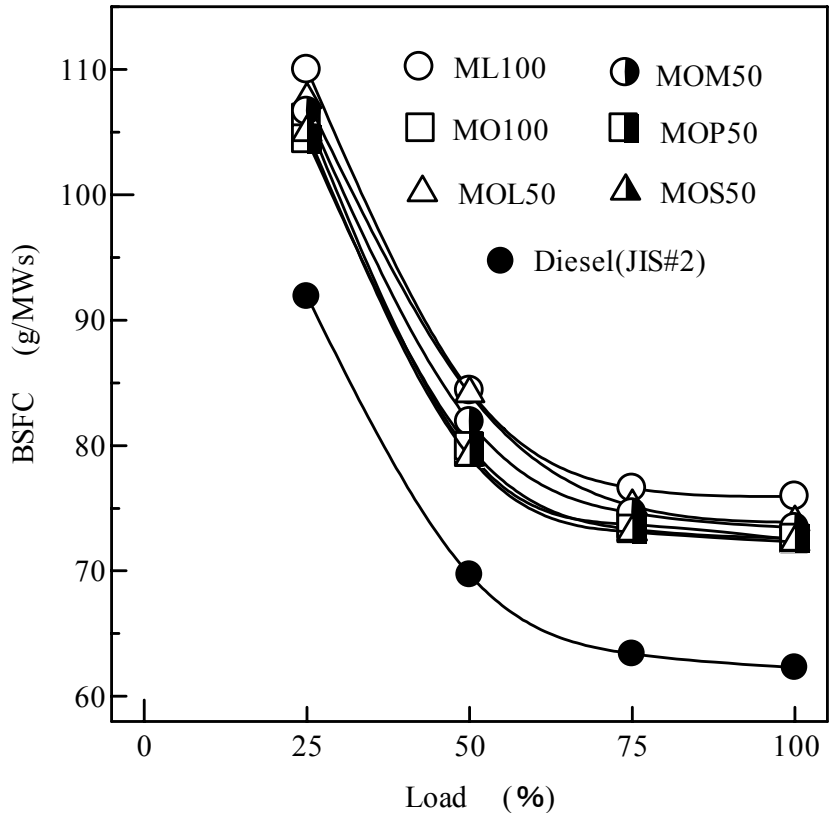

Figure 4.8 Brake specific fuel consumption of the test fuels

The HC emission from the test fuels are shown in Figure 4.9. The HC emission from ML100 is lowest and from MO100 is highest in the FAME fuels. Lower HC emission from ML100 may be related with the better combustion process. This is probably due to the more oxygen in MOL100 carries more complete combustion process. Furthermore, the lower kinematic viscosity and boiling point of ML100 (shown in Table 4.3) forms the better fuel air mixture and reduces fuel rich zone or incomplete combustion. The HC emissions from all FAME fuels are varying with the oxygen contents as well as kinematic viscosities and boiling points, and but lower than that of the diesel fuel. The CO emissions from the test fuels are shown in Figure 4.10. The CO emission from ML100 is lower and MO100 is higher than the other FAME fuels, in most of the load levels. The cause and formation of CO emission are similar as that of HC emission. At 100% load level the CO emissions from FAME fuels are lower than that of the diesel fuel.

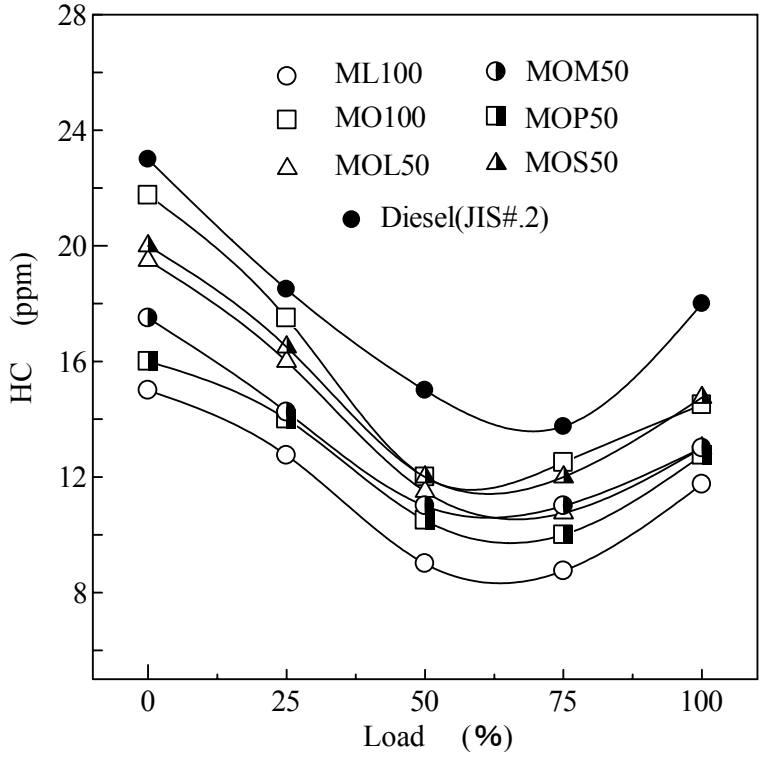

Figure 4.9 HC emissions of the test fuels

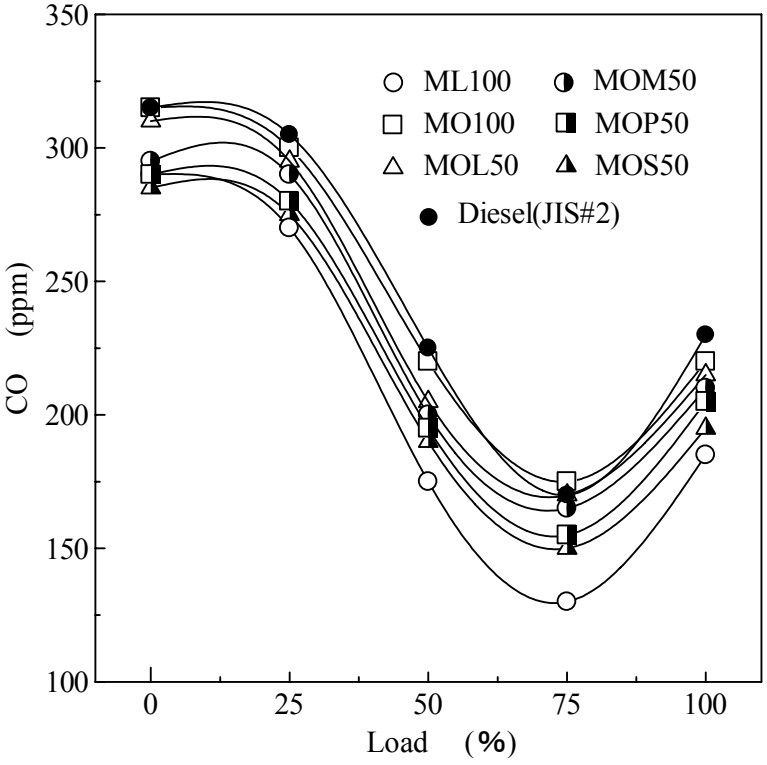

Figure 4.10 CO emissions of the test fuels

The NOx emissions from test fuels are illustrated in Figure 4.11. The NOx emission from ML100 is slight lower and MO100 and MOS50 are higher than the other FAME fuels. But the NOx emission differences in MOL50, MOM50 and MOP50 are very small. As described in the previous chapter, the NOx formation in combustion process is very complicated. Generally, the earlier combustion timing can result higher combustion temperature and higher NOx emission (35). Therefore, the NOx emissions from FAME fuels may concern and influence with the fuel injection timing and most of the NOx emissions are matching with the fuel injection timing as shown is Figure 4.3.

The smoke emissions of the test fuels are shown in Figure 4.12. The smoke emission in FAME fuels vary with the oxygen content of the fuel and the less smoke emission can be found in the fuel with the more oxygen content. Therefore the smoke emission from ML100 is the lowest and MOS50 is the highest in the FAME fuels. The smoke emissions from all FAME fuels are lower than that of the diesel fuel. The relation of smoke emissions and oxygen contents are shown in

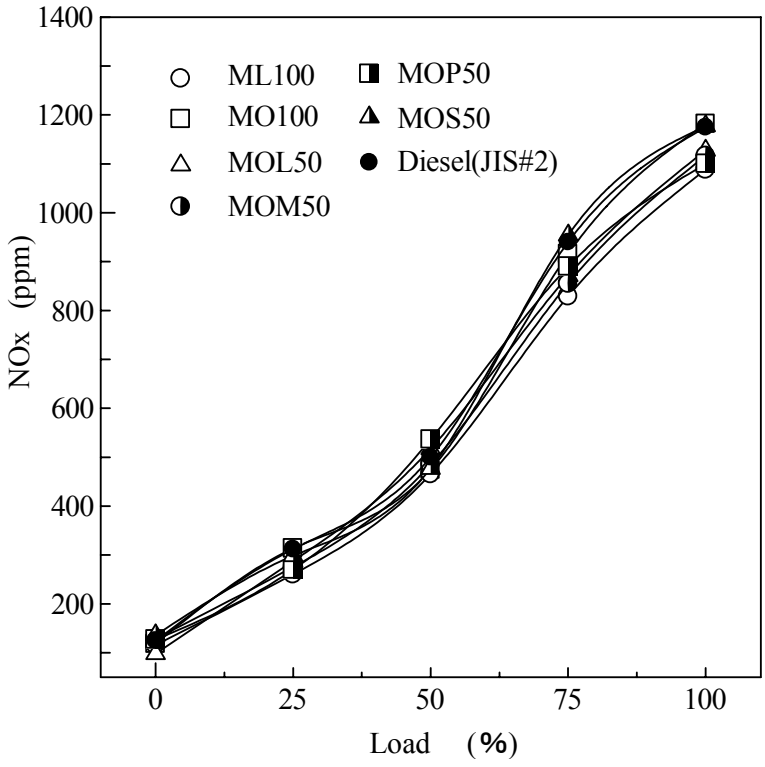

Figure 4.11 NOx emissions of the test fuels

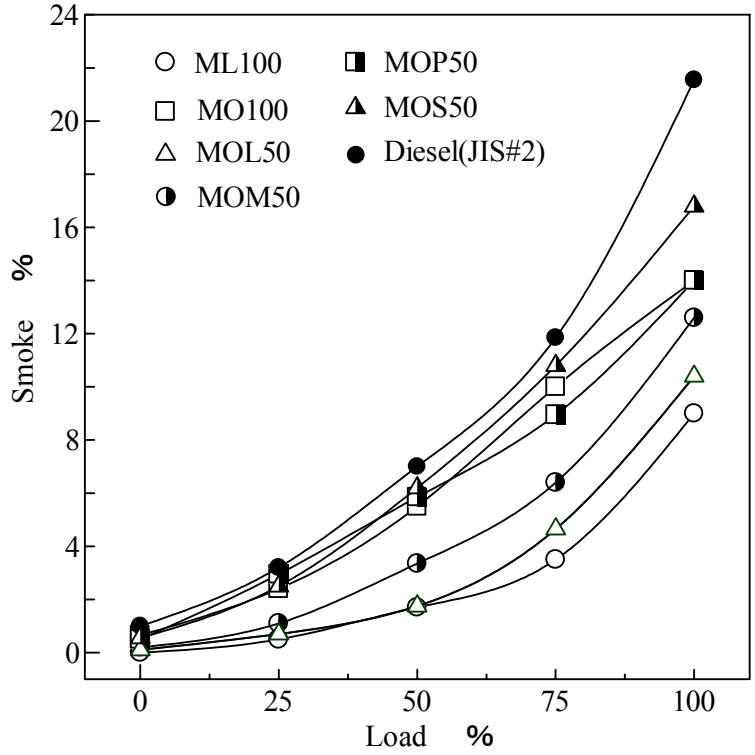

Figure 4.12 Smoke emissions of the test fuels

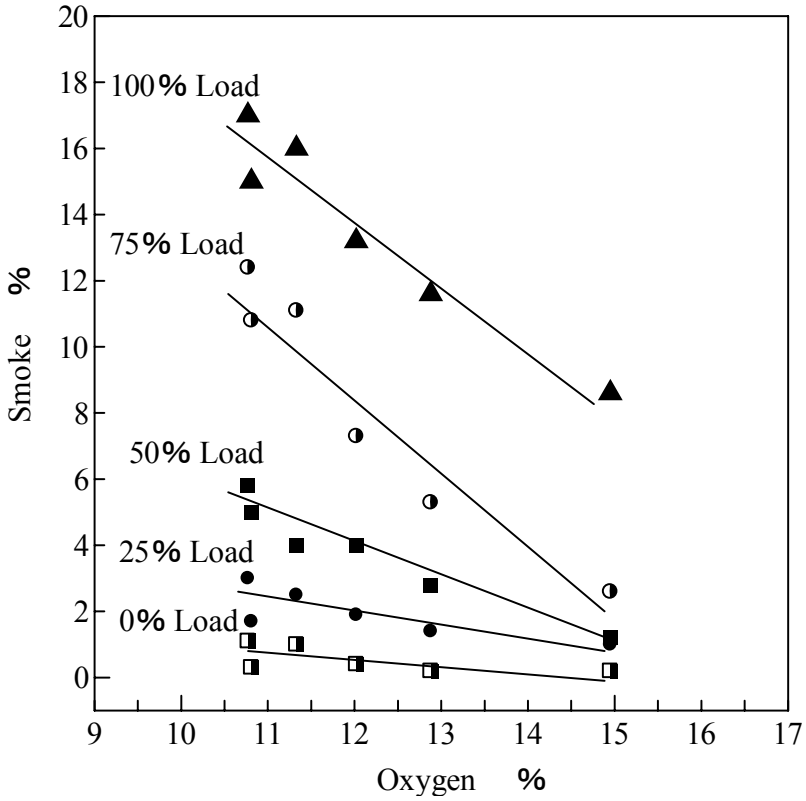

Figure 4.13 Relation of smoke emissions and oxygen contents

Figure 4.13. It can be seen from Figure 4.13, the more oxygen contents in fuel make the less smoke emissions and the more reduction in smoke emissions are found at the higher load levels. Therefore it can be said that, the oxygen contents of FAME fuels influence the smoke emission.

4.2.4 Conclusions

In order to investigate the combustion characteristics and exhaust emissions of various single composition of FAMEs those contain major composition in vegetable oils, the engine experiments were carried out by fueling with ML100, MO100, MOL50, MOM50, MOP50 and MOS50. From the experimental results of these FAME fuel, estimation for pure FAMEs can be drawn and the conclusions are as follow.

For six kinds of FAME fuels

(1) The ignition delay of MOS40 is shorter than those of the other FAME fuels and the ignition delay increases in the following order: MOS50<MOP50 <MOM50<MO100<MOL50<ML100.
(2) The peak of heat release rate of ML100 is the highest in the FAME fuels and the descending order of peak of heat release rate is ML100>MOL50>MO100 >MOM50>MOP50>MOS50.
(3) The brake thermal efficiencies of all FAME fuels are almost the same.
(4) The HC and CO emissions from ML100 are lowest and from MO100 are highest in the FAME fuels.
(5) The NOx emission from ML100 is lowest and from MO100 is highest in the FAME fuels.
(6) The smoke emission from MO100 is lower and from MOS50 is higher compared to the other FAME fuels.

For single composition of FAMEs

(1) The ignition delays of saturated FAMEs such as methyl laurate, methyl myristare, methyl palmitate and methyl stearate, may decrease with the longer straight chain and while FAMEs with the same carbon numbers like methyl

stearate and methyl oleate, the ignition delays may increase by increasing carbon-carbon double bonds.

(2) The ignition ability of methyl stearate may be better than those of methyl laurate, methyl myristare, methyl palmitate and methyl oleate.

(3) The NOx emission from methyl laurate may be less than those of methyl myristare, methyl palmitate methyl stearate, and methyl oleate.

(4) The smoke emission from methyl laurate may be less than those of methyl myristare, methyl palmitate methyl stearate, and methyl oleate.

4.3 Effect of Unsaturation Degree of Fatty Acid Methyl Ester on Diesel Combustion Characteristics

4.3.1 Test Fuels

In this experiment, to investigate the effect of unsaturation degree of fatty acid methyl esters (FAMEs) on the combustion characteristics in diesel engine, vegetable oils with three different unsaturation degrees of fatty acid such as high oleic safflower oil, high lonoleate safflower oil and linseed oil were used as substitutes for methyl oleate, methyl linoleate and methyl linolenate. High oleic safflower oil contains about 80% of oleic acid (18:1), high linoleate safflower oil contains about 77% of linoleic acid (18:2) and linseed oil contains about 59% of linolenic acid (18:3), in their fatty acid compositions respectively. The fatty acid compositions of high linoleate safflower oil, high linoleate safflower oil and linseed oil are shown in Table 4.4. In the test fuels preparing processes, high oleic safflower oil, high linoleate safflower oil and linseed oil and were transesterified to high oleic safflower oil methyl ester named as $SFME_{HO}$, high linoleate safflower oil methyl ester named as $SFME_{HL}$ and linseed oil methyl ester named as LME. In transesterification reaction, the molar ratio of oil to methanol was 6:1 and 1% mass of KOH to oil was used. The reaction was taken for two hours at reaction temperature 60˚C. After the end of the reaction, the mixture was kept at

Table 4.4 Fatty acid compositions of vegetable oils (31)

Fatty acid	C:N	Vegetable oil, wt%		
		H.O Safflower	H.L Safflower	Linseed
Myristic	14:0	0.34	-	-
Palmitic	16:0	5.46	8.6	4.92
Stearic	18:0	1.75	1.93	2.41
Oleic	18:1	79.36	11.58	19.7
Linoleic	18:2	12.86	77.89	18.03
Linolenic	18:3	-	-	54.94
Arachidic	20:0	0.23	-	-

Table 4.5 Properties of test fuels

Properties		$SFME_{HO}$	$SFME_{HL}$	LME	JIS#2
Cetane number		56*	50*	48*	56
Net calorific value	(MJ/kg)	36.33	36.21	36.14	43.12
Density@288K	(kg/m^3)	881	887	894	826
Kinematic viscosity@313K	(mm^2/sec)	3.93	3.24	2.98	2.5
Pour point	(^0C)	-10	-	-	-12.5
C	(% mass)	77	77.3	77.6	87.3
H	(% mass)	12.1	11.8	11.4	12.5
O	(% mass)	10.9	10.9	11	0
Sulphur	(ppm)	<6	<6	<6	<50
Water	(% mass)	0.08	0.07	0.11	-
Potassium	(mg/kg)	<5.0	<5.0	<5.0-	-
Methanol	(% mass)	<0.2	<0.2	<0.2	-
Monoglyceride	(% mass)	0.083	0.39	0.07	-
50% Distillation temperature	(^0C)	339	338	338	278
Stoichiometric air-fuel ratio		12.7	12. 8	12.6	14.2

* Estimated value

the ambient temperature 20- 25˚C for eight hours and then the settled down glycerin layer was drained off. At last the residual methanol in methyl ester mixtures was evaporated. For comparison, the diesel fuel (JIS #2) was also used as a test fuel.

The properties of test fuels are shown in Table 4.5. The cetane number of three FAME fuels were estimated from cetane number of single type FAMEs. The cetane number of $SFME_{HO}$ is 56 and it is the same as that of the diesel fuel, and the other two FAME fuels have smaller. The cetane number is reduced by increasing unsaturation of FAMEs. There are no differences in net calorific values between FAME fuels. But all are less than relative to the diesel fuel. The density of $SFME_{HO}$ is lowest and LME is highest in the FAME fuels. The kinematic viscosity of $SFME_{HL}$ is lowest and LME is highest in FAME fuels. Both density

and kinematic viscosity of FAME fuels are higher than that of the diesel fuel. The oxygen content of FAME fuels are about 11%.

4.3.2 Experimental Procedures

The experimental procedures of this experiment are the same procedures as expressed in the Chapter 3.

4.3.3 Results and discussion

Brake thermal efficiencies of test fuels are shown in Figure. 4.14. Brake thermal efficiencies of FAME fuels are not so different between them and they show higher brake thermal efficiencies than that of the diesel fuel. From this result, FAME fuels with more than 10% oxygen content may take better combustion and therefore they have better energy conversion rate compared to the diesel fuel. Brake specific fuel consumption of the test fuels are shown in Figure 4.15. In the FAME fuels, the differences in brake specific fuel consumptions are small. The brake specific fuel consumption is changing with the net calorific value of the fuel and application of loads. The higher brake specific fuel consumption of FAME fuels are due to the about 15% lower in net calorific value of these fuels compared to the gas oil.

Figure 4.16 shows the injection timing, the ignition delays, and the ignition timing of the test fuels. These values were derived from the needle lift of fuel injector and the heat release rate of the combustion chamber of the test engine. The fuel injection timings of FAME fuels are nearly the same as each other because of only small differences in density. But they are faster injection timing than that of the diesel fuel. The ignition delay times of $SFME_{HO}$ are shorter than the $SFME_{HL}$ and LME at all load levels. The ignition delay times order is the same order as the estimated cetane values of FAME fuels. Therefore, from this result, more unsaturated in FAMEs may cause longer ignition delay time or less ignition ability. The heat release rate of combustion chamber and the needle lift of fuel injector of test engine at 100% load level are shown in Figure. 4.13. The needle lift intervals among the FAME fuel are almost the same and longer than that of the diesel fuel. The reason for longer needle lift or fuel injection is the

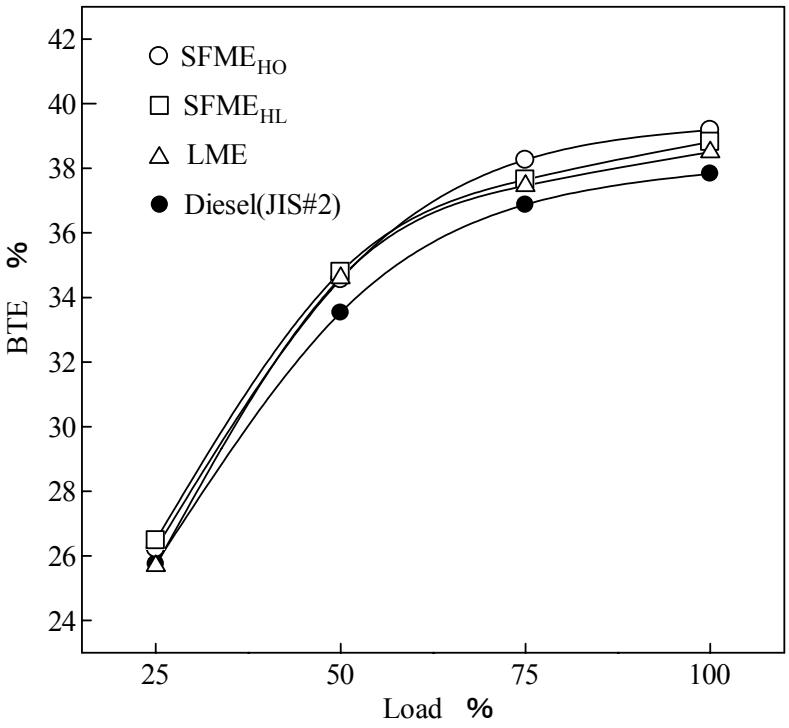

Figure 4.14 Brake thermal efficiency of the test fuels

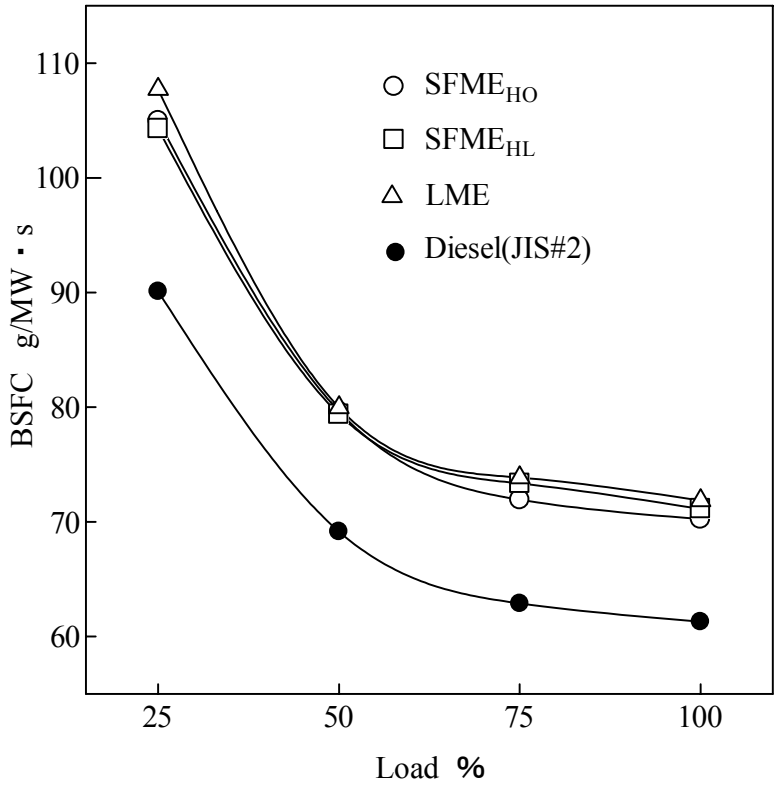

Figure 4.15 Brake specific fuel consumption of the test fuels

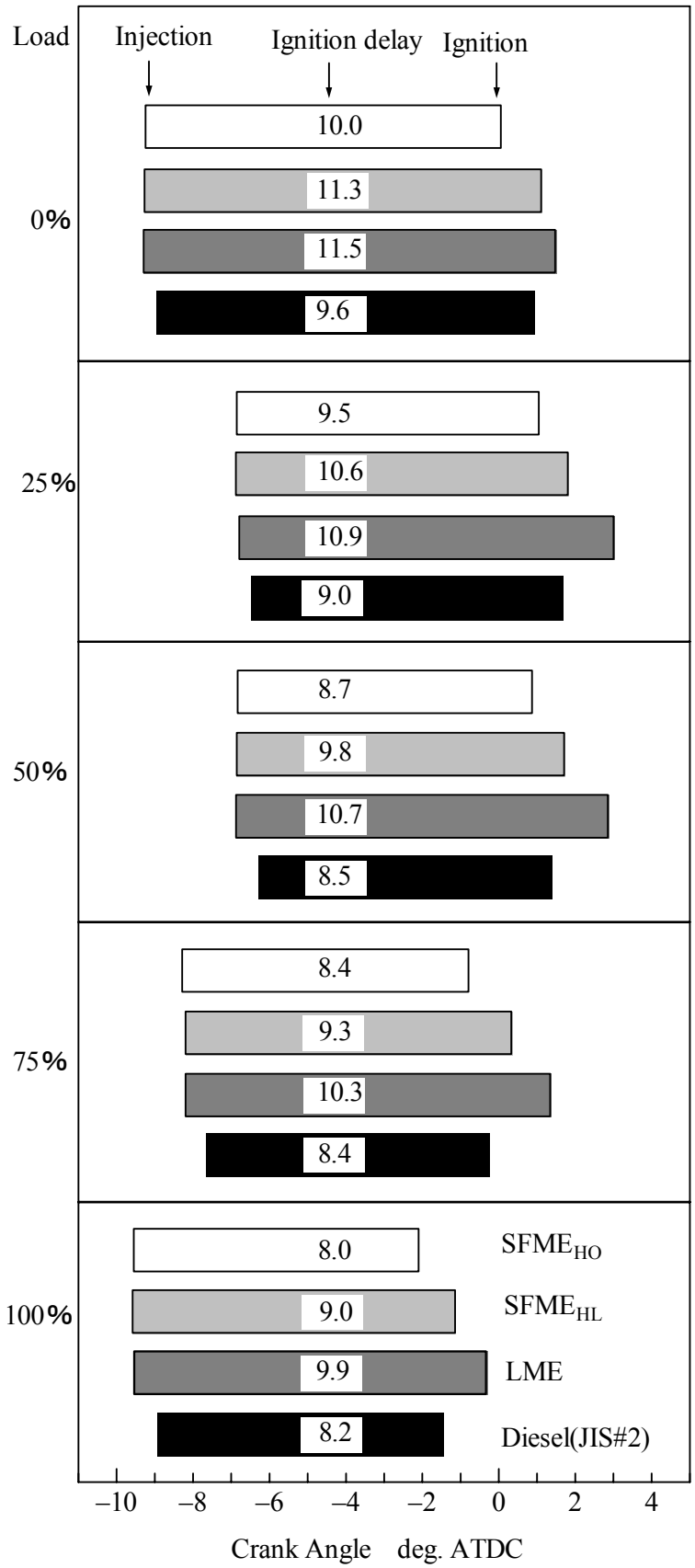

Figure 4.16 Injection, ignition delay and ignition

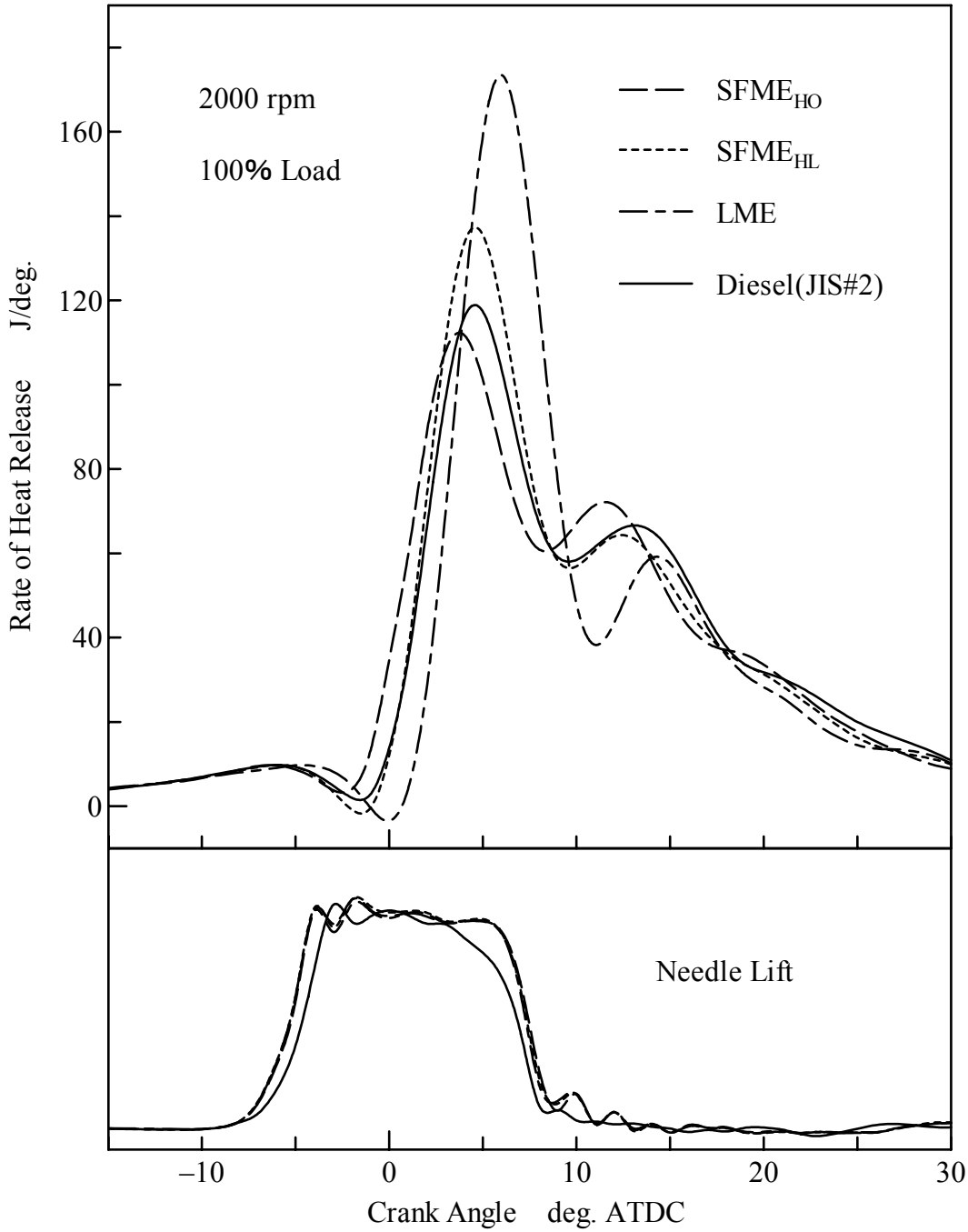

Figure 4.17 Heat release rate and needle lift

same reason explained in the section 4.2.3. The combustion start timing of $SFME_{HO}$ is faster than those of $SFME_{HL}$ and LME. The peak of heat release rate of LME is highest and $SFME_{HO}$ is lowest in the FAME fuel. It is probably concern with injection timing and ignition delay time. The faster injection timing and longer ignition delay time affect on the higher combustion temperature and heat

release rate. The combustion end timings of test fuels are likely the same.

The HC emission from the test fuels are illustrated in Figure 4.18. At 0% to 50% load levels, the HC emission from LME is the highest and $SFME_{HO}$ is the lowest. But there are small differences in 75% and 100% load levels. The cause and formation of HC emission is the same as discussed in the section 4.2.3. The CO emissions from test fuels are shown in Figure 4.19. The CO emission from $SFME_{HO}$ is the lowest and LME is the highest. The same trend of graph is found in both HC and CO emissions for FAME fuels. The NOx emission from the test fuels are shown in Figure 4.20. The NOx emissions of FAME fuels at 0-50% load levels are nearly the same and at 75% and 100% load levels, $SFME_{HO}$ is the lowest and LME is the highest. The smoke emissions from test fuel are shown in Figure 4.21. The smoke emission from $SFME_{HO}$ is lowest in the 0-25% load level. At 100% load level the smoke emission from LME is the lowest. The fluctuation of smoke emissions of FAME fuels is high from 0-100% load level.

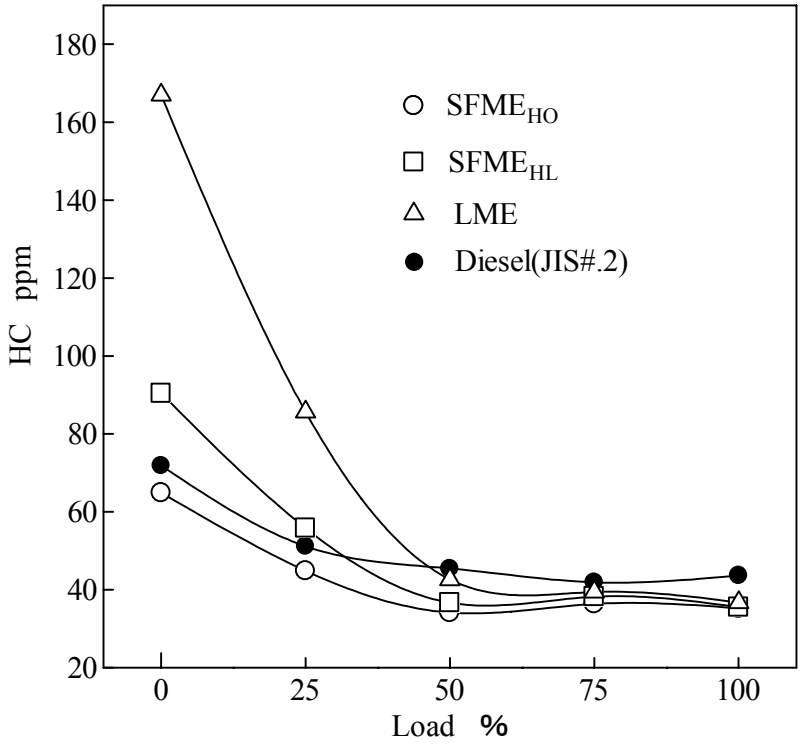

Figure 4.18 HC emissions of the test fuels

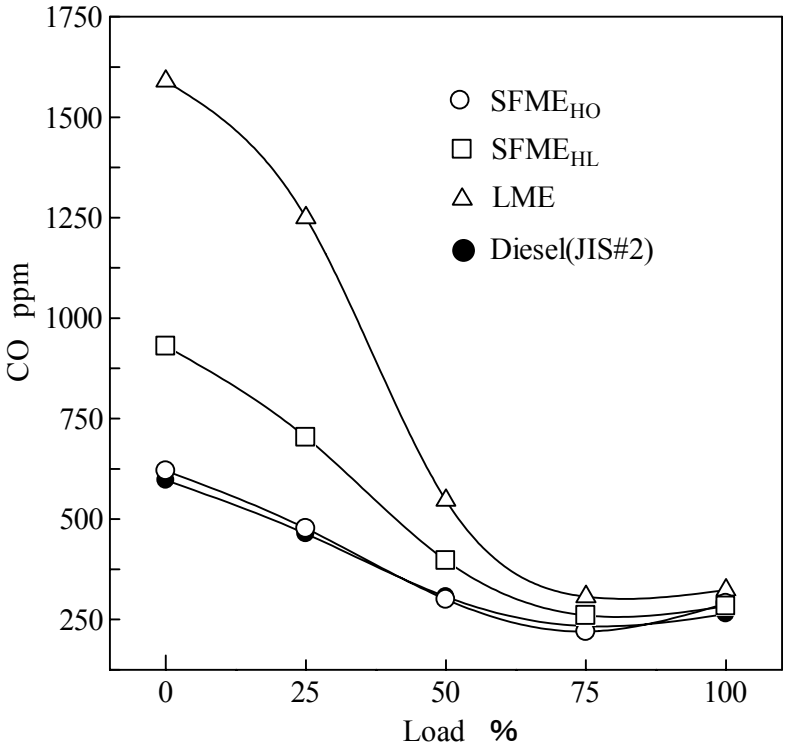

Figure 4.19 CO emissions of the test fuels

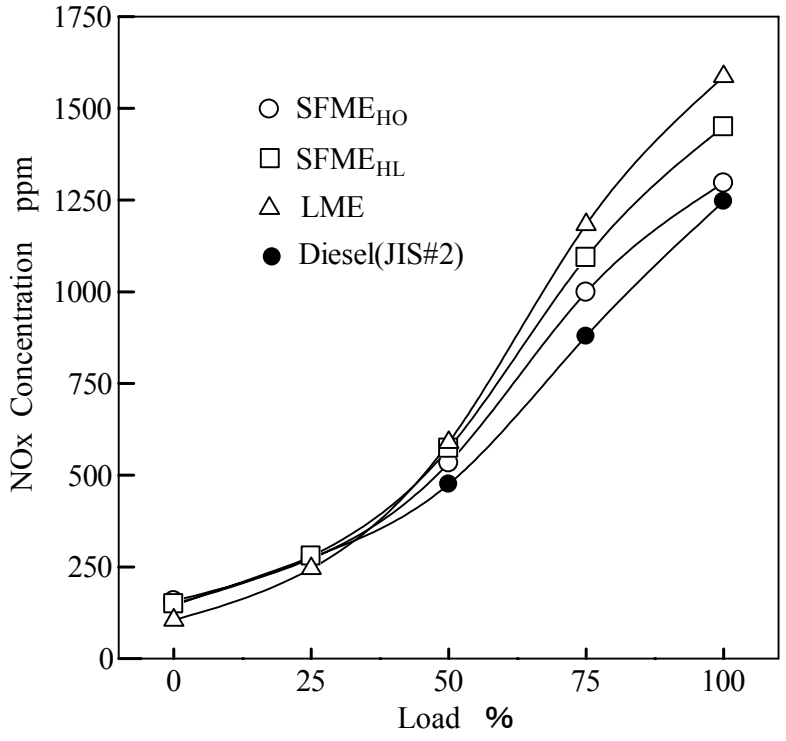

Figure 4.20 NOx emissions of the test fuels

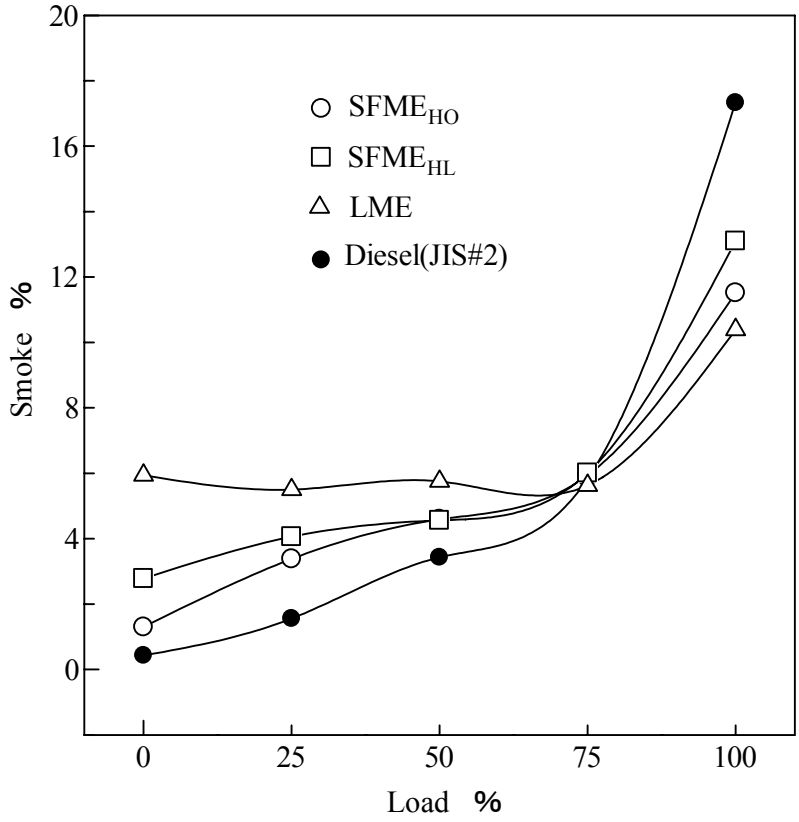

Figure 4.21 Smoke emissions of the test fuels

4.3.4 Conclusions

In order to investigate the combustion characteristics and exhaust emissions of three kinds of unsaturated FAMEs with the same carbon number and different degree of unsaturation, the engine experiments were carried out by fueling with $SFME_{HO}$, $SFME_{HL}$ and LME. From the experimental results the following conclusions can be drawn.

(1) Brake thermal efficiency and brake specific fuel consumption of $SFME_{HO}$, SFMEHL and LME are almost the same.
(2) The ignition delay of $SFME_{HO}$ is shorter than $SFME_{HL}$ and LME.
(3) The peak of heat release rate of $SFME_{HO}$ is lower than $SFME_{HL}$ and LME.
(4) The HC, CO, NOx and smoke emissions from $SFME_{HO}$ is lower than those of $SFME_{HL}$ and LME in most of the load levels.

5. THE EFFECT OF FATTY ACID COMPOSITION ON COMBUSTION CHARACTERISTICS OF BIO-DIESEL

5.1 Introduction

The effect of FAME composition on biodiesel can be seen by comparing the results of the engine experiments of vegetable oil methyl ester fuels and pure FAME fuels. Particularly, the FAME compositions clearly affect on the combustion characteristics of biodiesels. On the other hand, the combustion characteristics are affected by fuel properties such as physical and chemical properties of the fuel. In this chapter, the effect of fatty acid composition on fuel properties, combustion characteristics and exhaust emissions of biodiesel will be summarized and discussed.

5.2 Fatty Acid Composition and Fuel Properties of Biodiesel

Since biodiesel is produced from vegetable oils, animal fats and used cooking oil, the properties of finished biodiesel depend mainly on the feedstock. On the other hand, the main components of vegetable oils and animal fats are fatty acids and therefore fatty acid compositions influence the properties of biodiesel. These properties are both physical and chemical properties, including fuel properties such as cetene number, density, kinematic viscosity, bulk modulus and pour point. Generally, most of vegetable oils contain fatty acids usually with the carbon numbers ranging from C6 to C18. Some of these fatty acids are saturated, while others are unsaturated. The differing levels of saturation can affect some of the fuel properties. In addition, the experimental results have shown that differing biodiesel properties can also lead to different condition of combustion process and levels of exhaust emissions from diesel engine.

In this study, in order to understand the effect of fatty acid composition on the fuel properties of biodiesel, the cetane number, density, kinematic viscosity, distillation temperature and pour point of FAME fuels and vegetable oil methyl ester fuels from the experimental results will be summarized as follows.

5.2.1 Cetane Number

The cetane number is dimensionless descriptor of the ignition quality of a diesel fuel. As such, it is a prime indicator of diesel fuel quality. The cetane number of a diesel fuel is determined by the ignition delay time. The shorter the ignition delay time, the higher the cetane number and vice versa. Too high or too low cetane number can cause operational problems like incomplete combustion. Most diesel engine manufacturers designate a range of required cetane number usually 50-60 for their engines.

Generally, biodiesel or FAMEs has suitable cetane number for diesel engine. Long chain, saturated and unbranched hydrocarbons have suitable cetane number and good ignition ability while unsaturated and branched hydrocarbons have lower cetane number and poor ignition ability (36). Also cetane number generally increases with increasing chain length (40). From the experimental results of FAME fuels, MOS50 showed shorter ignition delay than the other FAME fuels and it may have higher cetane number. Therefore, from the experimental results of vegetable oil methyl ester fuels, the higher cetane number of PME than the other methyl ester fuels is because of higher content of larger carbon number saturated FAME like methyl palmitate. In case of CME and PKME, they are consisting smaller carbon number saturated FAMEs, methyl laurate, and so their cetane numbers are just enough as diesel fuels. It should be noted from the experimental results of vegitable oil methyl ester fuels and FAME fuels that, saturated FAMEs type biodiesels have much higher cetane numbers than the unsaturated FAMEs type biodiesels

5.2.2 Density

The density is usually expressed as a specific gravity. The density is directly proportional to the buck modulus. The density, speed of sound and buck modulus make the greatest effect on the injection timing of the diesel engine. Higher density and buck modulus make earlier injection timing. The early injection timing produces higher cylinder temperature or more NOx emission (35). The density, speed of sound and buck modulus increase as the chain length increase and higher for more unsaturated ester (33). Also the buck modulus of saturated

fatty acid methyl ester is lower than that of unsaturated fatty acid methyl ester. It can be seen from the FAME fuels in this study, the density of unsaturated FAMEs, MO100 and LME are higher than the other saturated FAME fuels. By contrasting among saturated FAMEs, slightly higher densities can be found in larger carbon number saturated FAMEs. Therefore lower density of CME and PKME are expected due to the higher content of small carbon number saturated FAMEs such as methyl laurate and higher density of SME and RME may be because of more unsaturated FAME such as methyl oleate and methyl linoleate. It can be seen from the experimental results of vegitable oil methyl ester fuels and FAME fuels that, saturated FAMEs type biodiesels have lower density than the unsaturated FAMEs type biodiesels

5.2.3 Kinematic Viscosity

Viscosity is a measure of a fluid resistance to flow. The greater the viscosity, the less readily the liquid flows. In diesel combustion, high viscosity leads to poorer atomization of the fuel spray, less accurate operation of fuel injector and more deposit formation in fuel injector and combustion chamber (41). Also it is known that when the viscosity of the fuel increases, the cone angle of fuel spray decreases, and the diameter of fuel droplets and their penetration increase. Thus, the liquid of fuel spray can touch the combustion chamber wall and the piston surface, causing heavy carbon deposits on the walls, piston ring sticking and breaking, and diluting the lubricating oil (42). Moreover high viscosity can cause early fuel injection due to high line pressure, which moves the combustion of the fuel closer to top dead center, increasing maximum pressure and temperature in the combustion chamber (43,44). In FAMEs, when chain length increases, the viscosity increases, and when the degree of unsaturation increases, the viscosity decreases (45). Comparing kinematic viscosity of FAME fuels in this study, ML100 and MOL50 have lower kinematic viscosity and their values are closed enough to that of the diesel fuel. So it can be said that the proper kinematic viscosity of CME and PKME are because of higher contents of methyl laurate. Alternatively, the higher RME and SME are probably because of higher contents of methyl oleate and methyl linoleate. It would be remarked from the

experimental results of vegetable oil methyl ester fuels and FAME fuels that, saturated FAMEs type biodiesels have lower kinematic viscosity than the unsaturated FAMEs type biodiesels

5.2.4 Distillation Temperature

The distillation temperature of a fuel is to determine the fuel volatility. Lower distillation temperature means higher or good fuel volatility and it make better fuel air mixture formation in the combustion process. The boiling points of FAMEs increase with the carbon number increases and decrease when the degree of unsaturated increases (46). In this study, the lower distillation temperatures of CME and PKME may be because of higher content of lower boiling point FAMEs such as methyl laurate and their distillation temperatures are almost the same as that of the diesel fuel (JIS#2). Therefore comparing the experimental results of vegetable oil methyl ester fuels and FAME fuels, much constituent of smaller carbon number saturated FAMEs lower the distillation temperature of biodiesels.

5.2.5 Pour Point

The pour point is a measure of cold flow property of a fuel. At pour point temperature, the fuel can not be flown. The pour point temperatures become higher as the chain length increases in saturated FAMEs and become lower for more unsaturated FAMEs (46). From the fuel properties of FAME fuels in this study, it can be seen that, the pour point temperature MO100 is the lowest and MOS50 is the highest among the FAME fuels. Therefore, PME with the higher content of larger carbon number saturated fatty acid (methyl palmitate) has higher pour point and RME with the higher content of unsaturated FAMEs (methyl oleate) has lower pour point among the vegetable oil methyl ester fuels. Although the pour point of RME, -7.5˚C, is the lowest in the vegetable oil methyl ester fuels used in this study, but it is 5˚C higher than that of the diesel fuel (JIS#2). Therefore, the vegetable oil methyl ester fuels in this study have not sufficient cold flow property to use in the cold region and it is necessary to improve the cold flow properties of these fuels by using cold flow improver or some additives to lower the pour point.

5.2.6 Summarization

Comparing the fuel properties of vegetable oil methyl ester fuels and FAME fuels, the summarization of pros and cons of saturated and unsaturated composition of FAME fuels and vegetable oil methyl ester fuels are as expressed in Table 5.1 and 5.2.

Table 5.1 Summarization of some fuel properties of biodiesels

Properties	High Saturated Bio CME, PKME	Medium Saturated Bio PME	High Unsaturated Bio RME, SME
Cetane no.	Medium	High	Low
Density	Low	High	High
Kinematic Viscosity	Low	High	High
Distillation temperature	Low	High	High
Pour point	Medium	Higher	Medium

Table 5.2 Summarization of some fuel properties of FAMEs

Properties	ML100, MOL50	MOM50, MOP50	MOS50	MO100, $SFME_{HO}$	$SFME_{HL}$, LME
Cetane no.	Medium	High	High	Medium	Low
Density	Low	Medium	Medium	High	High
Kinematic Viscosity	Low	High	High	Medium	Medium
Distillation temperature	Low	Medium	High	Medium	Low
Pour point	High	High	Higher	Low	Lower

5.3 Fatty Acid Composition and Combustion Characteristics of Biodiesel

It should be required to understand the basic concept of combustion in diesel engine before discussing about the combustion characteristics of biodiesel. Since the combustion process, including physical and chemical processes taking place in the combustion chamber are very complex and difficult to understand. In combustion process, the fuel is injected into a combustion chamber under high pressure, and then it atomizes into small droplets and begins to evaporate as it moves away from the fuel injector. The fuel air ratio at any point in the combustion chamber may range from zero, at a point with no fuel, to infinity, inside a fuel droplet that has not yet vaporized. In general, the fuel-air ratio is high near the fuel injector tip and low away from it, but because of the complexity of the mixing process, the fuel-air ratio does not change uniformly within the combustion chamber. Combustion can only occur within a certain range of the fuel-air ratio; if the ratio is too low, there is not enough fuel to support combustion, and if the ratio is too high, there is not enough air to take combustion process. As the injected fuel vaporizes into the hot air, it starts to oxidize. As more fuel vaporizes and mixes with air, the number of the oxidation reaction increase until the end of the ignition delay period, when ignition occurs at many locations independently and combustion propagates very rapidly in regions which have fuel-air ratio in the combustible range. This initial combustion after ignition is called the premixed combustion phase; it consumes only about 5% to 10% of the fuel used by the engine at typical full-load operation. At the end of the premixed combustion phase, most of the fuel has yet to be injected or is still in a region that is too rich to burn. But injection continues and fuel continues to vaporize and mix with air, aided by heat release and turbulence generated by the premixed combustion. This quickly generates more gas with the required fuel-air ratio and combustion continues. This is the diffusion controlled phase of combustion and, ideally consumes all of the remaining fuel.

Most of the biodiesels have suitable cetane numbers to occur the diesel combustion process. Furthermore, biodiesel is an oxygenated fuel which containing 10% to 15% oxygen by weight and that provides biodiesel to take more complete combustion. In this study, in order to understand the combustion

characteristics of biodiesel, fuel injection timing, fuel injection interval, and combustion start timing, ignition delay time and heat release rate of FAME fuels and vegetable oil methyl ester fuels from the experimental results will be discussed as follows.

5.3.1 Fuel Injection Timing

The fuel injection timing is mainly influenced by the physical properties of the fuel, especially the density, bulk modulus and kinematics viscosity of the fuel. The higher density, bulk modulus and kinematics viscosity fuel have less damping action and lead faster needle lift and injection timing. The faster injection timing causes the faster combustion and relating the increase of maximum pressure and temperature in the combustion chamber, and higher exhaust emissions. From the experimental results of FAME fuels, the higher density and kinematic viscosity of MO100, MOP50, MOS50, $SFME_{HO}$, $SFME_{HL}$ and LME showed faster fuel injection timings relative to other FAME fuels with lower density and kinematic viscosity. Also it was found in vegetable oil methyl ester fuels experiment, higher density and kinematic viscosity of PME, RME and SME showed faster fuel injection timing compared to lower density and kinematic viscosity fuels, CME and PKME.

5.3.2 Fuel Injection Interval

The fuel injection interval is the duration of fuel injection from fuel injector into the combustion chamber of diesel engine. The fuel injection interval varies with the heating value or net calorific value of the fuel. The lower net calorific value fuel is needed extra amount of fuel to occur the same amount of heat and to take the combustion process. Therefore, lower net calorific fuel take longer fuel injection time compared to the higher one. From the experimental results of FAME fuels, the lower net calorific value of ML100 and MOL50 showed longer fuel injection interval relative to other FAME fuels. Also it can be seen in vegetable oil methyl ester fuels experiment, lower net calorific value of CME and PKME were needed longer fuel injection interval compared to those of PME, RME and SME.

5.3.3 Combustion Start Timing

The combustion start timing is greatly important for the combustion process of the diesel engine. Improper combustion start timing causes incomplete combustion process and other negative effects like HC, CO and smoke emission increases. The combustion start timing is affected by the faster injection timing and the higher cetane number. Therefore from the experimental results of FAME fuels, the faster combustion start timings of MO100, MOP50 and MOS50 are likely to be the result of faster fuel injection and higher cetane number relative to other FAME fuels and the diesel fuel. From the experimental results of vegetable oil methyl ester fuels, PME which mainly contained methyl plamitate, has higher cetane number and faster fuel injection timing relative to the other test fuels. Therefore, PME showed faster combustion timing compared to the other methyl ester fuels.

5.3.4 Ignition Delay Time

The ignition delay time shows the ignition ability of a diesel fuel. It is the period between the start of injection and the start of combustion. The ignition delay time is mainly influenced by the cetane number of the fuel. It is known that, the larger cetane number fuel has the shorter ignition delay time. From the experimental results of FAMEs fuels, MOS50 showed shorter ignition delay time and LME exhibited longer ignition delay time relative to the other FAME fuels. It is the fact that, the long chain, saturated and unbranched hydrocarbons have suitable cetane number and good ignition ability as diesel fuel while unsaturated and branched hydrocarbons have lower cetane number and poor ignition ability (36). Therefore, from the experimental results of vegetable oil methyl ester fuels, it is clear that PME which contains mainly larger carbon number saturated FAMEs such as methyl palmitate, showed shorter ignition delay time and SME with higher content of unsaturated FAMEs like methyl linoleate showed longer ignition delay time. It should be noted from the experimental results of vegetable oil methyl ester fuels and FAME fuels that, saturated FAMEs type biodiesels (CME, PME and PKME) have better ignition ability than the unsaturated FAMEs type biodiesels (RME and SME).

5.3.5 Heat Release Rate

The heat release rate or combustion rate is the rate of heat emits rapidly just after the ignition. Generally, cetane number, ignition delay time, fuel volatility, amount of combustible mixture and net calorific value of the fuel affect on the heat release rate. To determine the heat release rate, the ignition delay time and fuel volatility are two most important fuel properties. The fuel with the higher cetane number is expected to shorten the ignition delay period and thus lower amount of fuel in the premixed combustion portion of the combustion process. The premixed combustion is the initial period of rapid combustion that follows ignition. It involves fuel that was prepared to burn during the ignition delay period. High levels of premixed combustion are often associated with early start of combustion with high temperature and pressure. But lower amount of premixed combustion is expected to be a result of shorter ignition delay, which provides less time for the preparation of premixed fuel. From the experimental results of FAMEs fuels, ML100, MOL50 and LME showed higher heat rates than the other FAME fuels and the diesel fuel. The higher heat release rate of ML100, MOL50 and LME were expected due to the higher level of premixed combustion associated with longer ignition delay times compared to the other FAME fuels.

Lower distillation temperature of fuel means higher volatility or vaporization of fuel. Therefore CME and PKME are higher volatility fuels. Higher volatility of CME and PKME allow much amount of fuel that vaporizes during ignition delay period, and increasing the amount of combustible mixture in the combustion chamber and premixed portion of the combustion. Thus, the peak of heat release rate of CME and PKME are higher than that of PME, even PME has slightly shorter ignition delay time that of CME and PKME. The higher peak of heat release rate of RME and SME are expected due to the longer ignition delay and higher net calorific value compared to those of CME and PKME. Longer ignition delay time makes more combustible mixture and premixed combustion and if the same amount of fuel combust, the higher net calorific value fuel may emit more heat quantity in the combustion process. Thus, higher peak of heat release rate of RME and SME compared to those of CME, PME and PKME are probably due to higher net calorific values.

5.3.6 Summarization

Comparing the experimental results of vegetable oil methyl ester fuels and FAME fuels, saturated FAMEs such as methyl laurate, methyl plamiate and methyl stearate, and saturated fatty acid type biodiesel such as CME, PME and PKME have better combustion characteristics. The summarization of combustion characteristics from experimental results is as shown in Table 5.3 and 5.4.

Table 5.3 Summarization of combustion characteristics of boidiesels

Properties	High Saturated Bio CME, PKME	Medium Saturated Bio PME	High Unsaturated Bio RME, SME
Fuel injection timing	Proper	Faster	Fast
Fuel injection interval	Longer	Long	Long
Combustion start timing	Proper	Faster	Proper
Ignition delay time	Short	Shorter	Long
Heat release rate	Low	Lower	High

Table 5.4 Summarization of combustion characteristics of FAMEs

Properties	ML100/ MOL50	MOM50/ MOP50	MOS50	MO100/ $SFME_{HO}$	$SFME_{HL}$/ LME
Fuel injection timing	Proper/ Fast	Fast	Faster	Faster	Faster
Fuel injection interval	Longer	Long	Short	Long	Longer
Combustion start timing	Proper	Faster	Faster	Fast	-
Ignition delay time	Short	Shorter	Shorter	Long	Longer
Heat release rate	High	Low	Lower	High	Too high

5.4 Effect of Fatty Acid Composition and Exhaust Emissions of Biodiesel

Exhaust emissions are the Achilles` heel of diesel engine. Diesel exhaust tends to be high in NOx and particulate matters (PM), both visible smoke and invisible emissions. But diesel exhaust contains much less unburned or partially burned hydro carbon (HC) emission and carbon monoxide (CO) emission. Several studies on biodiesels have shown that the exhaust emissions from biodiesel are different on the feedstock used to make biodiesels. Indirectly, this means the different compositions of fatty acids emit different exhaust emission levels of biodiesels. One of the distinctive properties of biodiesel is an oxygenated fuel containing 10% to 15% oxygen by weight. That leads biodiesel to more complete combustion and less most of the exhaust emissions from diesel engine.

In this study, in order to understand the effect of fatty acid composition on the exhaust emission of biodiesel, the unburned hydro carbon (HC) emission, carbon monoxide (CO) emission, nitrogen oxides (NOx) emission and smoke emission of FAME fuels and vegetable oil methyl ester fuels from the experimental results will be summarized as follows.

5.4.1 HC Emission

The HC emission can be either unburned or partially burned fuel. Therefore the cause of HC emission is entirely depending on the combustion process. Incomplete combustion process produces HC emission or unburned fuel emission. In the combustion process, if a fuel-rich mixture does not get enough oxygen to react with all the carbon, result higher level of HC emission. From the experimental results of FAME fuels, ML100 emitted lower and MO100 emitted higher HC emission relative to the other FAME fuels. The most unsaturated FAME fuel LME emitted the highest CO emission. Most of HC emissions of FAME fuels at 0-100% load are descending along with the more oxygen content in the FAME fuels. It may be because of more oxygen in fuel support the combustion process by reducing fuel rich zone or incomplete combustion. Therefore, from the experimental results of vegetable oil methyl ester fuels, it is clear that CME and PKME which contain about 3wt% much oxygen than the other methyl ester fuels emitted the lowest HC emissions. But higher HC

emissions from RME and SME are probably due to the less content of oxygen compared to CME and PKME.

5.4.2 CO Emission

The cause of CO emission from diesel combustion is similar as HC emission. Generally, CO is generated when there is not enough oxygen to convert all carbon to CO_2, some fuel does not get burned and some carbon ends up as CO. The other factors of CO emission are poor fuel air mixing, local fuel rich region and incomplete combustion will create some CO. From the experimental results of FAME fuels, the CO emission from ML100 is the lowest and MO100 is the highest. Also most unsaturated FAME fuel LME emitted the highest CO emission. Most of CO emissions of FAME fuel at 0-100% load are descending along with the more oxygen content in the fuel. From the experimental results of vegetable oil methyl ester fuel, higher methyl laurate fuels, CME and PKME exhibited lower CO emissions. But higher CO emissions from RME and SME are expected due to the less content of oxygen and incomplete combustion processes.

5.4.3 NOx Emission

NOx emission from diesel engine is a primary concern. NOx emission can be described generally by three methods, these are thermal NOx, fuel NOx and prompt NOx. Each of these three pathways contributes to the overall NOx emission. But thermal NOx formation is the main contributer of NOx emission from the diesel engine. Thermal NOx is formed at high temperature in the combustion chamber when the oxygen and nitrogen in the air combines. The NOx emission is increase with the combustion temperature increase. NOx are formed in significant quantities starting above 1500˚C and the formation increase rapidly as the temperature increases (35). Additionally, the combustion rate also affects significant effect on the NOx emission. More premixed combustion means a high initial rate of combustion, which causes the fuel to burn earlier, and resulting higher gas temperatures and increased NOx emission (35). From the point of view of fuel properties, NOx emissions increase with increasing fuel density or decreasing fuel cetane number. From the point of view of fatty acid composition

of the fuel, increasing the number of double bonds or degree of unsaturation (quantified as iodine number) correlated with increasing emissions of NOx emission. For saturated fatty acid, the NOx emission increased with decreasing chain length from 18-12 carbon numbers (35). Nevertheless the saturated FAMEs type biodiesel exhibits lower NOx emission than unsaturated.

From the experimental results of FAME fuels, MO100 showed the higher NOx emission than the other FAME fuels and ML100 showed the lower NOx emission. In unsaturated FAME fuels, the highest NOx emission was found in the highest degree of unsaturated fuel, LME. Also the higher density and kinematic viscosity, faster injection timing of these fuels make higher NOx emission. From the experimental results of vegetable oil methyl ester fuels, saturated type biodiesels, CME, PME and PKME emitted lower NOx emissions compared to unsaturated type RME and SME. The lower NOx emission from CME and PKME are expected because of higher contents of methyl laurate and alternatively because of their lower density, kinematic viscosity and proper cetane number. Also not faster or proper injection timing of CME and PKME may be related with the lower NOx emissions. Furthermore, shorter ignition delay time of PME reduced less premixed combustion and less combustion temperature resulting less NOx emission from PME.

5.4.4 Smoke Emission

The exhaust of diesel engines contains solid carbon soot particles or particulate matter (PM), these are seen as smoke emission. Particulate matters are often fractioned in term of sulfate, soluble organic fraction (SOF) or volatile organic fraction (VOF) and carbon or soot (47). In the diesel combustion process, some of fuel droplets may never vaporize, and thus, never burn. But the fuel does not remain unchanged; the high temperatures in the combustion chamber cause it to decompose. Later, these droplets may be partly or completely burned in the turbulent flame. If they are not completely burned, they will be emitted as droplet of heavy liquid or carbon particles. The conversion of fuel to PM is most likely to occur when the last bit of fuel is injected in a cycle, or when the engine is being operated at high speed and high load. At higher speeds and loads, the total

amount of fuel injected increases and the time available for combustion decreases resulting higher smoke emission. Also, fuel rich region or no enough oxygen and mistimed fuel injection can substantially increase PM or smoke emission.

There are several ways or methods to measure the PM and smoke emissions. The most common ways are extracted SOF measurement, Bosch type smoke density measurement and opacity type measurement. In this study, also as explained in Chapter 2, the smoke emissions were measured by light transmitting opacity type smoke meter. From the experimental results of FAME fuels, ML100 and MOL50 emitted lower and MO100 and MOS50 emitted higher smoke emission than the other FAME fuels. The smoke emission in FAME fuels vary with the oxygen content of the fuel and the less smoke emission can be found in the fuel with the more oxygen content. The lower smoke emissions from ML100 and MOL50 are expected to the higher oxygen contents of these fuels, which provide to better combustion process. Moreover their proper injection timing as diesel fuel may contribute to occurring better combustion process and less smoke emission. In case of LME, it emitted higher smoke emission compared to SFME $_{HO}$ and SFME$_{HL}$ at lower load levels. This may be because of poor combustion process, which takes place in the lower load levels. From the experimental results of the vegetable oil methyl ester fuels, CME and PKME emitted lower smoke emission relative to PME, RME and SME. The lower smoke emissions from CME and PKME are higher content of methyl laurate and alternatively they contain larger amount of oxygen in fuels. Also their complete combustion process may reduce the smoke emissions from them.

5.4.5 Summarization

Based on the experimental results of vegetable oil methyl ester fuels and FAME fuels, smaller carbon number saturated FAMEs such as methyl laurate showed lower exhaust emissions and saturated fatty acid type biodiesel such as CME, PME and PKME emitted less emissions compared to unsaturated fatty acid type biodiesels, RME and SME. The summarizations of exhaust emissions from the experimental results are as shown in Table 5.5 and 5.6.

Table 5.5 Summarization of exhaust emissions of biodiesels

Emission	High Saturated Bio CME, PKME	Medium Saturated Bio PME	High Unsaturated Bio RME, SME
HC	Lower	Low	High
CO	Lower	Low	High
NOx	Lower	Low	High
Smoke	Lower	Low	High

Table 5.6 Summarization of exhaust emissions of FAMEs

Emission	ML100/ MOL50	MOM50/ MOP50	MOS50	MO100/ $SFME_{HO}$	$SFME_{HL}$/ LME
HC	Lower/ High	Low	High	Higher	Higher
CO	Lower/ Higher	High	Low	Higher	Higher
NOx	Lower/ Low	Low	Low	High	Higher
Smoke	Lower	Low	High	Higher	Higher

5.5 Development of Correlation Program between Fatty Acid Composition and Exhaust Emissions of Biodiesel

From the experimental emissions data of seven kinds of vegetable oil methyl esters (CME, PME, RME, SME, $SFME_{HO}$, $SFME_{HL}$ and LME) and five kinds of FAMEs (ML100, MOM50, MOP50, MOS50 and MO100), a correlation program was developed between FAMEs compositions and exhaust emissions. By analysing the experimental exhaust emissions data of vegetable oil methyl esters and FAMEs fuels, the assumption of the exhaust emissions (HC, CO, NOx and smoke emissions) of seven kinds of pure FAMEs (methyl laurate, methyl myristate, methyl palmitate, methyl stearate, methyl oleate, methyl linoleic and methyl linolenic) were conducted. Therefore the basic estimation on exhaust emission of vegetable oil methyl ester can be carried out by the exhaust emissions of seven kinds of pure FAMEs. The equation for the exhaust emission of vegetable oil methyl ester can be written as follow.

$$(EG)_{VOME} = \sum_{n=1}^{7} (EG)_n \chi_n$$

Where,

$(EG)_{VOME}$: exhaust emission of vegetable oil methyl ester

n: pure FAME constituent

χ_n: mass fraction of n (kg/kg)

$(EG)_n$: exhaust emission of n

Base on this equation, a computer program was drawn to estimate the exhaust emissions vegetable oil methyl ester accurately. The out line of flow diagram of correlation program is shown in Figure 5.1. By using this correlation program, the HC, CO, NOx and smoke emission estimations of vegetable oil methyl esters were carried out. The comparisons of experimental data and estimation data of exhaust emissions of vegetable oil methyl esters are shown in Figure.5.2 to 5.5. These figures give the percentage of differences between the experimental data and estimation data. In HC, CO and smoke emissions of

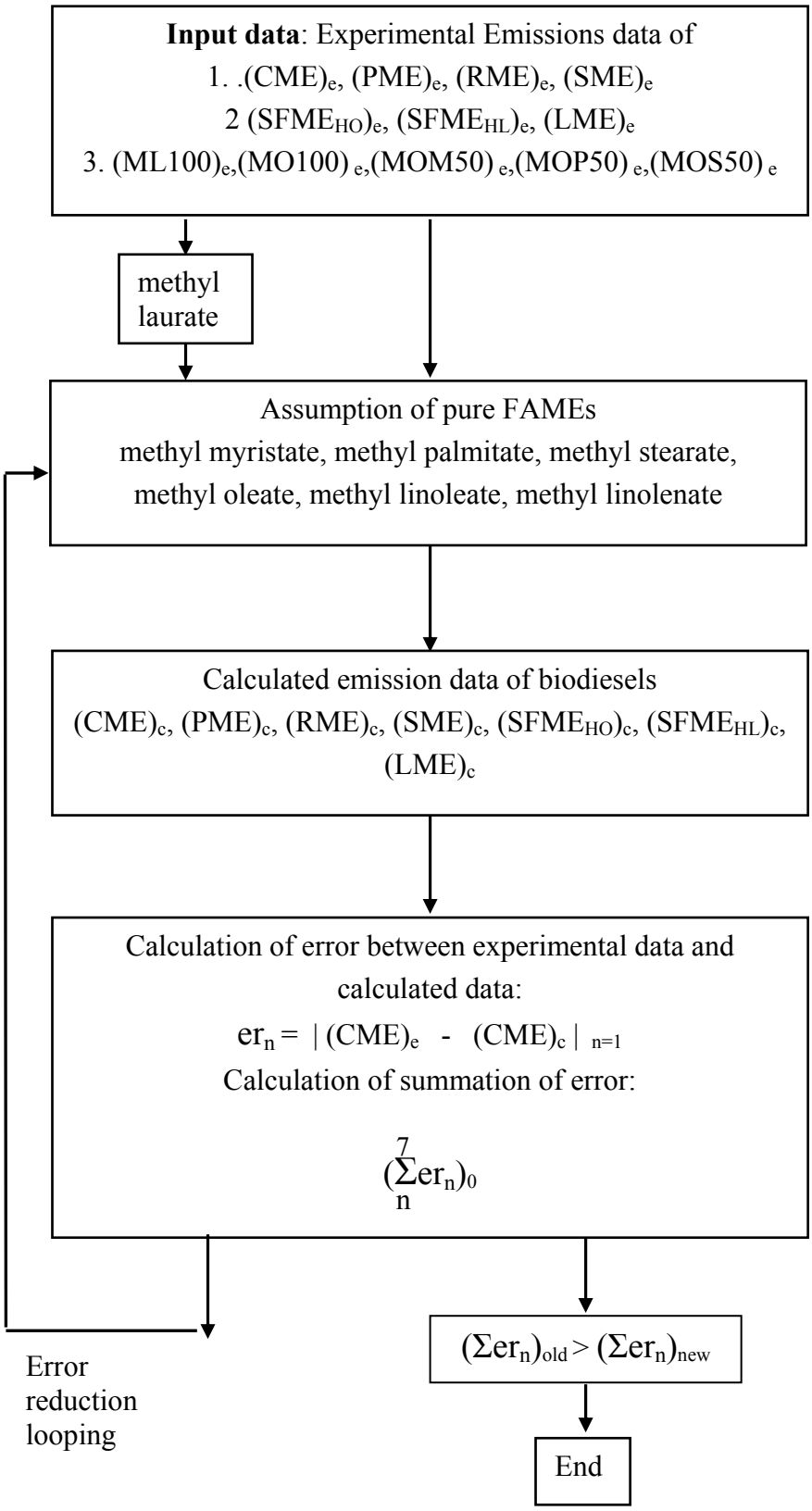

Figure 5.1 Flow diagram of correlation program

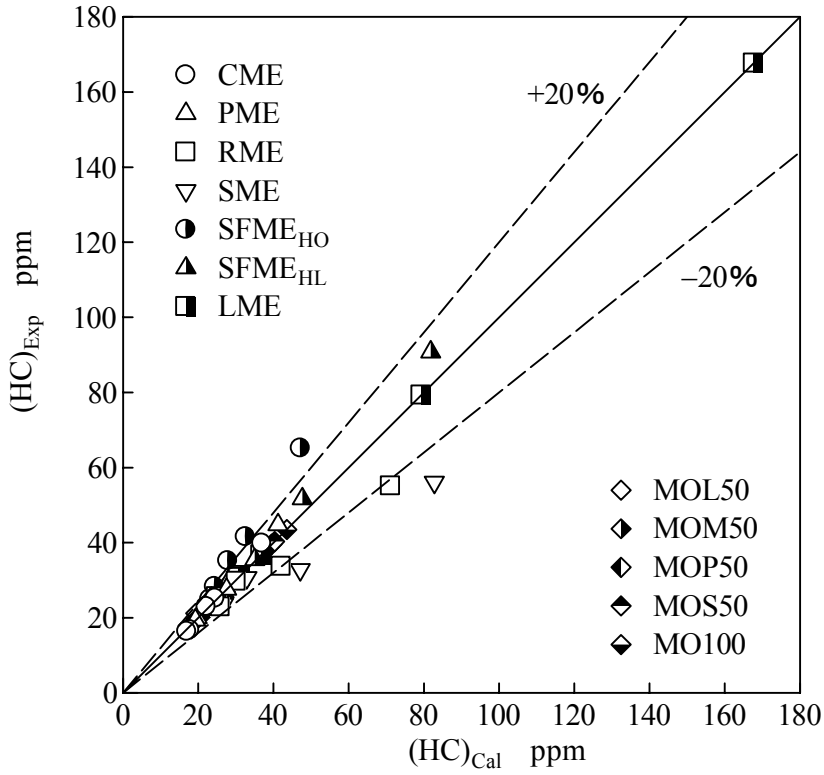

Figure 5.2 Comparison of $(HC)_{Exp}$ and $(HC)_{Est}$

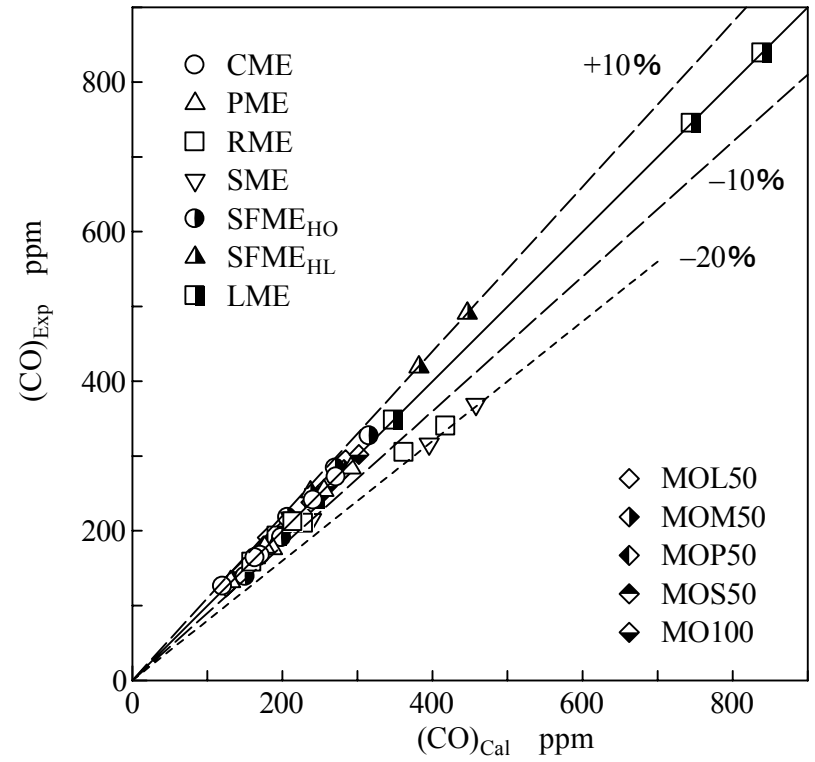

Figure 5.3 Comparison of $(CO)_{Exp}$ and $(CO)_{Estl}$

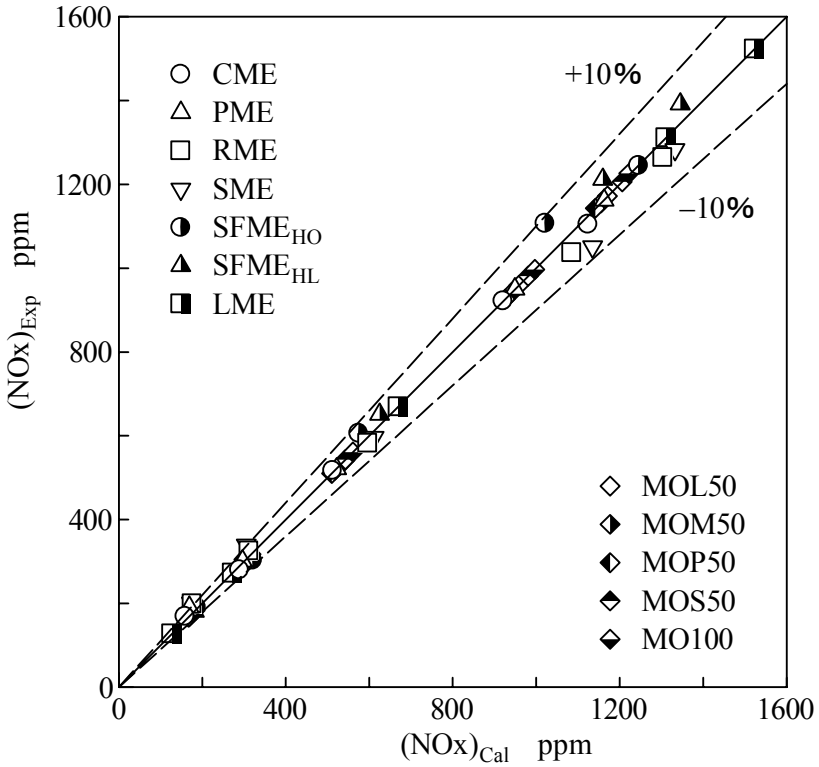

Figure 5.4 Comparison of $(NOx)_{Exp}$ and $(NOx)_{Est}$

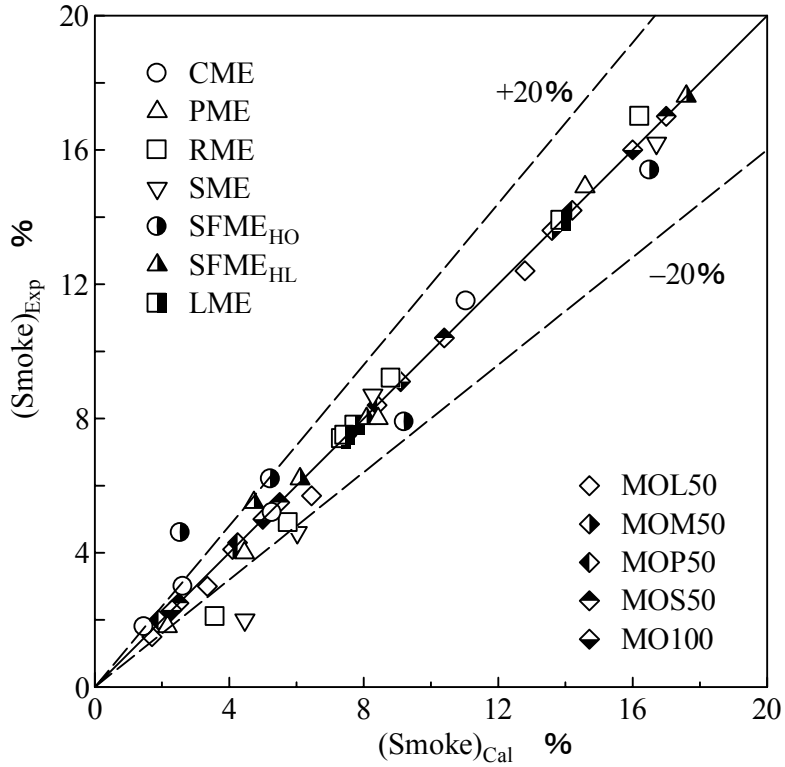

Figure 5.5 Comparison of $(Smoke)_{Exp}$ and $(Smoke)_{Est}$

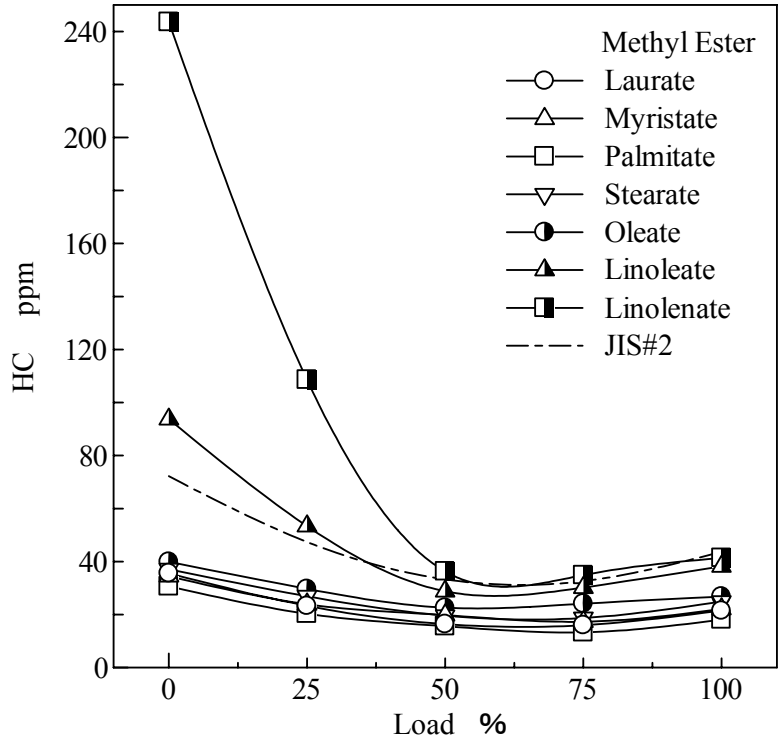

Figure 5.6 HC emission comparison of pure FAMEs

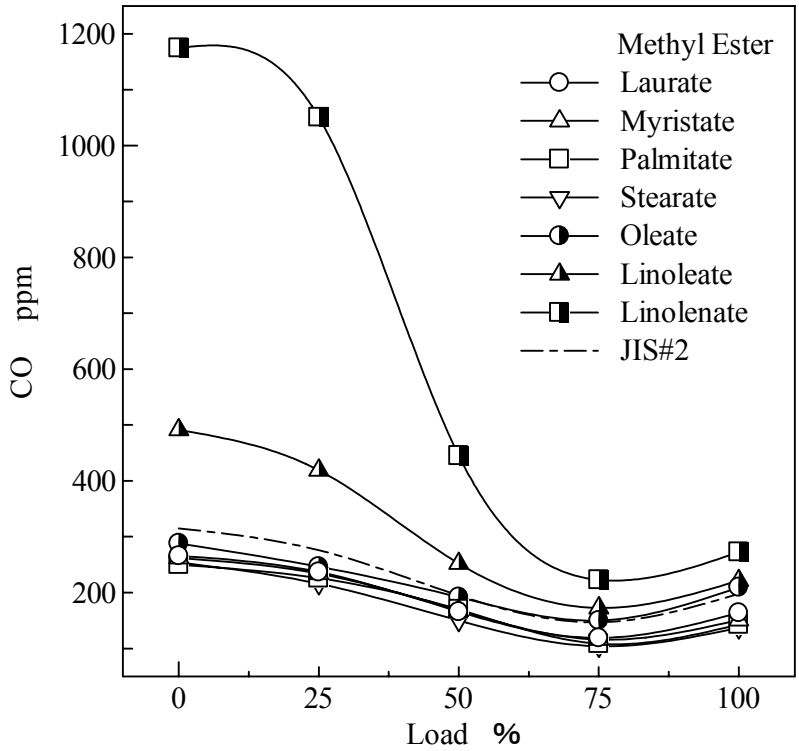

Figure 5.7 CO emission comparison of pure FAMEs

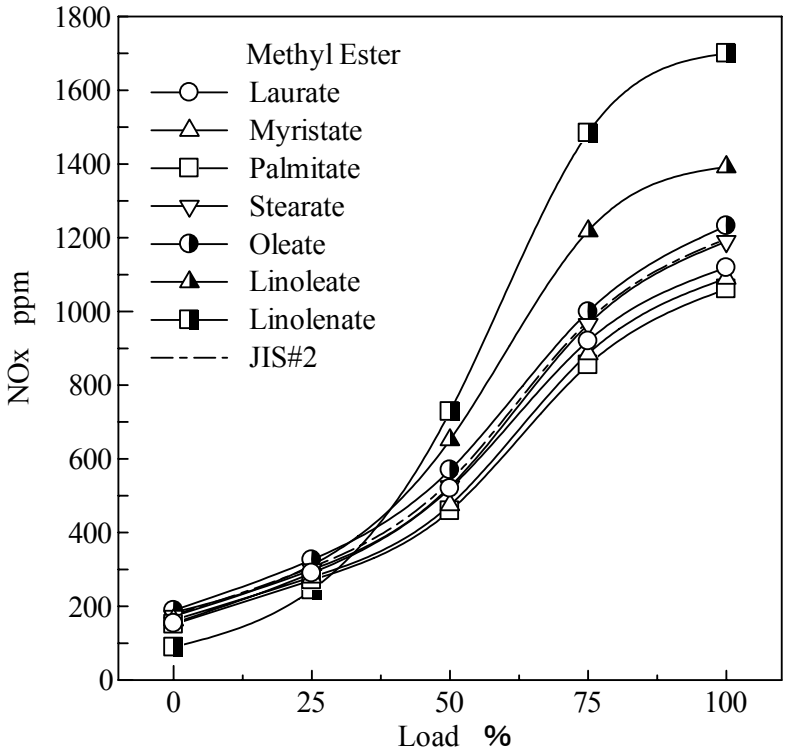

Figure 5.8 NOx emission comparison of pure FAMEs

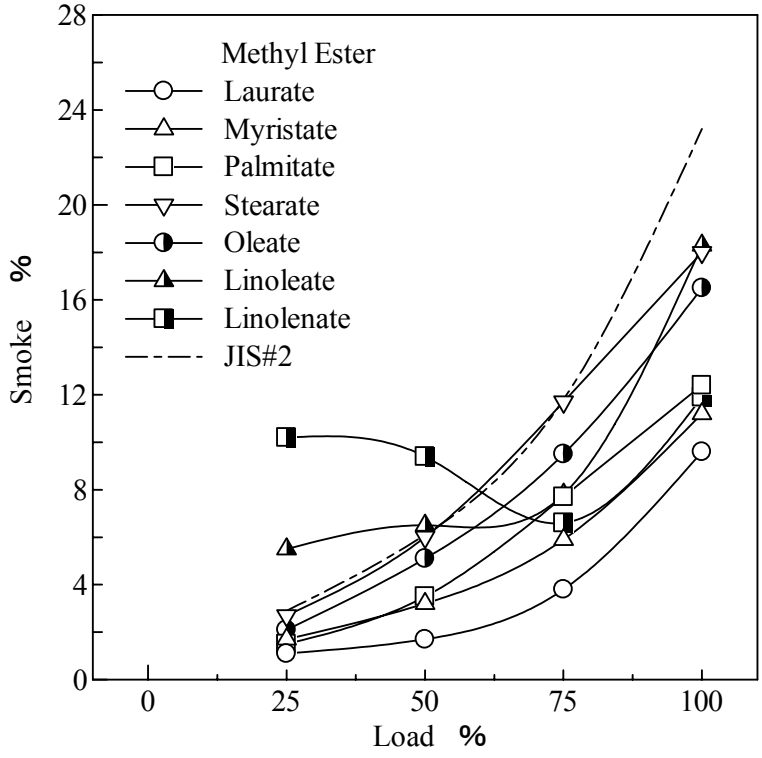

Figure 5.9 Smoke emission comparison of pure FAMEs

vegetable oil methyl esters, the most of the differences between experimental data and estimation data are within the range of ±20% and while NOx emissions are found in the range of ±10%. The trends of pure FAMEs are shown in Figure 5.6 to 5.9. These figures are drawn by the assumption data of exhaust emission of pure FAMEs. From these figures it can be seen that the trends of emissions of linolenate methyl ester are dramatically higher and quite different from the other methyl esters. It may be affected by because of the experimental emission data of LME. But the rest of methyl ester fuels show almost the same trends of graph at all load levels. Therefore, it is necessary to amend and re-assume the possible trend of linolenic methyl ester as similar pattern to the other methyl esters. The comparison of experimental and calculation emission data of FAMEs fuels and vegetable oil methyl ester fuels after the amendment are shown in Figure 5.10-5.21. These figures show the trends of emissions of the fuels against the load levels. It can be noticed from these figures, most of the estimation data are acceptable close to the experimental data, but some data need further amendment.

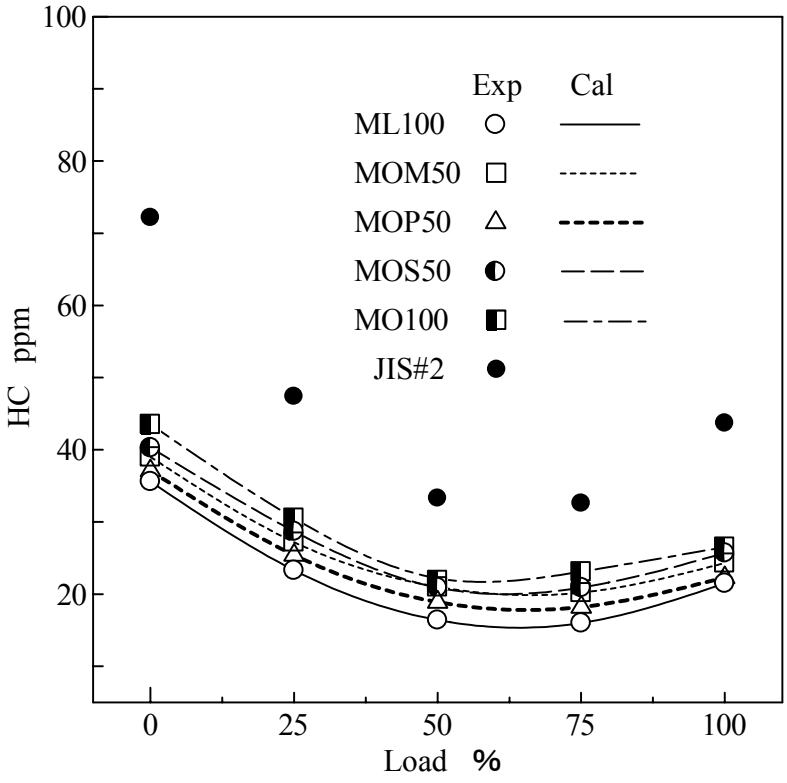

Figure 5.10 HC emission comparison of FAMEs

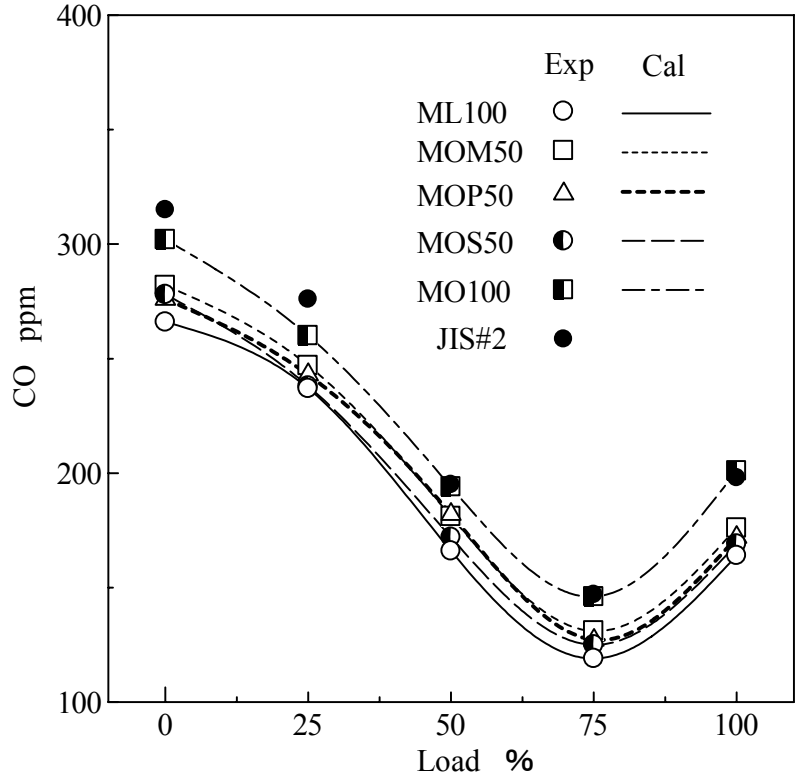

Figure 5.11 CO emission comparison of FAMEs

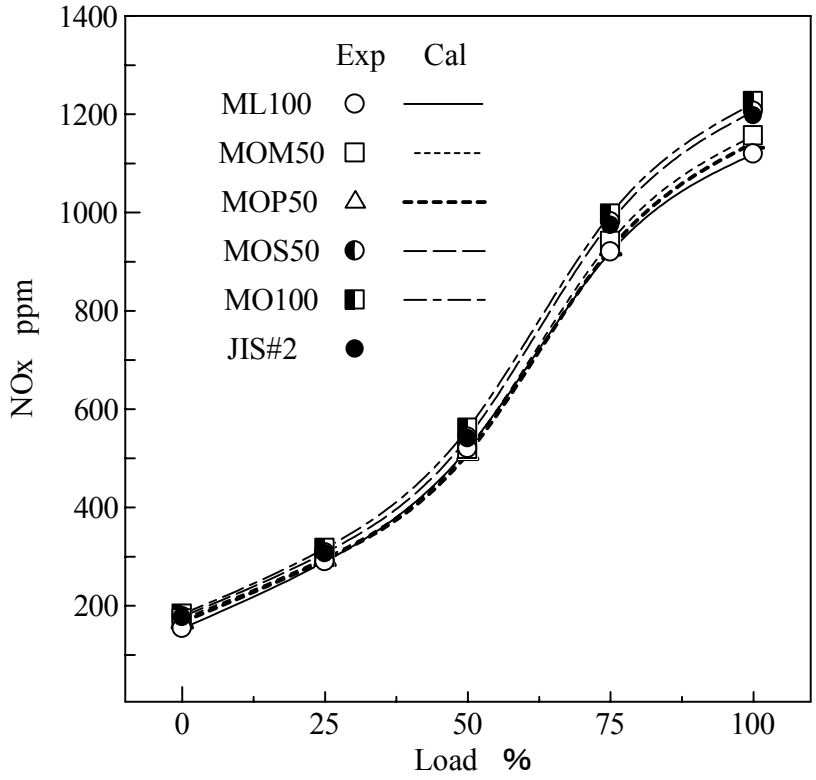

Figure 5.12 NOx emission comparison of FAMEs

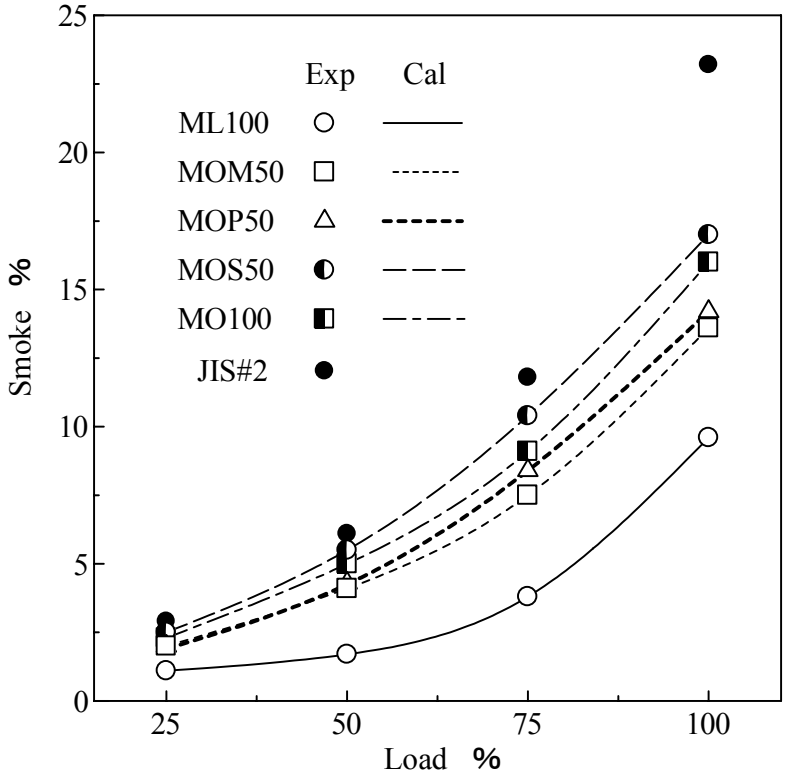

Figure 5.13 Smoke emission comparison of FAMEs

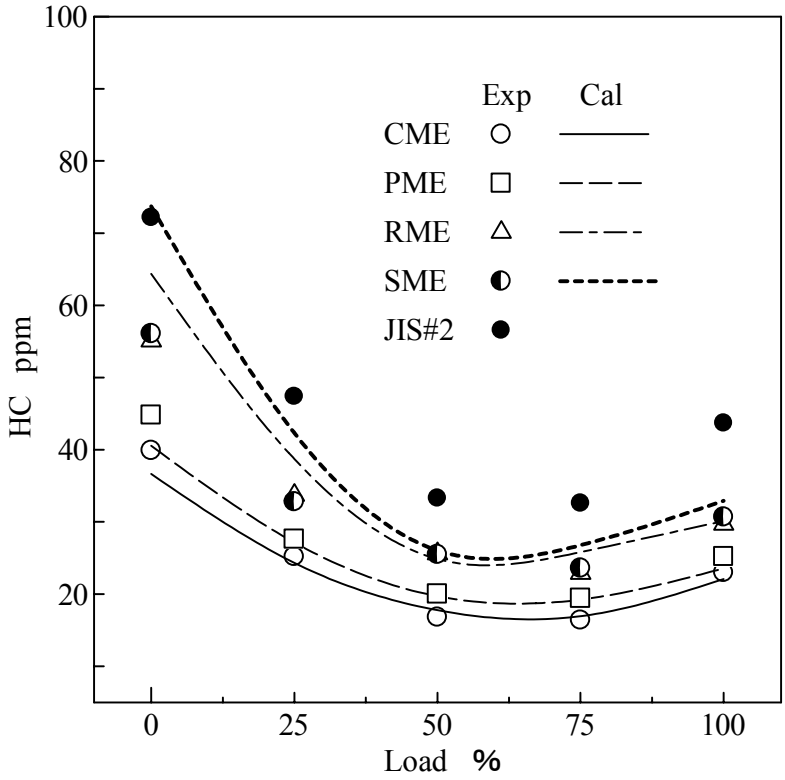

Figure 5.14 HC emission comparison

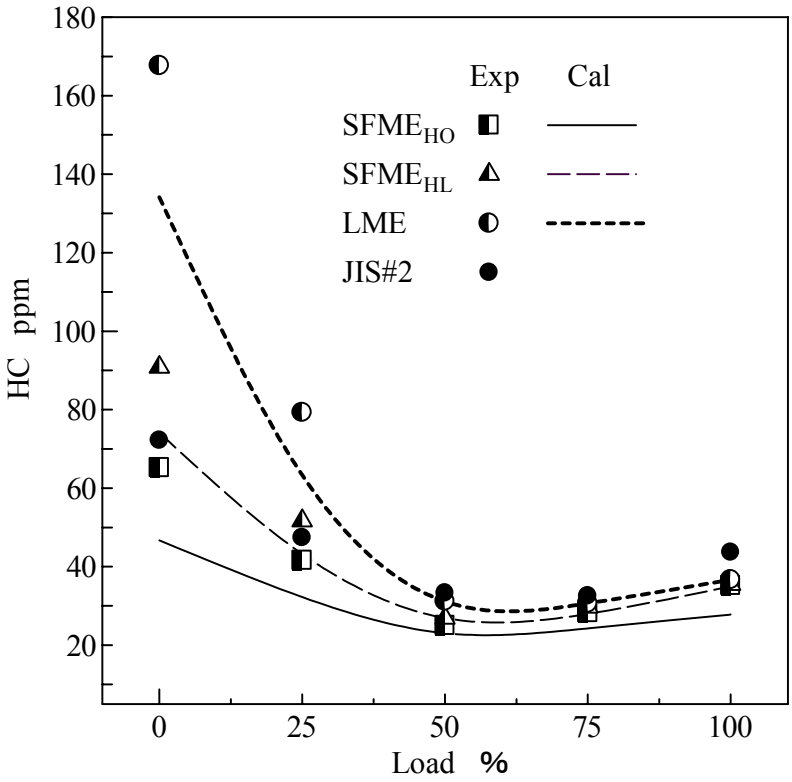

Figure 5.15 HC emission comparison

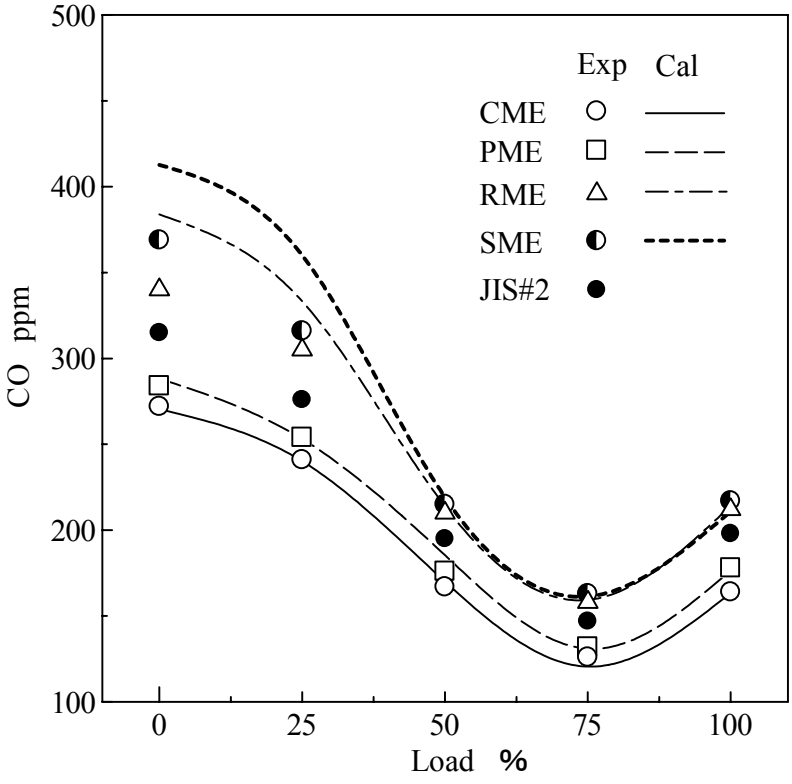

Figure 5.16 CO emission comparison

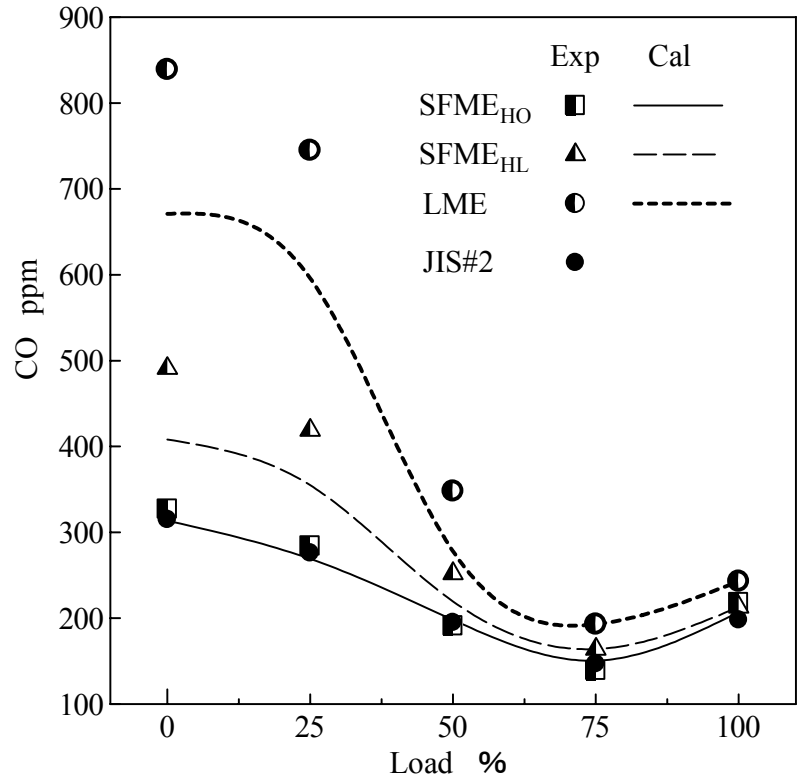

Figure 5.17 CO emission comparison

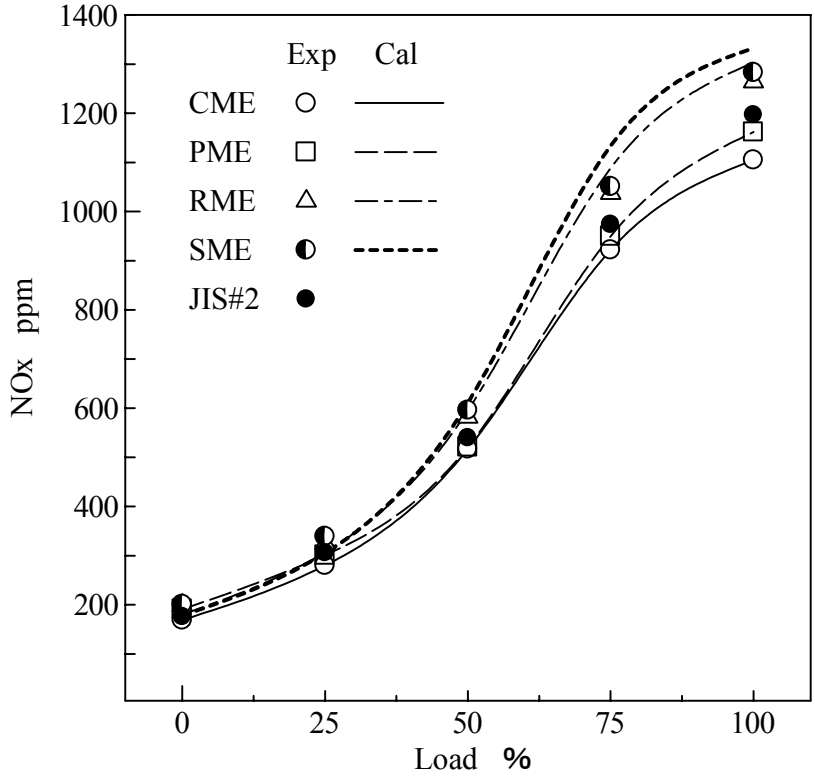

Figure 5.18 NOx emission comparison

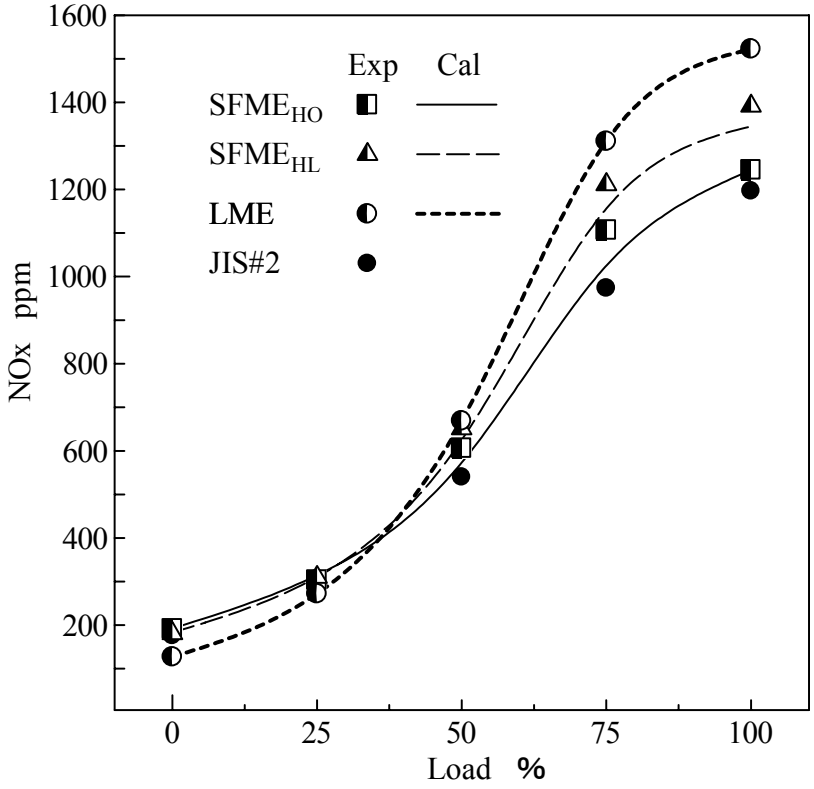

Figure 5.19 NOx emission comparison

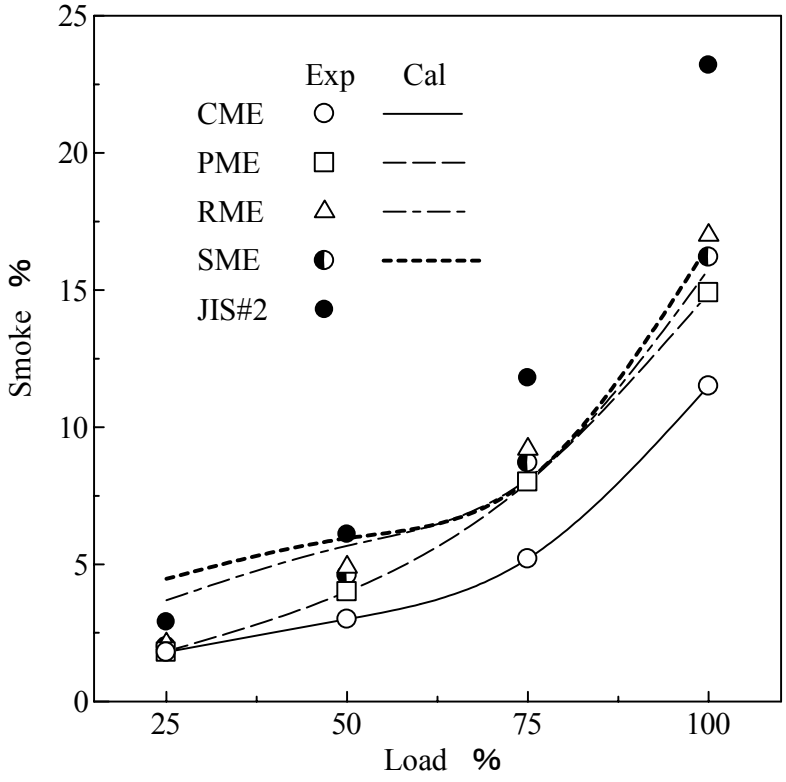

Figure 5.20 Smoke emission comparison

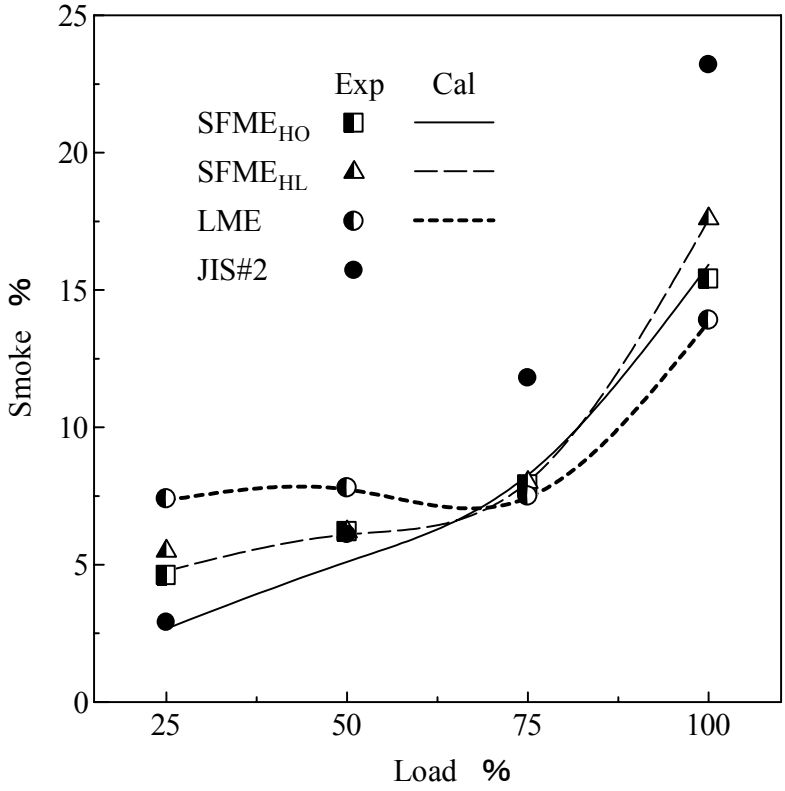

Figure 5.21 Smoke emission comparison

After reviewing these data and graphs of comparison between experimental and estimation emissions, some further assumption on experimental data were taken to improve the estimation. Therefore, the experimental emission data of $SFME_{HL}$ and LME were omitted from estimation because of their emission trends are dramatically higher at lower load levels. It may be related with their fuel properties such as residual impurity in these fuels make poor combustion process of $SFME_{HL}$ and LME in lower load levels. Thus the assumptions made only on CME, PME, RME and SME were better for emission estimations. The HC, CO, NOx and smoke emissions of seven kinds of pure FAMEs and four kinds of vegetable oil methyl ester graph drawn by after assumption data are shown in Figure 5.22 to 5.29. Comparing before and after assumptions figures, amendment on emission can be found mostly in the HC, CO, NOx and smoke emission of methyl linoleate and linolenate. Also it is expected that the result of the assumptions are reliable and possible trend of emissions of seven kinds of pure FAMEs and four kinds of vegetable oil methyl ester. Finally, the relation of FAME

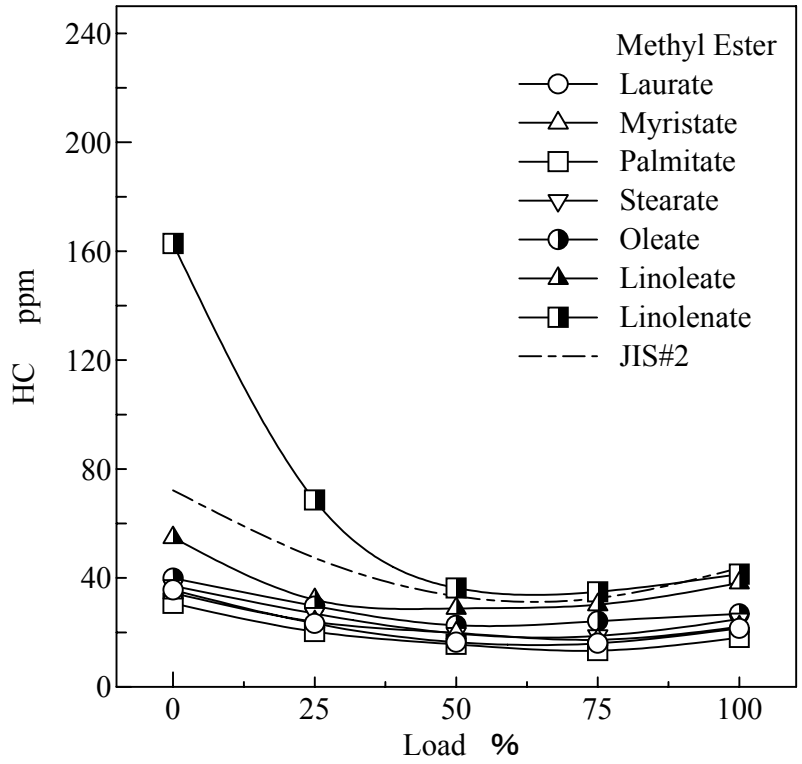

Figure 5.22 HC emission of pure FAMEs

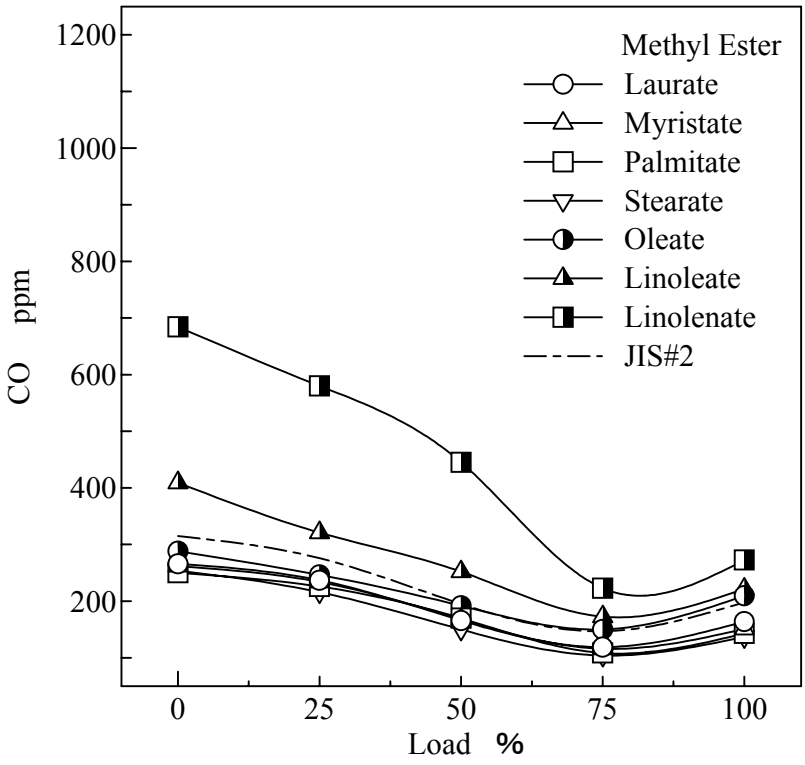

Figure 5.23 CO emission of pure FAMEs

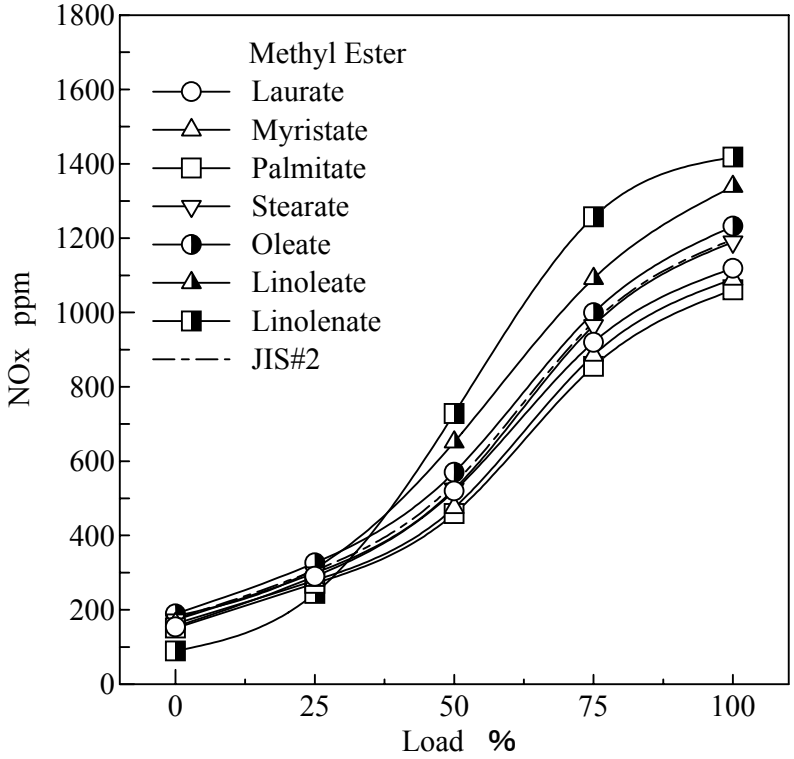

Figure 5.24 NOx emission of pure FAMEs

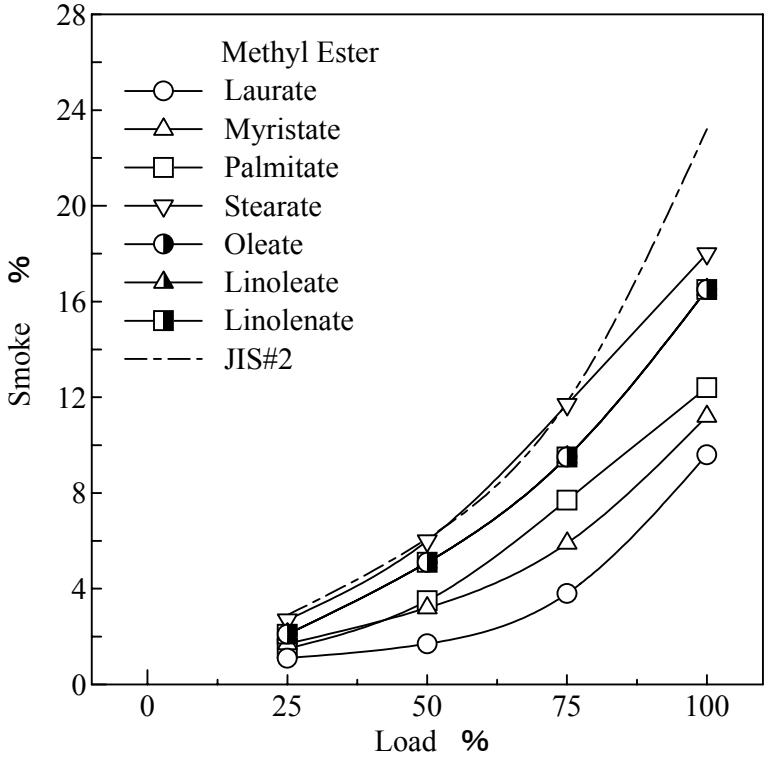

Figure 5.25 Smoke emission of pure FAMEs

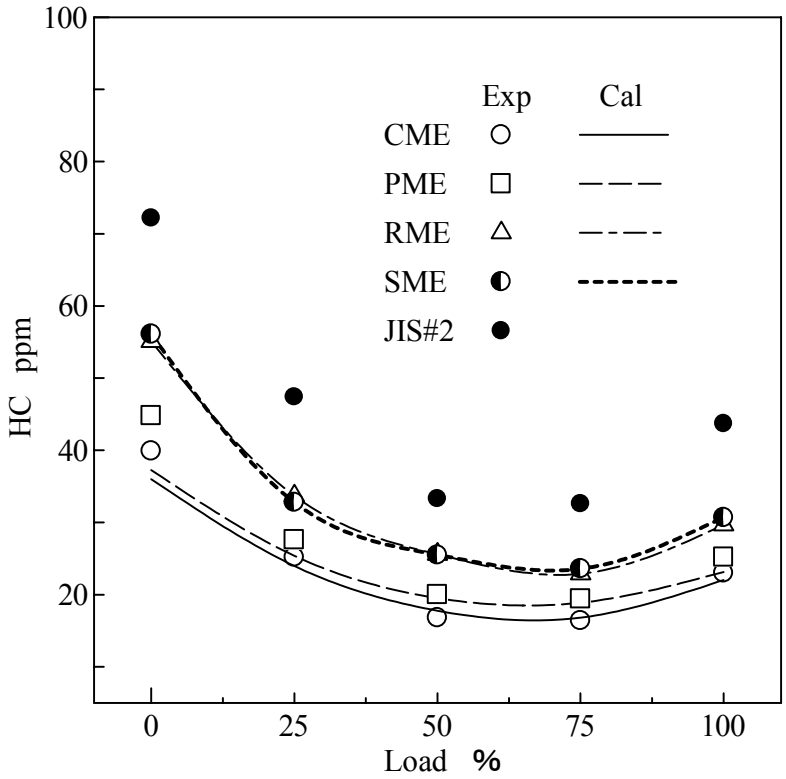

Figure 5.26 HC emission of vegetable oil methyl esters

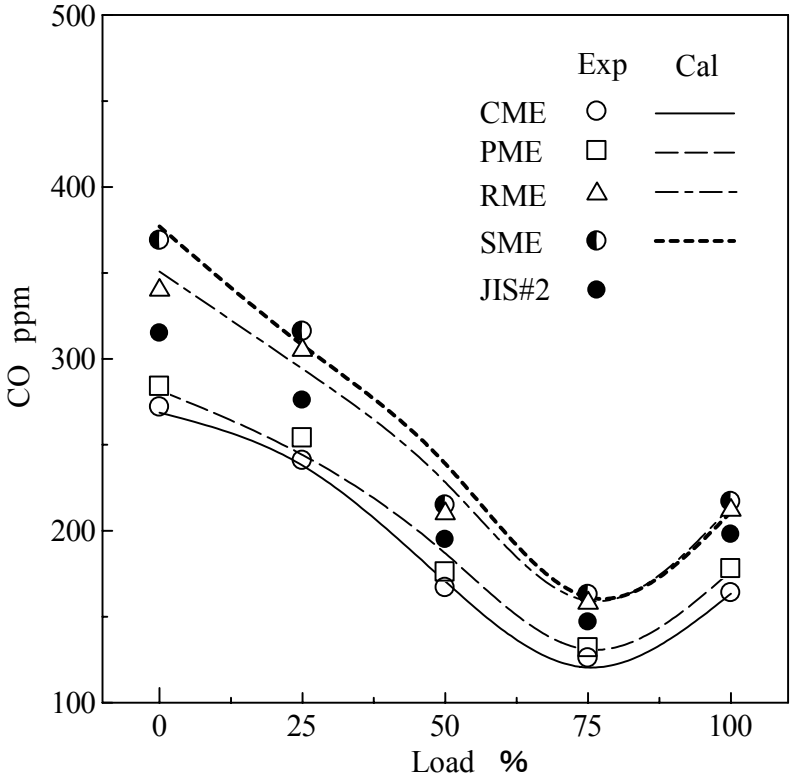

Figure 5.27 CO emission of vegetable oil methyl esters

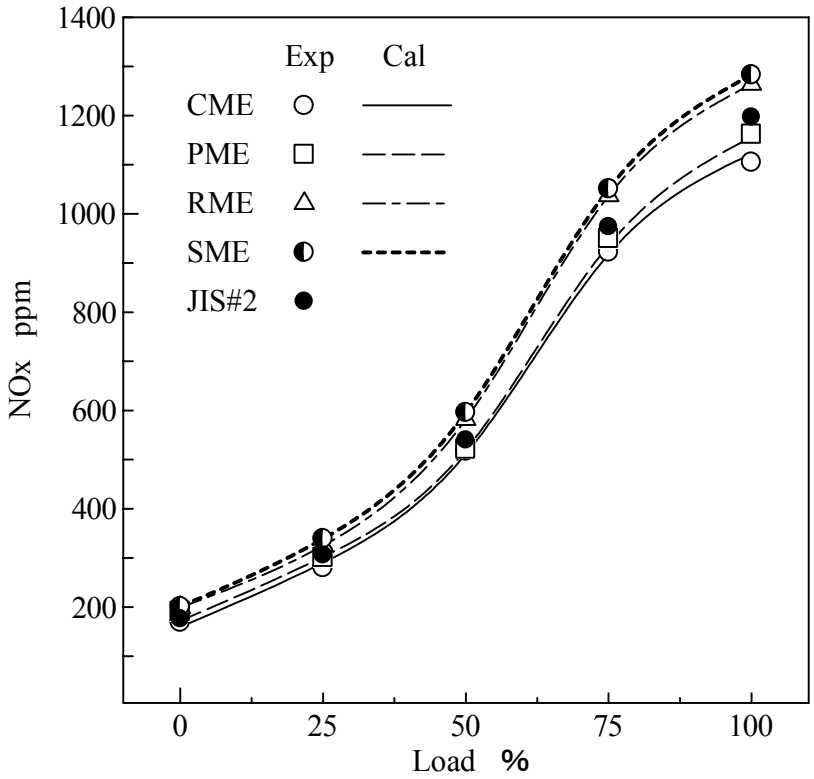

Figure 5.28 NOx emission of vegetable oil methyl esters

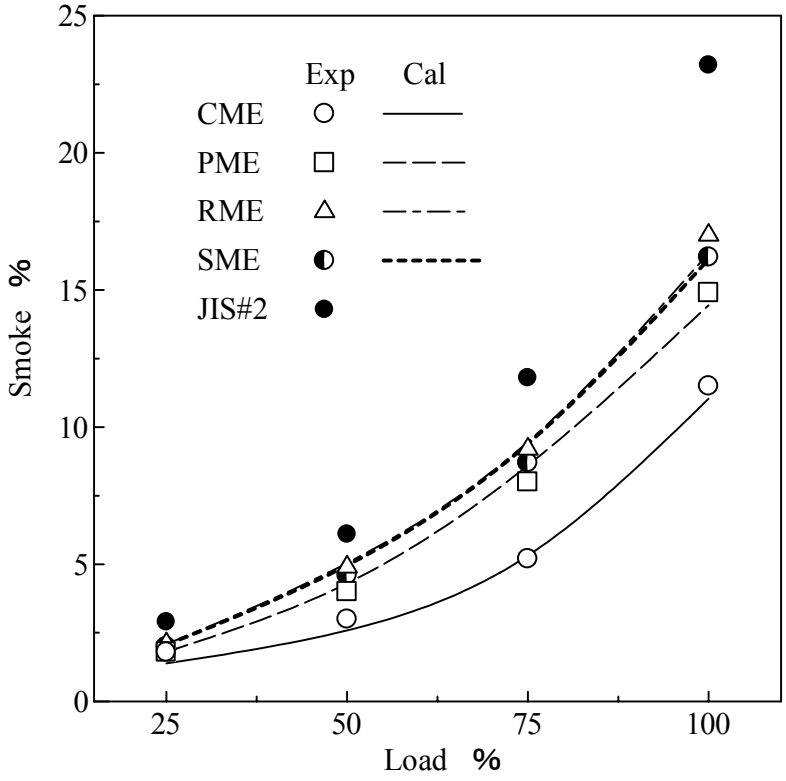

Figure 5.29 Smoke emission of vegetable oil methyl esters

Table 5.7 Determined data for NOx emission of pure FAMEs (ppm)

Methyl Ester	Load %				
	0	25	50	75	100
Laurate	154	290	520	920	1119
Myristate	163	279	475	885	1090
Palmitate	151	271	459	855	1061
Stearate	173	299	525	965	1190
Oleate	189	326	570	999	1232
Linoleate	183	312	652	1092	1339
Linolenate	89	244	728	1257	1418

Table 5.8 Determined data for smoke emission of pure FAMEs(%)

Methyl Ester	Load %				
	0	25	50	75	100
Laurate	0	1.1	1.7	3.8	9.6
Myristate	0	1.7	3.2	5.9	11.2
Palmitate	0	1.5	3.5	7.7	12.4
Stearate	0	2.7	6.0	11.7	18
Oleate	0	2.1	5.1	9.5	16.5
Linoleate	0	2.1	5.1	9.5	16.5
Linolenate	0	2.1	5.1	9.5	16.5

Table 5.9 Determined data for HC emission of pure FAMEs (ppm)

Methyl Ester	Load %				
	0	25	50	75	100
Laurate	35.6	23.3	16.4	16	21.5
Myristate	34.5	23.9	19.8	17.3	22.1
Palmitate	30.7	20.3	15.6	13.3	18.1
Stearate	37.1	26.9	19.6	18.7	24.9
Oleate	39.9	29.7	22.6	24.1	26.8
Linoleate	54.8	32.0	28.8	30.2	38.2
Linolenate	162.8	68.6	36.3	34.9	41.4

Table 5.10 Determined data for CO emission of pure FAMEs (ppm)

Methyl Ester	Load %				
	0	25	50	75	100
Laurate	266	237	166	119	164
Myristate	262	234	168	116	151
Palmitate	250	226	170	109	143
Stearate	254	216	150	104	137
Oleate	288	246	192	150	210
Linoleate	409	321	252	173	222
Linolenate	684	580	445	223	273

composition and the exhaust emissions (HC, CO, NOx and smoke) obtained from these assumptions are determined for the correlation program. The determined data for exhaust emission are shown in Table 5.7 to 5.10.

Therefore, by inputting the FAME composition of biodiesel in this correlation program, the basic estimation on HC, CO, NOx and smoke emission of methyl ester type biodiesel can be carried out before the engine experiment. This estimation of emissions covers for a steady state engine test with the same facility of experimental set up used in this study. In case of the different experimental facility and set up, it is possible to estimate the HC, CO, NOx and smoke emission of methyl ester type biodiesel by making proportional comparison of the common experimental emission data such as the emission data of the diesel fuel.

In order to carry out the estimation on the HC, CO, NOx and smoke emissions of jatropha oil and lard (pork fat), the developed correlation program was applied. By inputting the FAME composition of jatropha oil and lard (pork fat) in the correlation program, the estimated emission data on HC, CO, NOx and smoke emission were obtained. From these estimated data, the exhaust emission graph were drawn and shown in Figure 5.30 to 5.33. Also the estimated emissions of coconut oil, rapeseed oil and palm kernel oil methyl esters are shown in these figures for comparison.

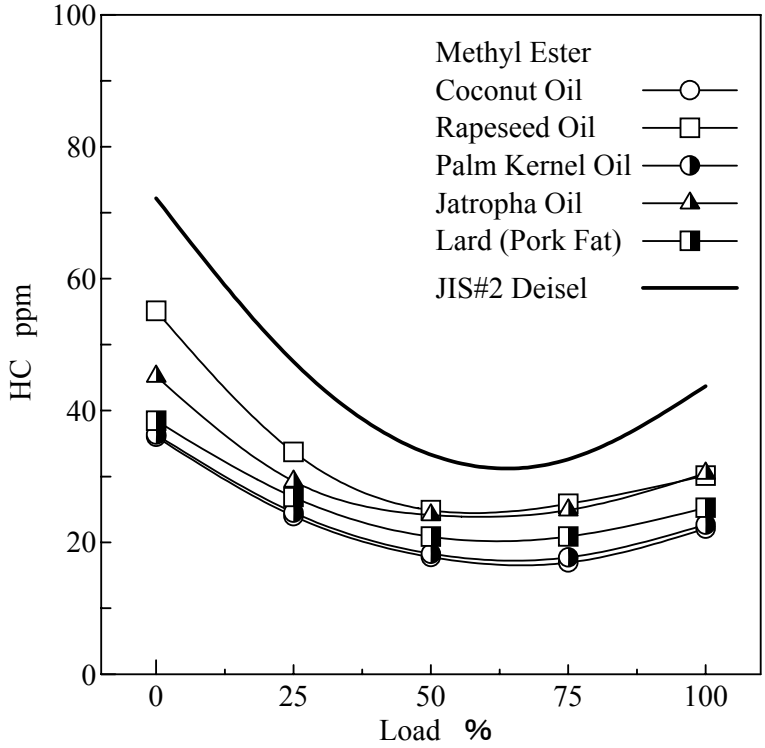

Figure 5.30 Estimated HC emission

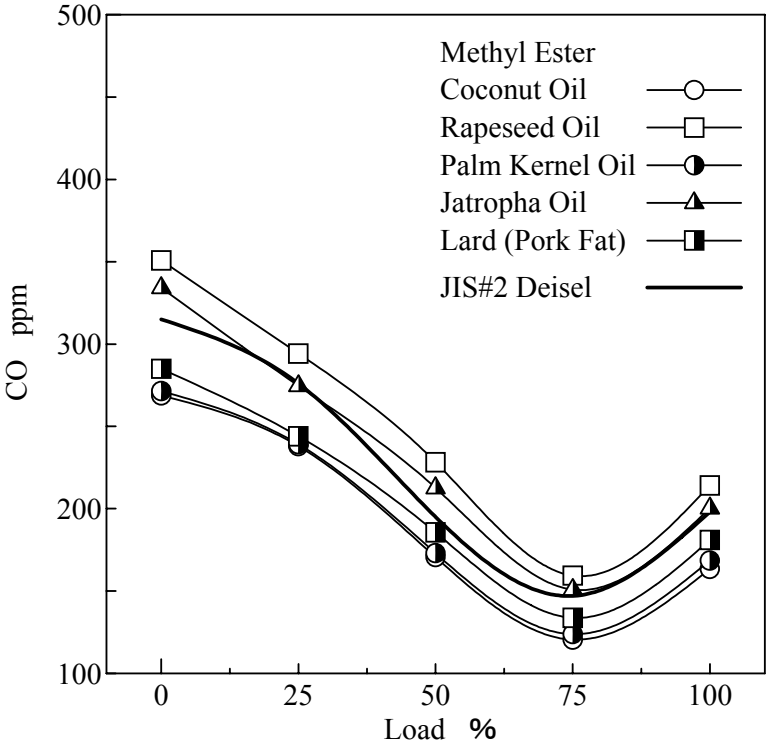

Figure 5.31 Estimated CO emission

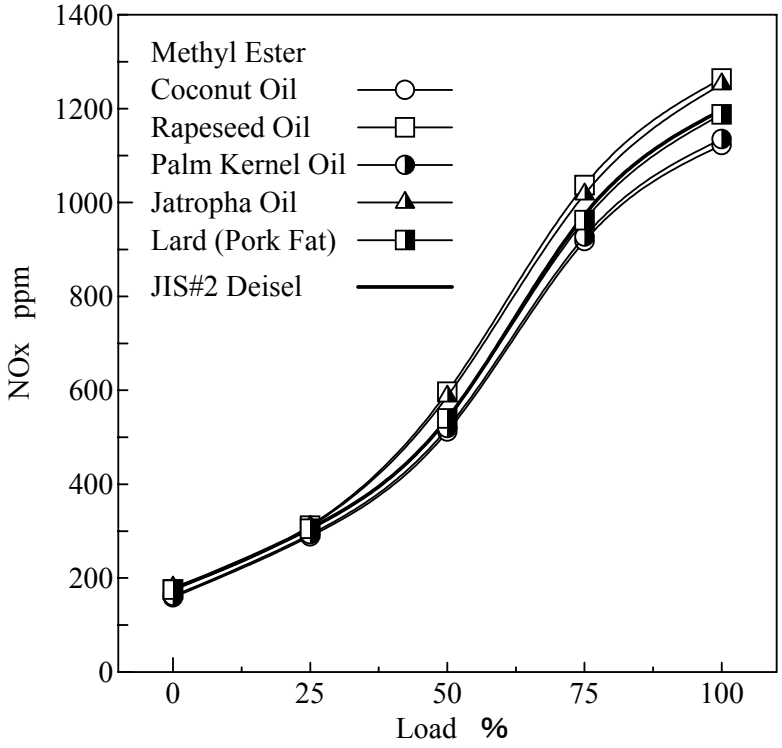

Figure 5.32 Estimated NOx emission

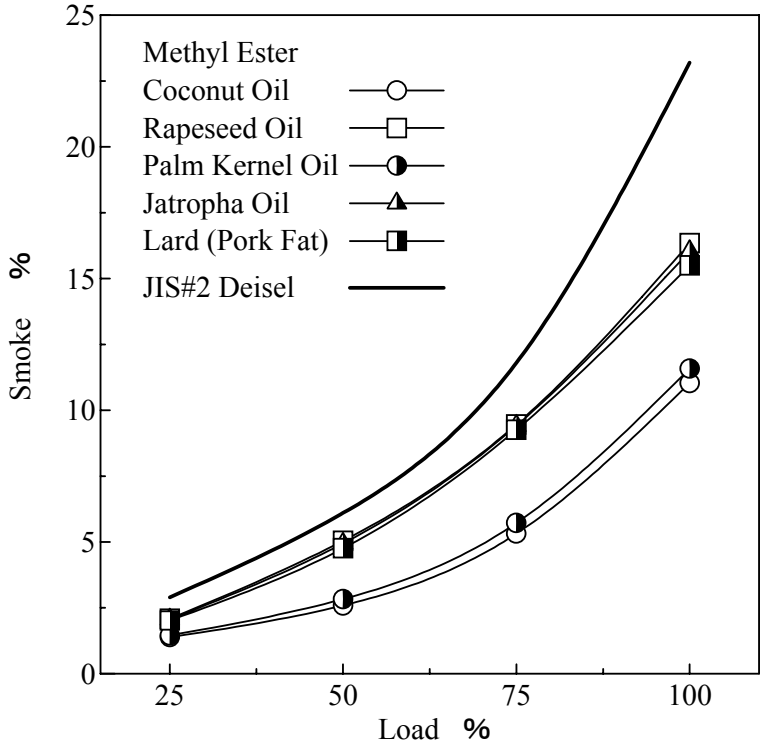

Figure 5.33 Estimated smoke emission

6. CONCLUSIONS

As expressed in Chapter 1, the objective of this study is to investigate the effect of fatty acid composition on the combustion characteristics of biodiesel. Therefore, to accomplish this objective, the experiments were carried out.

Firstly, five kinds of vegetable oils were selected based on the different level of saturation of fatty acids. These are coconut oil (over 90% saturated), palm oil (over 50% saturated), palm kernel oil (over 80% saturated), rapeseed oil (over 90% unsaturated) and soybean oil (over 80% unsaturated). Methyl ester type biodiesels were processed from these vegetable oils. Engine test experiments were conducted on a DI diesel engine by fuelling these five kinds of methyl ester fuels and JIS No. 2 diesel fuel. From the experimental results, saturated FAMEs type biodiesels, coconut oil methyl ester (CME), palm oil methyl ester (PME), palm kernel oil methyl ester (PKME) have better combustion characteristics and lower emissions compared to unsaturated FAMEs type biodiesels, rapeseed oil methyl ester (RME) and soybean oil methyl ester (SME). Specifically, higher content of saturated FAMEs fuels, CME and PKME, have suitable fuel properties, good combustion characteristics and less exhaust emissions.

For more detail investigation, five kinds of pure FAMEs and three kinds of unsaturated FAMEs with different degree of unsaturation, were chosen for the experiments. They are methyl laurate, methyl myristate, methyl palmitate, methyl stearate, methyl oleate, high oleate safflower oil methyl ester ($SFME_{HO}$), high linoleate safflower oil methyl ester ($SFME_{HL}$) and linseed oil methyl ester (LME). Because of purity and availability of methyl linoleate and methyl linolenate, high linoleate safflower oil methyl ester ($SFME_{HL}$) and linseed oil methyl ester (LME) were processed and used as substitutes. Test fuels were pure and blending types of the methyl esters. Two set of engine test experiments were conducted on a DI diesel engine. In the first experiment, test fuel are methyl laurate (ML100), methyl oleate (MO100), methyl laurate 50wt%+methyl oleate 50wt% blend (MOL50), methyl myristate 50wt%+methyl oleate 50wt% blend (MOM50), methyl palmitate 50wt%+methyl oleate 50wt% blend (MOP50) and methyl stearate 50wt%+methyl oleate 50wt% blend (MOL50) respectively. While in the second experiment,

$SFME_{HO}$, $SFME_{HL}$ and LME were used. In both experiments JIS No. 2 diesel fuel was used as a test fuel. From the experimental results of these two experiments, the better combustion characteristics and lower emissions were found in saturated FAMEs and poor combustion characteristics and higher emission can be seen in unsaturated FAMEs. Among the saturated FAMEs the combustion characteristics becomes better with the longer chain length or higher carbon number. But medium carbon number methyl laurate has acceptable combustion ability, because it ignition ability is better than that of the JIS No.2 diesel fuel. One distinguish property of methyl laurate is, it emits lower HC, CO, NOx and smoke emissions compared to JIS No.2 diesel fuel. In unsaturated FAMEs, the combustion characteristics are descending with increasing degree of unsaturation. On the other hand, more unsaturation makes poorer combustion characteristics and resulting higher emissions.

Therefore, by deducing the results of all experiments, it can be said that more saturated FAMEs composition in biodiesel improves the combustion characteristics and reduces the exhaust emissions. Furthermore, the smaller carbon number saturated FAMEs especially methyl laurate has suitable diesel fuel properties, good diesel combustion characteristics and less exhaust emissions.

Additionally a correlation program between FAMEs compositions and the exhaust emissions was developed in this study. By applying this program, basic estimation on exhaust emission (HC, CO, NOx and smoke) of methyl ester type biodiesel is possible. Finally, this study gave valuable knowledge on the fuel properties, combustion characteristics and exhaust emissions of five kinds of methyl ester type vegetable oils biodiesels, five kinds of pure fatty acid methyl esters (FAMEs) and three kinds of unsaturated FAMEs with different degree of unsaturation.

REFERENCES

(01) International Energy Outlook 2007 by Energy Information Adminstration, Office of Integrated Analysis and Forecasting, U.S. Department of Energy, Washington, DC 20585. (5.2007)

(02) IPCC Fourth Assessment Report: Climate Change 2007 by Intergovernmental Panel on Climate Change (IPCC). (2.2007)

(03) Jon H, Van Gerpen, Charles L. Peterson, Carroll E. Goering, Biodiesel: An Alternative Fuel for Compression Ignition Engines. ASABE Distinguished Lecture Series No. 31, American Society of Agriculture and Biological Engineers. (2.2007)

(04) Knothe, G. Dependence of Biodiesel Fuel Properties on the Structure of Fatty Acid Alkyl Ester. Fuel Processing Technology 86 (2005)

(05) Ferguson, C.R. Internal Combustion Engine: Applied Thermoscience. John Wiley and Sons, New York (1986)

(06) Technical Review, Diesel Fuels. By Chevron Products Company, 575 Market Street, San Francisco, CA94105 (1998)

(07) Taylor, C.F. The Internal Combustion Engine in Theory and Practice Thermodynamic, Fluid Flow, Performance. Vol. 1. MIT Press, Cambridge, MA. (1985)

(08) Taylor, C.F. The Internal Combustion Engine in Theory and Practice Combustion, Material Design. Vol. 2. MIT Press, Cambridge, MA. (1985)

(09) Engler, C.R., Lepori, W.A., Johnson, L.A., and Yarbrough, C.M., Process Requirement for Plant Oil as Alternative Diesel Fuels. Proceeding on Alternative Energy Conference. ASAE, St. Joseph MI. (1992)

(10) Japan Oil Chemists' Society. Standard Methods for the Analysis of Fats, Oil and Related Materials. (1996) (in Japanese)

(11) Freedman, B., Pryde, E.H., and Kwolek, W.F. Variables Affecting the Yields of Fatty Acids from Transesterified Oil. JAOCS. Vol. 61(7), pp.1638-1642

(12) Noureddini, H. and Zhu. D. Kinetic of Transesterification of Soybean Oil. JAOCS. Vol. 74(11), pp. 1457-1463

(13) Allen, C.A.W. and Watts, K.C. A Batch Type Transesterification Unit for Biodiesel Fuels. CSAE paper 96404. CSAE, Saskatoon, SK.

(14) Knothe, G. Cetane numbers- The History of Vegetable Oil-based Diesel Fuels. The Biodiesel Handbook. American Oil Chemist's Society Press (2005)

(15) Peterson, C.L., Reece, D.L., Cruz, R., and Thompson, J. A Comparison of Methyl and Ethyl Esters of Vegetable Oils as Diesel Fuel Substitutes. Proceeding of Alternative Energy Conference. ASAE, St. Joseph, MI. (1992)

(16) Schumacher, L.G. The Use of Strata-Fuel in Blends of Soydiesel. ASAE paper 946533. ASAE, St. Joseph, MI. (1994)

(17) Zubik, J., Sorenson, S. C., and Goering, C.E. Diesel Conbustion of Sunflower Oil Fuels. Transaction of ASAE. Vol 27(3), pp. 1252-1259

(18) Ali, Y., Eskiridge, K.M., Hanna, M.A. Testing of Alternative Fuel from Tallow and Soybean Oil in Cummins N14-410 Diesel Engine. Biosource Technology. Vol 53, pp.243-254 (1995)

(19) Wagner, L.E., Clarke, S.J. and Schrock, M.D. Effect of Soybean Oil Esters on the Performance, Lubricating Oil, and Water of Diesel Engines. Paper no. 841385. International Conference on Combustion Engineering. (1984)

(20) Van Gerpen, J. Cetane Number Testing of Biodiesel. Report Data Base, National Biodiesel Board, Jefferson City, Missouri 65110 (1996)

(21) Mittelbach, M. and Trillhart, P. Diesel Fuels Derived from Vegetable Oils, ш Emission Test Using Methyl Esters of Used Frying Oil. JAOCS, Vol 65(10), pp. 1185-1190

(22) Shaheed, A. and Swain, E. Performance and Exhaust Emission Evaluation of a Small Diesel Engine Fuelled with Coconut Oil Methyl Esters. SAE Paper no. 981156 (1998)

(23) Hamasaki, K., Tajima, H., Takasaki, K., Satohira, K., Enomoto, M. and Egawa, H. Utilization of Waste Vegetable Oil for Diesel Fuel. SAE paper no. 2001-01-2021. (2001)

(24) Kinoshita, E., Hamasaki, K. and Jaqin, C. Diesel Combustion of Palm Oil Methyl Ester. SAE paper no. 2003-01-1929. (2003)

(25) Clarke, S.J., Wagner, L, Schrock, M.D., and Piennaar. P.G. Methyl and Ethyl Esters as Alternative Fuels for Diesel Engines. JAOCS. Vol 55, pp.

1632-1638 (1984)

(26) Goodrum, J.W., Patel, V.C., and McClendon, R.W. Diesel Injector Carbonization by Three Alternative Fuels. Transaction of ASAE. Vol. 39(3), pp. 817-821 (1996)

(27) Knothe, G., Matheaus., A.C. and Ryan Ⅲ., T.W. Cetane Numbers of Branched and Straight-Chain Fatty Esters Determined in an Ignition Quality Tester. Fuel, Vol 82 pp. 971-975 (2003)

(28) Knothe, G. and Steidley. K.R. Kinematic viscosity of Biodiesel Fuel Components and Related Compound. Influence of Compound Structure and Comparison to Petroldiesel Fuel Components. Fuel, Vol. 84 pp.1059-1065 (2005)

(29) Graboski. M.S. and McCormick. R.L. Combustion of Fat and Vegetable Oil Derived Fuels in Diesel Engines. Prog. Energy Combustion Science, Vol. 24, pp. 125-164 (1998)

(30) Yamane. K., Ueta. A. and Shimamoto. Y. Influence of Physical and Chemical Properties of Biodiesel Fuels on Injection, Combustion and Exhaust Emission Characteristics in a Direct Injection Compression Ignition Engine. Int J Engine Research, Vol.2 No.4, pp.1-13 (2001)

(31) Japan Oilseeds Processors Association. The Transition of Global Vegetable Oil Production. http://oil.or.jp/

(32) Kono. N., Fukumoto. J., Iizuka. M. and Takeda. H. Influence of FAME Blending into Diesel Fuel on Plugging Characteristics of Fuel Supply System in Diesel Vehicle at Low Temperature. Proceeding of 2005 JSAE Annual Autumn Conference, No. 117-05, pp. 25-30 (2005) (in Japanese)

(33) Tat. M.E., Van Garpen. J.H. Measurement of Biodiesel Speed of Sound and Its Impact on Injection Timing. NREL/SR-510-31462 (2003)

(34) Heywood. J.B. Internal Combustion Engine Fundamentals. McGraw-Hill: New York (1988)

(35) Fernando. S., Hall. C. and Jha. S. NOx Reduction from Biodiesel Fuels. Energy and Fuel, Vol. 20, pp. 376-382 (2006)

(36) Freedman. B., Bagby. M.O., Callahan. T.J. and Ryan Ⅲ., T.W. Cetane Numbers of Fatty Esters, Fatty Alcohols and Triglycerides Determined in a

Constant Volume Combustion Bomb. SAE Paper no. 900343 (1990)

(37) Freedman. B. and Bagby. M.O. Predicting Cetane Numbers of n-Alcohols and Methyl Esters from their Physical Properties. JAOCS, Vol. 67(9), pp. 565-570

(38) Graboski. M.S., McCormick. R.L. Alleman T.L. and Herring. A.M. The effect of Biodiesel Composition on Engine Emissions from a DDC Series 60 Diesel Engine. NREL/SR-510-31461 (2003)

(39) Knothe. G. Dunn. R.O. and Bagby. M.O. Biodiesel: The Use of Vegetable Oils and Their Derivatives as Alternative Diesel Fuel. Chapter 10 from Fuels and Chemicals from Biomass, ASC Symposium Series, V666, Ed. by Saha. B.C and Woodward. J. American Chemical Society, Washington, DC. (1997)

(40) Klopfenstein, W.E. Effect of Molecular Weights of Fatty Acid Esters on Cetane Numbers as Diesel Fuels. JAOCS, Vol. 62(6), pp. 1029-1031

(41) Walter, J., P. and Derry, J. The 1981 Flower Power, Field Testing Program. Vegetable Oil Fuels, Proceeding of International Conference on Plant and Vegetable Oils as Fuels, pp. 384-393 (1982)

(42) Baranescu, R.A and Lusco, J.J Preformance, Durability and Low Temperature Evaluation of Sunflower Oil As a Diesel Fuel Extender. Vegetable Oil Fuels, Proceeding of International Conference on Plant and Vegetable Oils as Fuels, pp. 312-328 (1982)

(43) Varde, K.S. Some Correlation of Diesel Engine Performance with Injection Characteristics Using Vegetable Oil As Fuel. Vegetable Oil Fuels, Proceeding of International Conference on Plant and Vegetable Oils as Fuels, pp. 303-311 (1982)

(44) Radu, R. and Mircea, Z. The Use of Sunflower Oil in Diesel Engines. SAE Paper no. 972979 (1997)

(45) Goering, C.E., Schwab, A.W., Daugherty, M.J., Pryde, E.H. and Heakin, A.J. Fuel Properties of Eleven Vegetable Oils. Transaction of ASAE 25(6), pp. 1472-1477 (1982)

(46) U.S. Department of Energy. 2004 Biodiesel Handling and Use Guidelines (2004)

(47) Schmidt, K. and Gerpen, J.V. The Effect of Biodiesel Fuel Composition on

Combustion and Emissions. SAE Paper no. 961086 (1996)

Appendix

Section A: Experimental data of vegetable oil methyl esters

Table A-1 BSFC of vegetable oil methyl esters (g/MW·s)

Load %	0	25	50	75	100
CME	-	109.5	83.8	76.2	75.1
PME	-	103.0	79.4	72.8	71.8
PKME	-	108.3	82.7	75.4	74.6
RME	-	104.1	78.9	72.7	71.8
SME	-	103.7	79.6	73	72.2
JIS#2	-	91.9	69.7	63.4	62.3

Table A-2 BTE of vegetable oil methyl esters (%)

Load %	0	25	50	75	100
CME	-	25.8	33.6	37.0	37.5
PME	-	26.4	34.2	37.3	37.8
PKME	-	26.0	34.1	37.4	37.8
RME	-	26.3	34.7	37.7	37.7
SME	-	26.3	34.1	37.2	37.8
JIS#2	-	25.2	33.3	36.6	37.2

Table A-3 HC emission of vegetable oil methyl esters (ppm)

Load %	0	25	50	75	100
CME	39.9	25.2	16.8	16.4	23.0
PME	44.8	27.6	20.0	19.4	25.2
PKME	38.4	25.1	16.2	15.9	21.1
RME	55.1	33.7	25.6	22.9	29.7
SME	57.8	35.5	25.9	23.1	31.7
JIS#2	72.2	47.4	33.3	32.6	43.7

Table A-4 CO emission of vegetable oil methyl esters (ppm)

Load %	0	25	50	75	100
CME	422	345	237	180	265
PME	436	352	258	197	273
PKME	420	348	247	180	255
RME	583	466	318	225	330
SME	590	488	325	236	335
JIS#2	553	417	287	220	310

Table A-5 NOx emission of vegetable oil methyl esters (ppm)

Load %	0	25	50	75	100
CME	169	280	517	922	1105
PME	191	301	521	950	1162
PKME	176	290	521	942	1141
RME	199	325	582	1037	1264
SME	202	342	617	1072	1317
JIS#2	176	306	540	974	1197

Table A- 6 Smoke emission of vegetable oil methyl esters (%)

Load %	0	25	50	75	100
CME	0.4	0.7	1.2	3.8	11.5
PME	1.1	2.0	3.1	8.0	14.9
PKME	0.4	0.9	1.6	5.0	12.4
RME	0.5	2.1	3.9	9.2	17.0
SME	0.5	1.5	4.3	9.8	18.0
JIS#2	0.7	1.7	5.0	11.8	23.2

CME: coconut oil methyl ester, PME: palm oil methyl ester

PKME: palm kernel oil methyl ester, RME: rapeseed oil methyl ester

SME: soy bean oil methyl ester, JIS#2: JIS no. 2 diesel fuel

Section B: Experimental data of pure fatty acid methyl esters

Table B-1 BSFC of fatty acid methyl esters (g/MW·s)

Load %	0	25	50	75	100
ML 100	-	110.0	84.4	76.6	76.0
MO 100	-	106.1	79.4	73.7	72.5
MOL 50	-	107.6	84.2	75.2	73.9
MOM 50	-	106.7	81.9	74.6	73.5
MOP 50	-	104.4	79.9	73.3	72.6
MOS 50	-	105.0	79.1	73.1	72.3
JIS#2	-	92.0	69.7	63.4	62.3

Table B-2 BTE of fatty acid methyl esters (%)

Load %	0	25	50	75	100
ML 100	-	24.8	32.4	35.6	36.0
MO 100	-	24.3	32.4	35.0	35.5
MOL 50	-	24.9	31.5	35.2	35.9
MOM 50	-	24.5	31.9	35.1	35.6
MOP 50	-	24.7	32.3	35.3	35.8
MOS 50	-	24.4	32.0	34.9	35.5
JIS#2	-	24.3	31.0	34.9	35.3

Table B-3 HC emission of fatty acid methyl esters (ppm)

Load %	0	25	50	75	100
ML 100	15.0	12.8	9.0	8.8	11.8
MO 100	21.8	17.5	12.0	12.5	14.5
MOL 50	19.5	16.0	11.5	10.8	13.0
MOM 50	17.5	14.3	11.0	11.0	13.0
MOP 50	16.0	14.0	10.5	10.0	12.8
MOS 50	20.0	16.5	12.0	12.0	14.8
JIS#2	23.0	18.5	15.0	13.8	18.0

Table B-4 CO emission of fatty acid methyl esters (ppm)

Load %	0	25	50	75	100
ML 100	290	270	175	130	185
MO 100	315	300	220	175	220
MOL 50	310	295	205	170	215
MOM 50	295	290	200	165	210
MOP 50	290	280	195	155	205
MOS 50	285	275	190	150	195
JIS#2	315	305	225	170	230

Table B-5 NOx emission of fatty acid methyl esters (ppm)

Load %	0	25	50	75	100
ML 100	116	261	466	829	1089
MO 100	119	314	475	916	1182
MOL 50	98	288	518	871	1128
MOM 50	129	276	485	855	1117
MOP 50	127	270	537	890	1100
MOS 50	136	299	477	954	1178
JIS#2	125	312	500	940	1175

Table B-6 Smoke emission of fatty acid methyl esters (%)

Load %	0	25	50	75	100
ML 100	0.0	0.5	1.7	3.5	9.0
MO 100	0.7	2.4	5.5	10.0	14.0
MOL 50	0.1	0.7	1.8	4.7	10.4
MOM 50	0.2	1.1	3.4	6.4	12.6
MOP 50	0.5	3.0	5.9	9.0	14.0
MOS 50	0.6	2.5	6.2	10.8	16.8
JIS#2	1.0	3.2	7.0	11.9	21.6

ML 100: methyl laurate 100%

MO 100: methyl oleate 100%

MOL 50: methyl oleate 50wt% + methyl laurate 50wt%

MOM 50: methyl oleate 50wt% + methyl myristate 50wt%

MOP 50: methyl oleate 50wt% + methyl palmitate 50wt%

MOS 50: methyl oleate 50wt% + methyl stearate 50wt%

JIS#2: JIS no. 2 diesel

Section C: Experimental data of unsaturated fatty acid methyl esters

Table C-1 BSFC of unsaturated fatty acid methyl esters (g/MW･s)

Load %	0	25	50	75	100
$SFME_{HO}$	-	105.0	79.6	71.9	70.3
$SFME_{HL}$	-	104.3	79.4	73.4	71.1
LME	-	107.7	80.0	73.9	71.9
JIS#2	-	90.1	69.2	62.9	61.3

Table C-2 BTE of unsaturated fatty acid methyl esters (%)

Load %	0	25	50	75	100
$SFME_{HO}$	-	26.2	34.6	38.3	39.2
$SFME_{HL}$	-	26.5	34.8	37.7	38.8
LME	-	25.7	34.6	37.5	38.5
JIS#2	-	25.8	33.5	36.9	37.8

Table C-3 HC emission of unsaturated fatty acid methyl esters (ppm)

Load %	0	25	50	75	100
$SFME_{HO}$	64.9	44.9	34.1	36.4	35.2
$SFME_{HL}$	90.4	55.8	36.7	38.2	35.5
LME	167.0	85.7	42.6	39.4	36.7
JIS#2	71.9	51.2	45.5	41.9	43.8

Table C-4 CO emission of unsaturated fatty acid methyl esters (ppm)

Load %	0	25	50	75	100
$SFME_{HO}$	620	477	300	220	290
$SFME_{HL}$	930	703	397	260	283
LME	1590	1250	547	307	323
JIS#2	597	463	307	233	263

Table C-5 NOx emission of unsaturated fatty acid methyl esters (ppm)

Load %	0	25	50	75	100
$SFME_{HO}$	158	273	534	999	1297
$SFME_{HL}$	150	280	573	1094	1450
LME	105	246	589	1183	1587
JIS#2	145	276	476	879	1247

Table C-6 Smoke emission of unsaturated fatty acid methyl esters (%)

Load %	0	25	50	75	100
$SFME_{HO}$	1.3	3.4	4.6	5.9	11.5
$SFME_{HL}$	2.8	4.1	4.6	6.0	13.1
LME	5.9	5.5	5.8	5.6	10.4
JIS#2	0.4	1.6	3.4	5.8	17.3

$SFME_{HO}$: high oleic safflower oil methyl ester

$SFME_{HL}$: high linolenic safflower oil methyl ester

LME: linseed oil methyl ester

JIS#2: JIS no. 2 diesel

ACKNOWLEDGEMENTS

I wish to express my sincere gratitude to everyone who contributed to the successful completion of my study.

Special thank to Major General Saw Lwin, Minister for Ministry of Industry No.2 Union of Myanmar for giving me a chance for further study. I also deeply thank to Minister's Office and Myanma Automobile and Diesel Engine Industries for supports for my study. I would like to express my gratitude to Japanese Government (Monbukagakusho) Scholarship Program for financial support through my Master of Engineering and Ph.D. courses.

I would like to acknowledge the excellent guides provided by Professor Kazunori Hamasaki, Associate Professor Eiji Kinoshita, Professor Hisayoshi Kado, Professor Minoru Fukuhara, Professor Shunpei Kamitani and Associate Professor Hiroshi Katanoda throughout my study. Special thanks to Professor Kazunori Hamasaki and Associate Professor Eiji Kinoshita for their kindness, hospitality and supports that, they extended to me from the beginning through finishing of this study. A great thank to lab engineer Mr. Akio Kameda and my lab colleagues for their cooperation. Also thank to the staffs of Mechanical Engineering Department and Graduate School of Science and Engineering, Kagoshima University.

I also would like to thank my father Dr. Thoung Nyunt, my mother Daw Nyunt Nyunt Shane and my brothers for their support throughout my education.

Most important of all, the deepest gratitude to, my wife Hay Mundar Thaung, my daughter Shunn Mya Thet Myo and my son Hein Thet Myo for giving me tremendous supports and encouragement throughout my study career.